Characterization of metabolites in Mongolian S*aposhnikovia divaricata* roots by means of various analytical methods

Zolboo Batsukh

Section of Pharmacognosy

Institute of Natural Medicine

University of Toyama

2020

Characterization of metabolites in Mongolian S*aposhnikovia divaricata* roots by means of various analytical methods

A THESIS

Submitted to University of Toyama

For the degree of

DOCTOR OF PHILOSOPHY

In Pharmaceutical Science

Zolboo Batsukh

Section of Pharmacognosy

Institute of Natural Medicine

University of Toyama

2020

Content

Introduction

I. Saposhnikoviae Radix

Saposhnikovia divaricata (Turcz.) Schischkin is a sole species of genus *Saposhnikovia*, family Umbelliferae and distributed in Central Asia, Russia (Eastern Siberia, Far East), Mongolia, China, and Korea. The root and rhizome of *S. divaricata* is prescribed as Saposhnikoviae Radix (SR) in Japanese and Chinese Pharmacopoeia [1,2]. It has been widely applied for the treatment of pyrexia, rheumatism, headache, vertigo, generalized aching, and arthralgia for thousands of years in the traditional medicine of China, Japan, and Korea [3]. SR has been frequently used as an ingredient of Kampo formulae, such as "Bofutsushosan" in Japanese ("Fang-feng-tong-sheng-san" in Chinese) for the treatment of obesity and metabolic syndrome [4].

Phytochemical studies of SR showed numerous compounds such as chromones, coumarins, polyacetylenes, and polysaccharides [3,5-8]. Chromones are the major constituents in the roots of *S. divaricata,* and they can be classified into two chemical groups, linear dihydrofurochromones and dihydropyranochromones, which have dihydrofuran or dihydropyran rings in their chemical structures, respectively. Coumarins, the minor constituents, are classified into three chemical groups, linear dihydrofurocoumarins, linear furocoumarins, and simple coumarins [9]. Five polyacetylenes including panaxynol, falcarindiol, 8E-heptadeca-1,8-dien-4,6-diyn-3,10-diol, 9Z-1-methoxy-9-heptadecene-4,6-diyn-3-ol, and 8E-10-hydroperoxyl-1,8-heptadecadiene-4,6-diyn-3-ol have been isolated from *S. divaricata* roots [5,10]. Recently, three new coumarins, named divaricoumarin A-C, and two new pyranochromone glycosides were isolated from the roots of *S. divaricata* [11,12].

Many pharmacological studies of SR have indicated the various biological activities, including analgesic, anti-oxidant, anti-inflammatory, anti-proliferative, anti-allergic, and anti-tumor effects [3,6,13-15]. Pharmacological activities of the SR extracts and compounds are shown in Table 1.

Table 1. Pharmacological activities of SR and its constituents.

Group	Compound name	Activity
SR extracts	Ethanol extract [14,15]	antioxidant, anti-inflammatory, anti-proliferative
Dihydrofuro chromones	prim-*O*-glucosylcimifugin (**1**) [16,17]	anti-inflammatory, anti-tumor
	cimifugin (**2**) [6,18]	anti-allergic, analgesic, antioxidant
	4'-*O*-β-D-glucosyl-5-*O*-methylvisamminol* (**3**) [19-21]	anti-inflammatory, analgesic, anti-spasm
	5-*O*-methylvisamminol (**4**) [20]	antioxidant, anti-inflammatory
Dihydropyrano chromones	sec-*O*-glucosylhamaudol (**5**) [6]	analgesic, anti-inflammatory
	hamaudol (**6**) [6,22]	analgesic, anti-inflammatory
	3'-*O*-acetylhamaudol (**7**)	anti-tumor, anti-metastatic
	ledebouriellol (**8**) [6,22]	analgesic, anti-inflammatory
	3'-*O*-angeloylhamaudol (**9**) [22,23]	anti-inflammatory, antitumor
Furanocoumarins	psoralen (**10**) [6]	analgesic
	bergapten (**12**) [6]	analgesic
	xanthatoxin (**11**) [6]	analgesic
	phellopterin (**20**) [24]	GABA activity
Dihydrofuro coumarins	deltoin (**13**) [6,13]	anti-inflammatory, antioxidant
Pyranocoumains	praeruptorin B (**16**) [23,25]	anti-inflammatory, anti-tumor
Polyacetylenes	panaxynol (**15**) [6,26]	anti-inflammatory, anti-proliferative, antiplatelet aggregation activity
	falcarindiol (**17**) [27]	antiplatelet aggregation activity
Polysaccharides	[28,29]	antioxidant, anti-tumor, immunoregulatory

Forty-five compounds, including 13 chromones, 28 coumarins, and four others, were characterized by the HPLC-ESI-Q-TOF-MS technique [30]. Eleven compounds, including 5 chromones and 6 coumarins, were simultaneously determined by HPLC-

DAD and HPLC-MS/MS, and then the HPLC-DAD method was applied to quantify them in 51 batches of SR obtained from Chinese and Korean markets [31]. Four chromones were quantified and analyzed by LC-ESI/MS [32].

Among them, two chromones, prim-*O*-glucosylcimifugin (**1**) and 4'-*O*-*β*-D-glucosyl-5-*O*-methylvisamminol (**3**), were selected as marker compounds for quality control of SR in the Chinese Pharmacopoeia (CP) [2], while **3** is selected as the specific marker compound in the Japanese Pharmacopoeia (JP) [1]. The total content of **1** and **3** were prescribed to be more than 0.24% in the CP. Whereas, dilute ethanol-soluble extract not less than 20% was prescribed for the quality evaluation of SR in the JP. Compound **1** had a promising anti-inflammatory effect by inhibiting the activation of MAPK and NF-kB signaling pathway [33]. Compound **3** has been reported to be able to suppress histone H3 phosphorylation and make it be able to abrogate the mitotic cell cycle progression and immediate pro-inflammatory gene expression in the HeLa S-3 cell culture [21]. However, other compounds are also important for quality assessment of SR, because they possess more analgesic effects than **1** and **3** [6].

II. Metabolomic analysis

Metabolomic analysis/profiling is the study of the metabolism and metabolites in living organisms, such as biofluids, tissues, and cells. It is the most relevant to phenotypes as compared with other "omics" sciences such as exposomics, proteomics, genomics, and transcriptomics [34]. Metabolomic analysis has been rapidly growing as well as omics technologies, and it is important for understanding biological systems, having wide applications ranging from therapeutics, drug discovery, and biotechnology. In natural product research, bioactive secondary metabolites are considered to be new drug leads

[35]. In biotechnology, metabolomic engineering is routinely used for optimizing metabolite production [36]. The metabolomic analysis targets the qualitative and quantitative characterization of metabolites, which have a small molecular weight (< 1500 Da) with changes appearing in organisms in response to certain stimuli [34].

In living organisms, two types of metabolites are produced, primary metabolites which are involved in the metabolic pathways of an organism necessary for its growth, development, and reproduction and secondary metabolites which are involved in ecological functions and species interactions. Analysis of each of these types has different goals and requires the use of different analytical technologies. The analytical platforms commonly used in metabolomics include gas chromatography-mass spectrometry (GC-MS), liquid chromatography-mass spectrometry (LC-MS), high or ultrahigh performance liquid chromatography (HPLC/UPLC), and nuclear magnetic resonance (NMR) spectroscopy [37]. Among them, LC-MS and NMR are powerful means of generating multivariate metabolomic data and each of these tools has its own advantages and disadvantages. Briefly, LC-MS based metabolomics possesses high sensitivity and resolution but suffers from imprecise identification of compound structures and a lack of precise quantitation compared to NMR analysis. LC-MS based methods were recently developed and increasingly applied for metabolomics profiling in plants [38-41], due to their performance to analyze a wide variety of metabolites. In contrast, NMR-based metabolomics is advantaged in quantitation and requires little or no chromatographic separation and sample preparation but suffers from low sensitivity. In addition, NMR is practically amenable to detecting and characterizing compounds that are less tractable to LC-MS analysis, such as sugars, organic acids, alcohols, polyols, and other high polar compounds [42-45].

In the traditional HPLC method, a targeted quantification can be performed through the use of the authentic reference standards of the metabolites to construct calibration curves for each metabolite. The isolation of metabolites in a sufficient amount for detailed analysis is time-consuming, and the low yield of purification may not allow accurate calibration. On the other hand, ^{1}H NMR spectroscopy, which can provide direct quantitative information because the integral of the proton signal is proportional to the molar concentration of the analyte, does not need a chromatographic separation step and calibration curve preparation of reference standards. Therefore, NMR-based quantitation is becoming increasingly popular as well as LC-MS based quantitation. Numerous targeted methods based on LC-MS and NMR have been reported, mainly for primary metabolites [43-47].

Multivariate statistical analysis is widely used in the metabolomic analysis to assist the extraction of valuable information from large datasets [48]. It can be further classified into unsupervised and supervised techniques. PCA is one of the most popular unsupervised techniques in the LC-MS based metabolomic profiling to analyze multivariate data and give an overview of the information hidden in the data. In contrast, supervised techniques include partial least squares, orthogonal partial least squares, and orthogonal partial least squares-discriminant analysis (OPLS-DA). For instance, OPLS-DA is designed for discrimination of more than two classes of data to increase the class separation, simplify interpretation, and find potential markers.

In the present study, LC-IT-TOF-MS analysis combined with multivariate statistical analysis for comprehensive metabolomic profiling of *S. divaricata* roots from Mongolia, HPLC-DAD analysis combined with multivariate statistical analysis for accurate determination of 9 chromones and 4 coumarins in *S. divaricata* roots from Mongolia, and

^{1}H NMR and qHNMR analyses for rapid characterization and quantification of major chromones and polar compounds were performed.

III. *Saposhnikovia divaricata* in Mongolia

Mongolia is located in the hinterland of the eastern part of central Asia and shares a border with China in the south and Russia in the north. There is a vast floral resource that conforms to its an extreme continental climate characterized by long, cold winters and short summers. Among 3160 species of vascular plants distributed in Mongolia [49], 1100 species are efficacious medicinal plants, 200 species are used for dyeing, 480 species are ornamental plants, and more than 200 species have been used as formulaic ingredients in Mongolian traditional medicine [50,51]. For example, the roots of *Glycyrrhiza uralensis* Fischer, the aerial parts of *Ephedra sinica* Stapf., and the roots of *Astragalus mongholicus* Bunge are the most commonly used medicines in Mongolia, and they were identified as the source of Glycyrrhizae Radix, Ephedra Herba, and Astragali Radix, respectively, by the assessment of the qualities of these plants which were previously conducted by our group [52-55]. In addition, *S. divaricata* is also a commonly used medicinal plant, which distributes widely in 16 regions of Mongolia including Khentei, Khangai (East, Northeast), Mongol Daurian, Great Khingan, Middle Khalkha, and East Mongolia [56]. The aerial parts of *S. divaricata* called "Derveger Jirgeruu" has been used for the treatment of stomach disorders in Mongolian traditional medicine [57]. Therefore, the utilization of Derveger Jirgeruu has not disturbed the land by maintaining permafrost. Most medicinal plants, including *S. divaricata* are harvested in the wild, and the extent of the use has led to these species' endangerment and extinction. Thus, medicinal plant conservation has become urgent and the environmental policy of Mongolia is now protecting natural reserves of the medicinal plants for the restoration against diminishing

and desertification [58]. However, in the case of *S. divaricata*, due to increased demand for SR derived from wild plants, and its decreased production in China, Mongolian *S. divaricata* has been illegally collected by local inhabitants for export to their neighboring country.

IV. Aim of the study

The annual consumption of SR in Japan is approximately 150 tons and over 95% of this product was imported from China [59]. In China, 4500 tons of SR are consumed every year and 30% of it is produced through wild collection [60]. The difference between supply and demand for SR (particularly the SR derived from wild plants) was 200 tons in 2005 then rose to 3,000 tons in 2013 [60]. In recent years, instead of Chinese SR derived from wild plants, those from Russia and Mongolia were also available in the Chinese market [61]. Therefore, the over-exploitation of natural resources of SR has become a severe issue in Northeast Asia. To increase the sources of SR, a large scale of cultivation of SR has been practiced in China. However, SR derived from cultivated plants does not often meet the requirement of CP and JP due to the lower amounts of **1** and **3** and the higher yield of dilute ethanol-soluble extract, respectively [1,2,62]. Therefore, sustainable utilization of SR resources besides maintaining the quality of SR should be implemented through high-performance cultivation by selecting suitable plant resources and cultivation areas as well as through development of methods for cultivation and systematic harvesting. Mongolia was chosen for this study because of the large population of wild growing *S. divaricata*, especially in the eastern part and because of the conservation program for the efficient usage of medicinal plants by the heed of government. Moreover, few chemical studies of Mongolian *S. divaricata* have been reported. Therefore, a field investigation was conducted in the eastern part of Mongolia for three times in 2015, 2017,

and 2019, followed by a quality evaluation of *S. divaricata* roots from several regions using various analytical methods.

The aim of this study was to evaluate *S. divaricata* roots from Mongolia for scouting new natural sources of SR, to clarify geographical variation of *S. divaricata* roots from different regions of Mongolia, and to identify suitable areas for cultivation of *S. divaricata* in Mongolia. For these purposes, a combination of qualitative and quantitative metabolomic analyses was performed.

In chapter 1, the preparation of reference compounds including a new compound used for qualitative and quantitative determinations in chapter 2 and 3 was described.

In chapter 2, metabolomic profiling based on liquid chromatography–ion-trap–time-of-flight–mass spectrometer (LC-IT-TOF-MS) method combined with multivariate statistical analysis methods (PCA and OPLS-DA) was conducted to assess chemical differences between Mongolian *S. divaricata* roots and Chinese SR and to find out characteristic compounds attributed in the geographical variation of Mongolian *S. divaricata* roots.

In chapter 3, the quantitative analysis by means of high-performance liquid chromatography–diode array detection (HPLC-DAD) method was conducted to determine the contents of 9 chromones and 4 coumarins, followed by OPLS-DA based on HPLC data to support geographical variation. In addition, ^{1}H NMR analysis was conducted to characterize metabolites such as polyacetylenes and sugars as well as chromones and coumarins. Finally, qHNMR analysis was carried out to determine the levels of sucrose and polyacetylenes, and to develop the rapid quantification method of main chromones.

The workflow of the study is illustrated in Fig. 1.

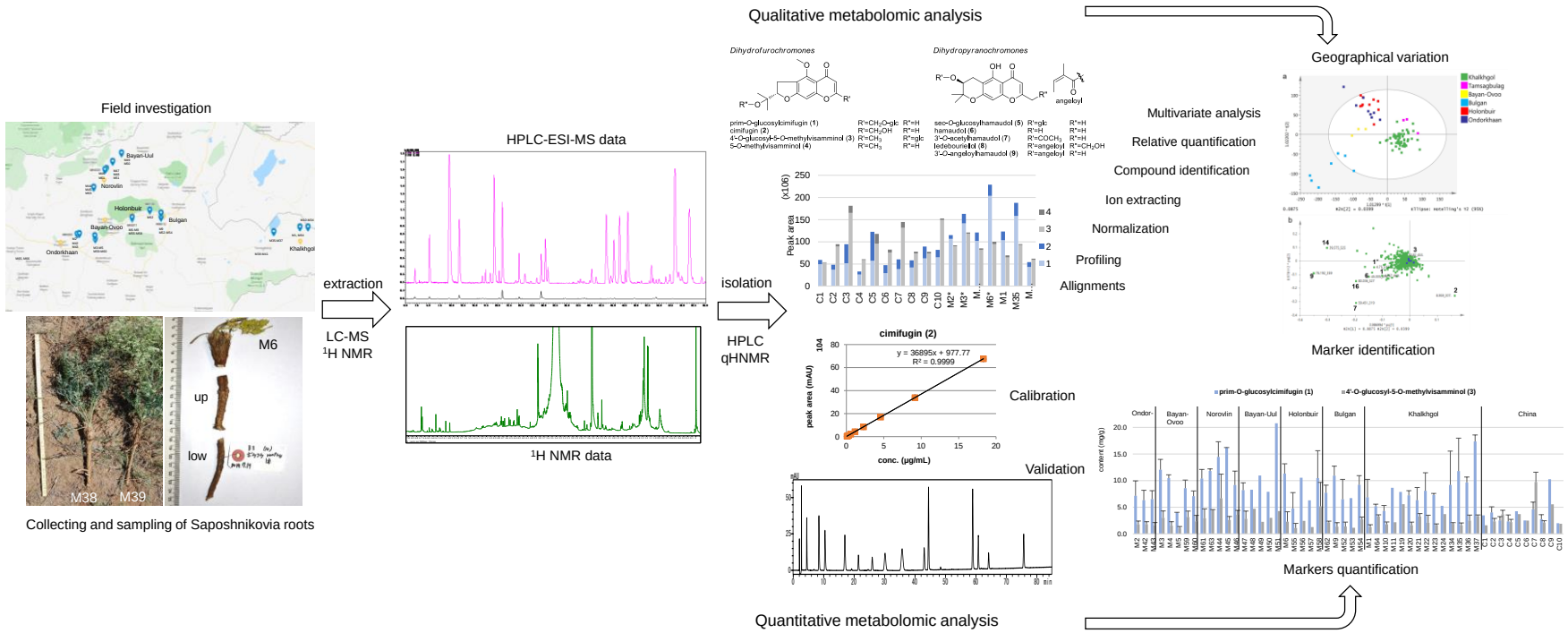

Fig. 1. The workflow of qualitative and quantitative metabolomic analysis of *Saposhnikovia divaricata* roots from Mongolia.

Chapter 1. Isolation and identification of constituents in *S. divaricata* roots

1.1 Extraction and isolation of compounds

1.1.1 Isolation of known compounds

Chopped root (SR sample C9, 1450 g) was extracted with methanol (MeOH, 3L × 3) at room temperature for 24 h. All extracts were combined and evaporated under reduced pressure to give the MeOH extract (360 g). A portion (140 g) of the MeOH extract was suspended in water and partitioned with ethyl acetate (EtOAc) and *n*-butanol (1-BuOH) to give the EtOAc layer (26.3 g), the *n*-BuOH layer (11.3 g), and the water residue (97.1 g), respectively. The LC-MS profiling of these layers revealed that the EtOAc layer contained numerous constituents, and the *n*-BuOH layer mainly contained major chromones. Therefore, the EtOAc and *n*-BuOH layers were selected for further isolation.

Firstly, the EtOAc layer (18 g) was fractionated by medium pressure liquid chromatography (MPLC) on a silica gel column (SNAP Ultra SiO_2 340 g) with UV detection at 254 and 290 nm at a flow rate of 100 mL/min; the column was eluted with *n*-hexane (Hex):EtOAc:MeOH (10:0:0 to 0:10:0, 0:0:10, *v*/*v*/*v*) to obtain 32 fractions (Fig. 1-1). Fr.5 (2.5 g), Fr.8 (0.5 g), and Fr.13 (0.4 g) contained primarily panaxynol (**15**), glycerol monolinoleate (**19**), and falcarindiol (**17**), respectively. Fr.11 (298 mg) and Fr.16 (58 mg) were recrystallized with MeOH to give the 3′-*O*-angeloylhamaudol (**9**, 10 mg) and bergapten (**12**, 10 mg), respectively. Fr.14 (177 mg) was separated by MPLC on silica gel (SNAP Ultra SiO_2 10 g, flow rate: 25 mL/min) with the solvent system Hex:EtOAc (10:0 to 0:10, *v*/*v*) to yield 14 subfractions (Fr.14-1–Fr.14-14) including 3′-*O*-acetylhamaudol (**7**) (Fr.14-4, 21 mg). Further purification of Fr.14-6 (7.7 mg) and Fr.14-

7 (5.9 mg) by preparative ODS HPLC [column: YMC ODS-A (19 × 250 mm, 5 μm); mobile phase: acetonitrile (MeCN) in H_2O containing 0.1% formic acid (20:80 to 0:100, *v*/*v*); flow rate 10 mL/min] resulted in the isolation of praeruptorin B (**16**, 4.7 mg). Similarly, Fr.15 (123 mg) was subjected to ODS MPLC (SNAP Ultra C18 12 g, flow rate: 12 mL/min) eluted with MeOH/H_2O (0:10 to 7:3, *v*/*v*) to afford psoralen (**10**, 4.6 mg) and bergapten (**12**, 0.6 mg), respectively. Phellopterin (**20**, 9.4 mg) was the main compound in Fr.15-16 and Fr.15-17. In the same way, Fr.17 (63 mg), Fr.18 (82 mg), and Fr.19 (133 mg) were subjected to ODS MPLC (SNAP Ultra C18 12 g, flow rate: 12 mL/min) eluted with MeOH/H_2O (0:10 to 10:0, *v*/*v*). Then, Fr.17 yielded xanthatoxin (**11**, 1.5 mg), bergapten (**12**, 1.8 mg), and deltoin (**13**, 18.8 mg). Fr.18 yielded xanthatoxin (**11**, 7.8 mg), isopimpinellin (**21**, 0.5 mg), and deltoin (**13**, 4.2 mg). Fr.19 yielded hamaudol (**6**, 11.6 mg), ledebouriellol (**8**, 14.8 mg), and virol C (**18**, 2.0 mg). Since Fr.32 and Fr.33 showed the same profile by LC-MS analysis, they were combined and subjected to silica gel MPLC (SNAP Ultra SiO_2 10 g, flow rate: 12 mL/min) with the elution system chloroform ($CHCl_3$)/MeOH (99:1 to 0:100, *v*/*v*) to yield 5-*O*-methylvisamminol (**4**, 16.8 mg), cimifugin (**2**, 25.9 mg), and sec-*O*-glucosylhamaudol (**5**, 12.8 mg). 4′-*O*-β-D-glucosyl-5-*O*-methylvisamminol (**3**, 0.4 mg) was purified from the combined Fr.32-5 and Fr.32-6 fractions (40 mg) by preparative TLC eluted with $CHCl_3$/MeOH (2:1, *v*/*v*), while prim-*O*-glucosylcimifugin (**1**, 0.3 mg) was purified from Fr.32-7 (23 mg).

Next, the *n*-BuOH layer (1.7 g) was subjected to ODS MPLC (MeOH/H_2O, 1:10 to 10:0, *v*/*v*) to obtain 9 fractions (Fr.B1–Fr.B9), including **1** (152.8 mg, Fr.B3), **3** (77.1 mg, Fr.B7), and **5** (50.8 mg, Fr. B9) (Fig. 1-1). Fr.B5 (190 mg) was further purified by silica gel MPLC (SNAP Ultra SiO_2 10 g, flow rate: 20 mL/min), eluting with a stepwise

gradient of $CHCl_3$/MeOH (10:0 to 1:1, *v*/*v*) to afford **1** (48 mg) and **2** (2.2 mg). Similarly, Fr.B6 (56.0 mg) was subjected to silica gel MPLC (SNAP Ultra SiO_2 10 g, flow rate: 20 mL/min) eluting with a stepwise gradient of $CHCl_3$/MeOH (10:0 to 1:1, *v*/*v*) to yield **2** (6.2 mg) and **3** (5.3 mg).

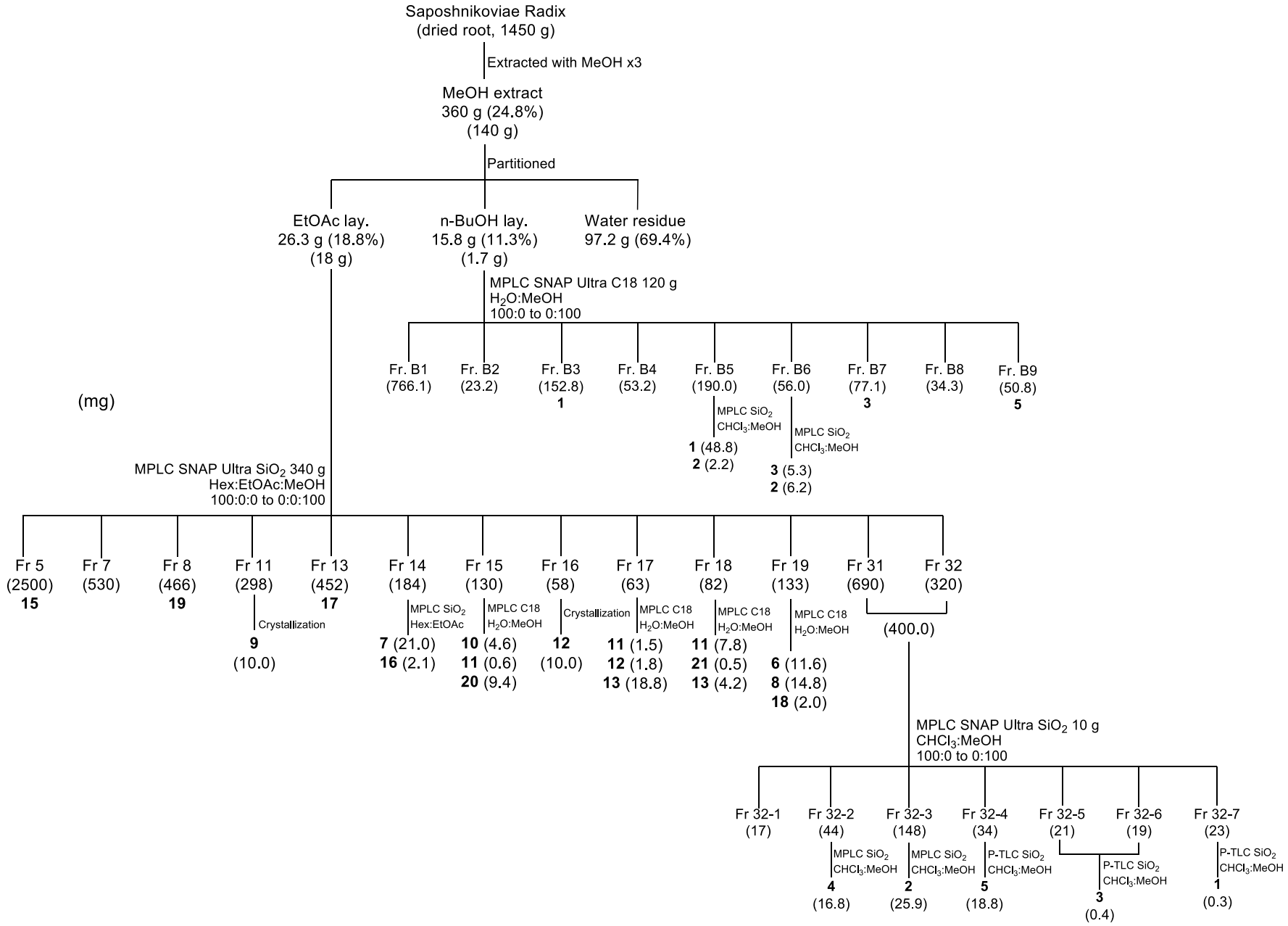

Fig. 1-1. Extraction and isolation of reference compounds from Saposhnikoviae Radix (SR).

Dihydrofurochromones

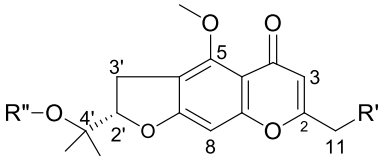

prim-*O*-glucosylcimifugin (**1**)	R'=O-glc	R"=H
cimifugin (**2**)	R'=OH	R"=H
4'-*O*-glucosyl-5-*O*-methylvisamminol (**3**)	R'=H	R"=glc
5-*O*-methylvisamminol (**4**)	R'=H	R"=H

Dihydropyranochromones

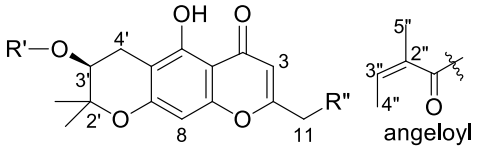

sec-*O*-glucosylhamaudol (**5**)	R'=glc	R"=H
hamaudol (**6**)	R'=H	R"=H
3'-*O*-acetylhamaudol (**7**)	R'=$COCH_3$	R"=H
ledebouriellol (**8**)	R'=angeloyl	R"=OH
3'-*O*-angeloylhamaudol (**9**)	R'=angeloyl	R"=H

Khellactone type coumarins

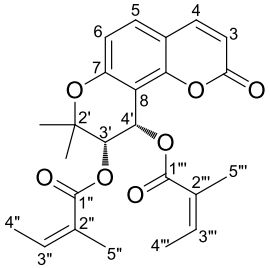

praeruptorin B (**16**)

Polyacetylenes

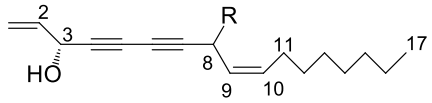

panaxynol (**15**) R=H
falcarindiol (**17**) R=OH

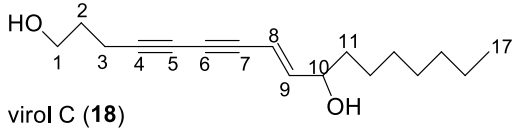

virol C (**18**)

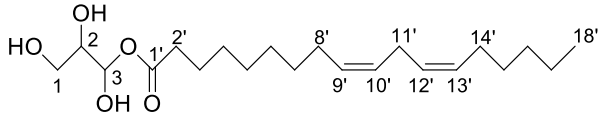

glycerol monolinoleate (**19**)

Dihydrofurocoumarins

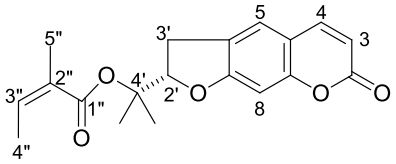

deltoin (**13**)

Furocoumarins

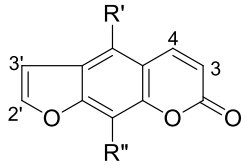

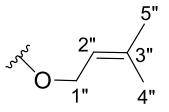

psoralen (**10**)	R'=H	R"=H
xanthatoxin (**11**)	R'=H	R"=OCH_3
bergapten (**12**)	R'=OCH_3	R"=H
isopimpinellin (**21**)	R'=OCH_3	R"=OCH_3
phellopterin (**20**)	R'=OCH_3	R"=3,3-dimethylallyoxy

Fig. 1-2. Structures of reference compounds.

1.1.2 Isolation of compound **14**

Another portion (109 g) of the MeOH extract was subjected to DAION HP-21 column (500 g) and eluted with a gradient mixture of H_2O/MeOH (100:0 to 0:100, *v*/*v*) to obtain five subfractions (Frs. 1–5, Fig. 1-3). Fr. 5 (100% MeOH eluent, 8.0 g) was dissolved in MeOH and partitioned with *n*-hexane (100 mL × 3). Then, the MeOH soluble portion (1.4 g) was fractionated by MPLC on an ODS column (SNAP Ultra C18, 120 g) with UV detection at 254 and 290 nm at a flow rate of 40 mL/min, and eluted with H_2O/MeOH (100:0 to 0:100, *v*/*v*) to obtain 55 fractions. Fr. 5.36 (6 mg) and Fr. 5.37 (12 mg) were combined and purified by preparative ODS HPLC [column: YMC ODS-A (19 × 250 mm, 5 μm); mobile phase: acetonitrile in water (MeCN/H_2O) containing 0.1% formic acid (20:80 to 0:100, *v*/*v*); flow rate 10 mL/min] to obtain **14** (3.5 mg).

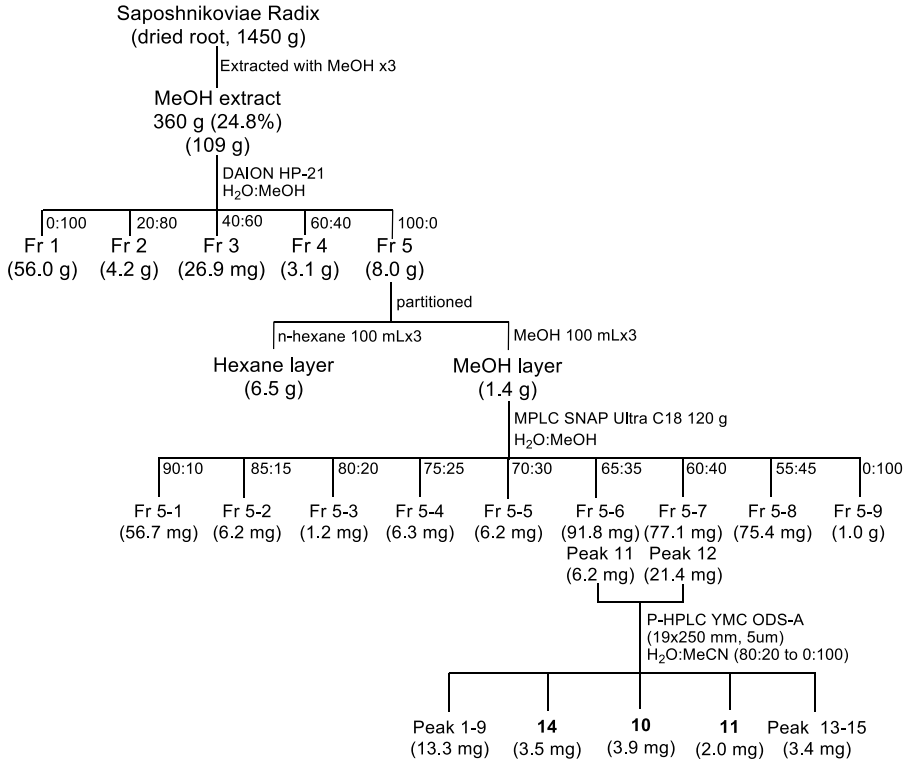

Fig. 1-3. Isolation of **14** from MeOH extract of SR sample C9.

1.2 Identification of known compounds and structure elucidation of **14**

1.2.1 Identification of known compounds

Compound **2** was obtained as colorless needles and its molecular formula was assigned as $C_{16}H_{18}O_6$ based on the $[M+H]^+$ ion peak at *m/z* 307.1185 (calcd. for $C_{16}H_{19}O_6$, 307.1176, Δ+0.9 mmu) in the HR-ESI-MS. The UV spectrum of **2** displayed absorption maximum at 213, 246, and 298 nm. The ^{1}H NMR spectrum (in DMSO-d_6) showed two sp^2 methines at δ_H 6.66 (1H, s) and δ_H 6.09 (1H, br s), an oximethine at δ_H 4.73 (1H, t, *J* = 8.5 Hz), and two singlet methyl signals at δ_H 1.17 and 1.18 (each 3H, s) (Table 1-1, Fig. 1-4). Based on these spectroscopic data, **2** was suggested to be cimifugin, and the ^{1}H NMR (in $CDCl_3$) data was identical with those of reported values [7]. Thus, **2** was identified as cimifugin .

Compound **1**, obtained as colorless amorphous solid, was shown to have the molecular formula $C_{22}H_{28}O_{11}$ on the basis of HR-ESI-MS data (*m/z* 469.1689, calcd. for $C_{22}H_{29}O_{11}$, 469.1704 $[M+H]^+$, Δ−1.5 mmu), with six more carbons, ten more hydrogens, and five more oxygens than that of **2**. The UV spectrum of **1** displayed similar absorption maxima (at 213, 248, and 300 nm) with that of **2** and the ESI-MS/MS showed a product ion peak at *m/z* 307 $[M+H– C_6H_{10}O_5]^+$ indicating that **1** might be a glucoside of **2**. In the ^{1}H NMR spectrum (in DMSO-d_6) of **1** (Fig. 1-4, Table 1-1), an absence of hydroxy group signal, downfield shifted oxymethylene signals (Δδ +0.3 ppm), and the H-3 signal (Δδ +0.24 ppm) indicated that a glucosyl moiety is linked to oxymethylene at C11. These spectroscopic data indicated **1** was prim-*O*-glucosylcimifugin. The ^{1}H NMR (in C_5D_5N) data was identical with those of reported values [7]. Thus, **1** was identified as prim-*O*-glucosylcimifugin.

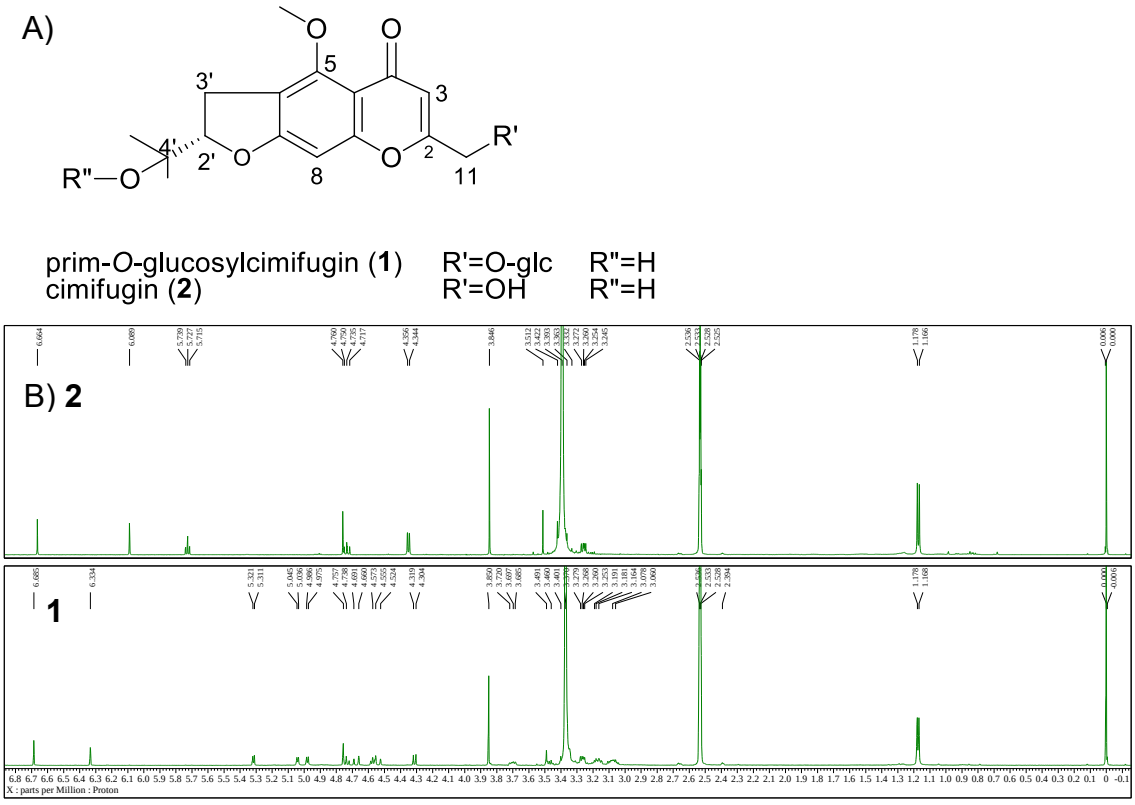

Fig. 1-4 Structures (A) and ^{1}H NMR spectrum (B) of **1** and **2**

Table 1-1. ^{1}H NMR data of **1** and **2** (500 MHz).

Position	δ_H (mult, *J* Hz)			
	prim-*O*-glucosylcimifugin (**1**) in DMSO-d_6	cimifugin (**2**) in DMSO-d_6	prim-*O*-glucosylcimifugin (**1**) in C_5D_5N	cimifugin (**2**) in $CDCl_3$
2				
3	6.33 (s)	6.09 (br s)	6.57 (s)	6.25 (br s)
5-OCH_3	3.85 (s)	3.85 (s)	4.00 (s)	3.94 (s)
8	6.69 (s)	6.66 (s)	6.74 (s)	6.51 (s)
2'	4.74 (t, 9.2)	4.73 (t, 8.5)	4.09 (t, 8.4)	4.74 (t, 9.1)
3'	3.26 (dd, 9.2, 5.4)	3.27 (dd, 9.2, 6.1)	4.24 (q, 9.2)	3.27 (d, 6.1)
gem-$(CH_3)_2$	1.17, 1.18 (s)	1.17, 1.18 (s)	1.38, 1.48 (s)	1.24, 1.37 (s)
11 a	4.54 (d, 15.3)	4.35 (d, 6.1)	4.65 (d, 14.5)	4.5 (br s)
b	4.68 (d, 15.3)		4.80 (d, 14.5)	
11-OH		5.71 (t, 6.1)		5.71 (t, 6.0)
1"	4.31 (d, 7.6)		4.98 (d, 7.6)	
2"	3.15-3.19 (2H, m)		3.32 (1H, dd, 16.1, 9.9)	
3"			3.60 (1H, dd, 16.1, 7.6)	
4"	3.04-3.11 (2H, m)		4.88 (1H, dd, 9.2, 7.6)	
5"			3.96-3.98 (1H, m)	
2", 3", 4"-OH	4.98 (d, 5.4)			
	5.04 (d, 4.6)			
	5.32 (d, 4.6)			
6" a	3.44-3.49 (m)		4.36 (1H, dd, 11.5, 6.1)	
6" b	3.68-3.72 (m)		4.56 (1H, dd, 11.5)	
6"-OH	4.57 (t, 6.1)			

Compound **4** was obtained as colorless needles and its molecular formula was determined as $C_{16}H_{18}O_5$ based on the $[M+H]^+$ ion peak at *m/z* 291.1230 (Calcd. for $C_{16}H_{19}O_5$, 291.1227, Δ+0.3 mmu) in the HR-ESI-MS, with one less oxygen than that of **2**. The UV spectrum of **4** displayed absorption maxima at 211 and 294 nm. The ^{1}H NMR spectrum (in DMSO-d_6) showed two sp^2 methines at δ_H 5.99 (1H, br s) and 6.67 (1H, s), an oxymethine at δ_H 4.73 (1H, t, J = 9.2 Hz), a methoxy at δ_H 3.84 (3H, s), an oxymethylene at δ_H 3.24 (2H, dd, J = 9.2, 4.6 Hz), and two methyl singlets at δ_H 1.17 and 1.18 (each 3H, s), suggesting similar structure with **2** (Fig. 1-5, Table 1-2). Additional downfield shifted methyl at 2.29 (3H, br s) was observed in **4** instead of OH signal that was observed at δ_H 5.71 in **2**. Based on these spectroscopic data, **4** was suggested to be 5-*O*-methylvisamminol and the ^{1}H NMR (in $CDCl_3$) data was identical with those of reported values [7]. Thus, **4** was identified as 5-*O*-methylvisamminol.

Compound **3** was obtained as colorless needles and was concluded to have the molecular formula $C_{22}H_{28}O_{10}$ (*m/z* 453.1762 $[M+H]^+$, calcd. for $C_{22}H_{29}O_{10}$, 453.1755, Δ+0.7 mmu) with one more $C_6H_{10}O_5$ unit than that of **4**, on the basis of HR-ESI-MS. The UV spectrum of **3** displayed absorption maxima at 203 and 294 nm similar with **4** and the ESI-MS/MS showed a product ion peak at *m/z* 291 $[M+H– C_6H_{10}O_5]^+$ indicating that **3** might be a glucoside of **4**. In the ^{1}H NMR spectrum (in DMSO-d_6), slightly downfiled shifted singlet methyl signals at δ_H 1.27 and 1.29 (each 3H, s) and an upfield shifted oxymethin at δ_H 4.34 (t, J = 5.4 Hz) indicated that glucosyl moiety is linked to quarterenaly carbon at C4′ of **4** (Fig. 1-5, Table 1-2). A doublet at δ_H 4.44 (1H, d, J = 7.6 Hz, H-1″) could be assigned to an anomeric proton of the β-glucopyranosyl moiety. These spectroscopic data indicated **3** was 4'-*O*-β-D-glucosyl-5-*O*-methylvisamminol. The ^{1}H NMR data (δ_H in C_5D_5N) was identical with those of reported values [7]. Thus, **3** was identified as 4'-*O*-β-D-glucosyl-

5-*O*-methylvisamminol.

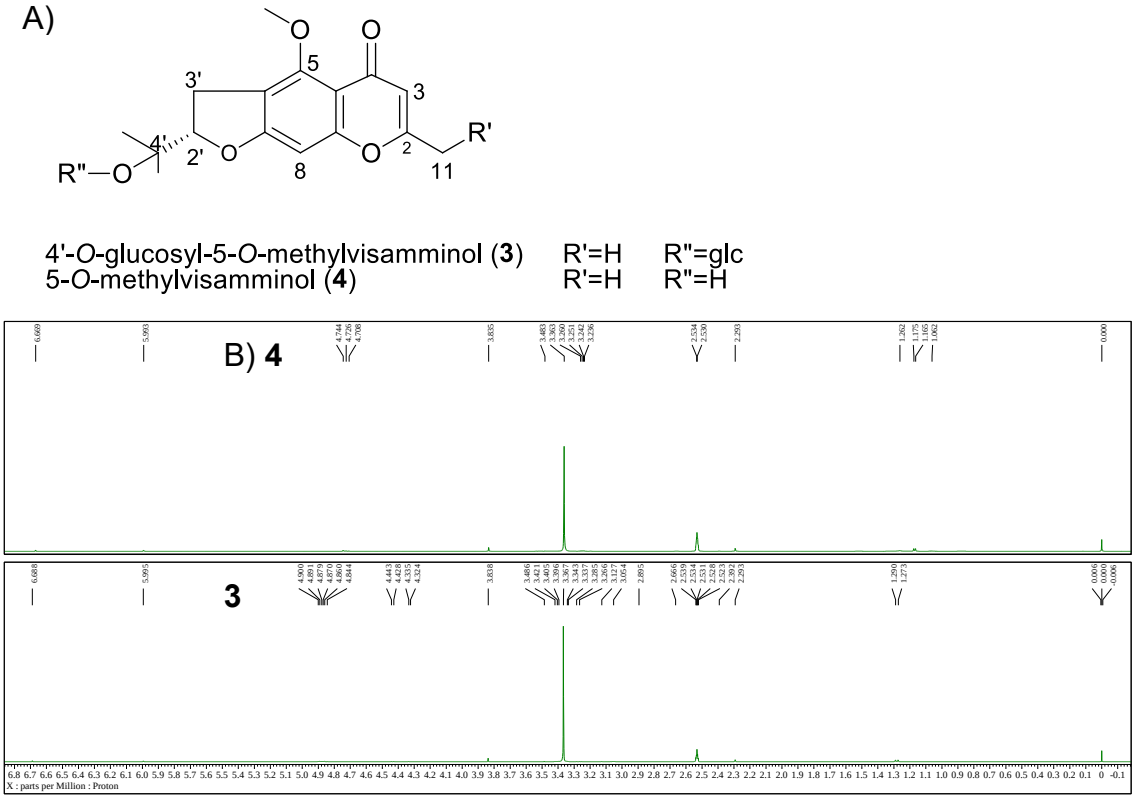

Fig. 1-5 Structures (A) and ^{1}H NMR spectrums (B) of **4** and **3**

Table 1-2. ^{1}H NMR data of **3** and **4** (500 MHz).

	δ_H (mult, *J* Hz) in DMSO-d_6		δ_H (mult, *J* Hz)	
Position	4'-*O*-glucosyl-5-*O*-methylvisamminol (**3**)	5-*O*-methylvisamminol (**4**)	4'-*O*-glucosyl-5-*O*-methylvisamminol (**3**) in C_5D_5N	5-*O*-methylvisamminol (**4**) in $CDCl_3$
2				
3	5.99 (s)	5.99 (br s)	6.08 (br s)	5.98 (br s)
5-OCH_3	3.84 (s)	3.84 (s)	3.98 (s)	3.94 (s)
8	6.69 (s)	6.67 (s)	6.58 (s)	6.53 (s)
2'	4.34 (t, 5.4)	4.73 (t, 9.2)	4.97 (t, 8.4)	4.74 (t, 8.5)
3' a	3.26 (dd, 9.2, 16.1)	3.24 (dd, 9.2, 4.6)	3.35 (dd, 16.1, 9.2)	3.22 (dd, 16.1, 8.4)
b			3.70 (dd, 16.1, 7.6)	3.28 (dd, 16.1, 9.2)
gem-$(CH_3)_2$	1.27, 1.29 (s)	1.17, 1.18 (s)	1.52, 1.53 (s)	1.24, 1.29 (s)
11	2.29 (s)	2.29 (br s)	2.01 (s)	2.27 (br s)
1"	4.44 (d, 7.6)		5.11 (d, 7.6)	
2"	3.13-3.19 (m)		3.83-3.87 (m)	
3"	3.02-3.09 (2H, m)		3.92 (t, 8.4)	
4"			4.15-4.30 (2H, m)	
5"	2.87-2.91 (m)			
2"3"4"5"-OH	4.84-4.90 (3H, m)			
6" a	3.41-3.44 (2H, m)		4.15-4.30 (2H, m)	
6" b				
6"-OH	4.33 (t, 5.4)			

Compound **6** was obtained as yellow needles and its molecular formula was assigned as $C_{15}H_{16}O_5$ based on the $[M+H]^+$ ion peak at *m/z* 277.1077 (calcd. for $C_{15}H_{17}O_5$, 277.1071, Δ+0.6 mmu) in the HR-ESI-MS. The UV spectrum of **6** displayed absorption maxima at 215, 250, 257, and 297 nm. The ^{1}H NMR spectrum (in DMSO-d_6) showed two sp^2 methines at δ_H 6.22 (1H, br s) and 6.40 (1H, s), two methylenes at δ_H 2.50 (1H, dd, J = 16.8, 6.9 Hz) and 2.81 (1H, dd, J = 16.8, 5.4 Hz), an oxymethine at δ_H 3.73 (1H, t, J = 6.1 Hz), and three singlet methyls at δ_H 1.26 and 1.32 (each 3H, s) and 2.38 (3H, br s) (Fig. 1-7, Table 1-3). A chelated hydroxy group at position C5 was observed at 13.20 (1H, br s) and another hydroxy signal was observed as doublet at δ_H 5.30 (1H, d, J = 4.6 Hz). Based on these spectroscopic data, **6** was suggested to be hamaudol, and ^{1}H NMR (in $CDCl_3$) data was identical with those of reported values [7]. Thus, it was identified as hamaudol.

Compound **5** was obtained as colorless needles, was shown to have the molecular formula $C_{21}H_{26}O_{10}$ on the basis of HR-ESI-MS data (*m/z* 439.1617, calcd. for $C_{21}H_{27}O_{10}$, 439.1599 $[M+H]^+$, Δ+1.8 mmu), with one more $C_6H_{10}O_5$ unit than that of **6**. The UV spectrum of **5** displayed absorption maxima at 210, 250, 257, and 298 nm similar with **6** and the ESI-MS/MS showed a product ion peak at *m/z* 277 $[M+H– C_6H_{10}O_5]^+$ indicating that **5** might be a glucoside of **6**. In the ^{1}H NMR spectrum (in DMSO-d_6), a downfield shifted oxymethine at δ_H 4.00 (1H, t, J = 5.8 Hz) and an absence of 3′-OH signal indicated that glucosyl moiety is linked to the C3′ of **6** (Fig. 1-6, Table 1-3). A doublet at δ_H 4.35 (1H, d, J = 7.8 Hz, H-1″) could be assigned to an anomeric proton of the β-glucopyranosyl moiety. These spectroscopic data indicated that **5** was sec-*O*-glucosyl hamaudol. This ^{1}H NMR data was identical with those of reported values [7]. Thus, **5** was identified as sec-*O*-glucosyl hamaudol.

Compound **7** was obtained as colorless needles and its molecular formula was determined as $C_{17}H_{18}O_6$ based on the $[M+H]^+$ ion peak at *m/z* 319.1190 (calcd. for $C_{17}H_{19}O_6$, 319.1176, Δ+2.4 mmu) in the HR-ESI-MS. The UV spectrum of **7** displayed absorption maxima at 221, 250, 258, and 295 nm similar with **6** and the ESI-MS/MS showed a pseudomolecular ion peak at *m/z* 319 $[M+H]^+$, and product ion peak at *m/z* 277 $[M+H–C_2H_2O]^+$ indicating a loss of acetyl moiety. The ^{1}H NMR (in DMSO-d_6) showed methyl of acetyl group at δ_H 2.04 (3H, s) and a downfield shifted oxymethine at δ_H 5.10 (1H, t, *J* = 4.5 Hz) (Fig. 1-6, Table 1-3). Based on these spectroscopic data, **7** was suggested to be 3′-*O*-acetylhamaudol. The ^{1}H NMR data (in $CDCl_3$) was identical with those of reported values [7]. Thus, **7** was identified as 3′-*O*-acetylhamaudol.

Compound **9**, obtained as colorless needles, was shown to have the molecular formula $C_{20}H_{22}O_6$ based on HR-ESI-MS data (*m/z* 359.1487, calcd. for $C_{20}H_{23}O_6$, 359.1489 $[M+H]^+$, Δ-0.2 mmu). The UV spectrum of **9** displayed similar absorption maxima at 223, 250, 257, and 295 nm with that of **6** and the ESI-MS/MS showed a product ion peak at *m/z* 277 $[M+H—C_5H_6O]^+$ indicating a loss of an angeloyl moiety. In the ^{1}H NMR spectrum (in DMSO-d_6) of **9**, an absence of hydroxy group signal and downfield shifted oxymethine signal at δ_H 5.18 (1H, t, *J* = 4.3 Hz) indicated that an angeloyl moiety is linked to the C3′ of **6** (Fig. 1-6, Table 1-3). Additional two methyls at δ_H 1.79 (3H, t, *J* = 1.5 Hz) and 1.83 (3H, dq, *J* = 7.2, 1.5 Hz) and a sp^2 methine at δ_H 6.15 (1H, dq, *J* = 7.2, 1.5 Hz) was observed. Based on these spectroscopic data, **9** was suggested to be 3′-*O*-angeloylhamaudol. The ^{1}H NMR data (in $CDCl_3$) was identical with those of reported values [7]. Thus, it was identified as 3′-*O*-angeloylhamaudol.

Compound **8** was obtained as colorless needles and its molecular formula was assigned as $C_{20}H_{22}O_7$ based on the $[M+H]^+$ ion peak at *m/z* 375.1455 (calcd. for $C_{20}H_{23}O_7$, 375.1438, Δ+1.7 mmu) in the HR-ESI-MS. The UV spectrum of **8** displayed similar absorption maxima at 221, 250, 259, and 297 nm with that of **6** and the ESI-MS/MS showed product ion peaks at *m/z* 359 $[M+H–OH]^+$ and *m/z* 277 $[M+H–OH–C_5H_7O]^+$ indicating sequantial loss of a hydroxy group and an angeloyl moiety. The ^{1}H NMR (in DMSO-d_6) showed signals due to a hydroxymethyl at δ_H 4.43 (2H, d, J = 5.5 Hz, H_2-11) and hydroxy group at δ_H 5.86 (1H, t, J = 5.5 Hz, 11-OH) instead of methyl signal (δ_H 2.33) observed in **6** (Fig. 1-6, Table 1-3). These spectroscopic data indicated that **8** was ledebouriellol. The ^{1}H NMR (in $CDCl_3$) data was identical with those of reported values [7]. Thus, **8** was identified as ledebouriellol.

A)

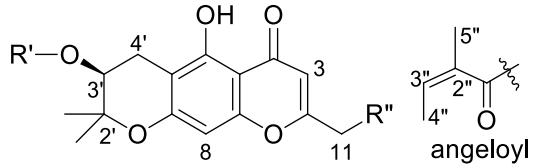

sec-*O*-glucosylhamaudol (**5**)	R'=glc	R"=H
hamaudol (**6**)	R'=H	R"=H
3'-*O*-acetylhamaudol (**7**)	R'=$COCH_3$	R"=H
ledebouriellol (**8**)	R'=angeloyl	R"=OH
3'-*O*-angeloylhamaudol (**9**)	R'=angeloyl	R"=H

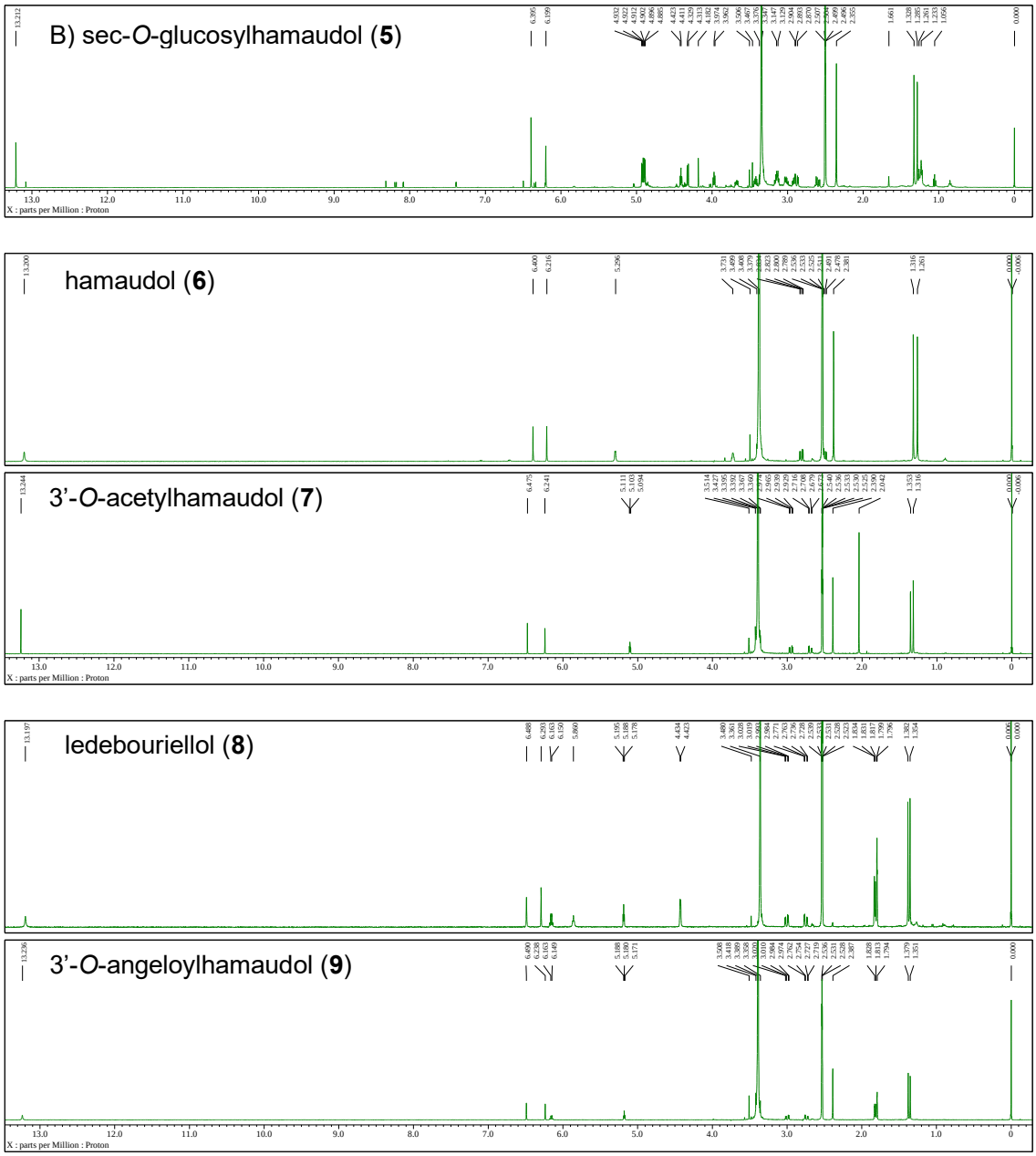

Fig. 1-6 Structures (A) and ^{1}H NMR spectrums (B) of **5**–**9** in DMSO-d_6.

Table 1-3. ^{1}H NMR data of **5**–**9** (500 MHz).

Position	δ_H in DMSO-d_6 (m, *J* Hz)					δ_H in $CDCl_3$ (m, *J* Hz)			
	sec-*O*-glucosylhamaudol (**5**)	hamaudol (**6**)	3'-*O*-acetyl hamaudol (**7**)	ledebouriellol (**8**)	3'-*O*-angeloyl hamaudol (**9**)	hamaudol (**6**)	3'-*O*-acetyl hamaudol (**7**)	ledebouriellol (**8**)	3'-*O*-angeloyl hamaudol (**9**)
2									
3	6.23 (s)	6.22 (br s)	6.24 (br s)	6.29 (s)	6.24 (br s)	5.99 (br s)	6.00 (br s)	6.30 (s)	5.99 (br s)
5-OH	13.24 (s)	13.20 (br s)	13.24 (br s)	13.19 (br s)	13.24 (br s)	13.03 (br s)	13.02 (br s)	12.91 (br s)	13.00 (br s)
8	6.42 (s)	6.40 (s)	6.47 (s)	6.49 (s)	6.49 (s)	6.33 (s)	6.34 (s)	6.34 (s)	6.33 (s)
3'	4.00 (t, 5.8)	3.73 (q, 6.1)	5.10 (t, 4.3)	5.19 (t, 4.3)	5.18 (t, 4.3)	3.88 (q, 5.5)	5.11 (t, 3.8)	5.19 (t, 5.4)	5.18 (t, 5.4)
3'-OH		5.30 (d, 4.6)							
3' OAc			2.04 (s)				2.07 (s)		
4' a	2.91 (dd, 5.3, 17.1)	2.81 (dd,16.8, 5.4)	2.95 (dd, 17.6, 4.6)	3.01 (dd, 17.6, 4.6)	3.00 (dd, 17.6, 4.6)	2.96 (dd, 17.6, 5.4)	2.99 (dd, 17.6, 3.8)	3.04 (dd, 17.6, 4.6)	3.03 (dd, 17.6, 5.4)
b	2.63 (dd, 6.5, 17.1)	2.50 (dd, 16.8, 6.9)	2.69 (dd, 17.6, 3.8)	2.75 (dd, 17.6, 3.8)	2.74 (dd, 17.6, 3.8)	2.74 (dd, 17.6, 5.4)	2.77 (dd, 17.6, 4.6)	2.81 (dd, 17.6, 5.4)	2.79 (dd, 17.6, 5.4)
gem-$(CH_3)_2$	1.31, 1.36 (s)	1.26, 1.32 (s)	1.32, 1.35 (s)	1.35, 1.38 (s)	1.35, 1.38 (s)	1.35, 1.39 (s)	1.34, 1.36 (s)	1.37, 1.38 (s)	1.37, 1.38 (s)
11				4.43 (d, 5.5)				4.55 (d, 6.1)	
11-OH				5.86 (t, 5.5)					
11-CH_3	2.38 (s)	2.38 (br s)	2.39 (br s)		2.39 (br s)	2.33 (br s)	2.34 (br s)		2.33 (br s)
Angeloyl 3"				6.15 (dq, 1.5, 7.5)	6.15 (dq, 1.5, 7.2)			6.09 (dq, 7.6, 1.2)	6.08 (dq, 7.6, 1.5)
4"				1.79 (t, 1.5)	1.79 (t, 1.5)			1.85 (t, 1.5)	1.85 (t, 1.5)
5"				1.83 (dq, 1.5, 7.5)	1.83 (dq, 1.5, 7.2)			1.91 (dq, 7.6, 1.5)	1.90 (dq, 7.6, 1.5)
Glucosyl 1"	4.35 (d, 7.8)								
2"	3.14-3.18 (2H, m)								
3"	3.02-3.07 (m)								
4"									
5"	2.93-2.97 (m)								
2"3"4"-OH	4.91-4.95 (3H, m)								
6" a	3.44-3.47 (m)								
6" b	3.69-3.72 (m)								
6"-OH	4.42 (t, 6.0)								

Compound **10** was obtained as colorless needles and its molecular formula was assigned as $C_{11}H_6O_3$ based on the $[M+H]^+$ ion peak at *m/z* 187.0394 (calcd. for $C_{11}H_6O_3$, 187.0390, Δ+0.4 mmu) in the HR-ESI-MS. In the ^1H NMR (in DMSO-d_6) spectrum, two characteristic pairs of doublets [δ_H 6.47 (1H, d, *J* = 9.5 Hz, H-3), 8.21 (1H, d, *J* = 9.5 Hz, H-4)] and [δ_H 8.15 (1H, d, *J* = 2.3 Hz, H-2′), 7.13 (1H, d, *J* = 2.3 Hz, H-3′)] and two sp^2 methines at δ_H 8.05 (1H, br s, H-8) and 7.78 (1H, s, H-5) were observed, due to furanocoumarin skeleton (Fig. 1-7, Table 1-4). Based on these spectroscopic data, **10** was suggested to be psoralen. The ^1H NMR data (in $CDCl_3$) was identical with those of reported values [63]. Thus, **10** was identified as psoralen.

Compound **11** was obtained as colorless needles and was concluded to have the molecular formula $C_{12}H_8O_4$ on the basis of HR-ESI-MS data (*m/z* 217.0525 $[M+H]^+$, calcd. for $C_{12}H_9O_4$ 217.0495, Δ+3.0 mmu), with one more carbon, two more hydrogens, and one more oxygen than that of **10**. The ^1H NMR spectra (in DMSO-d_6) of **11** was similar to that of **10** indicating that **11** has the furanocoumarin skeleton (Fig. 1-7, Table 1-4). Additional methoxy signal at δ_H 4.21 (3H, s) instead of a broad singlet of H-8 proton indicated that the methoxyl group is linked to the C8. These spectroscopic data indicated that **11** was 8-*O*-methoxypsoralen (xanthatoxin). The ^1H NMR data (in $CDCl_3$) was identical with those of reported values [63]. Hence, **11** was identified as xanthatoxin.

Compound **12** was obtained as colorless needles and its molecular formula was assigned as $C_{12}H_8O_4$ same as **11** based on the $[M+H]^+$ ion peak at *m/z* 217.0517 (Calcd. for $C_{12}H_9O_4$ 217.0495, Δ+2.2 mmu) in the HR-ESI-MS. The ^1H NMR spectrum (in DMSO-d_6) of **12** was similar with that of **10** and **11** (Fig. 1-7, Table 1-4). An absence of a singlet proton of H-5 and the presence of additional methoxy group δ_H 4.30 (3H, s) indicated that the

methoxy group is linked to the C5. Based on these spectroscopic data, **12** was suggested to be 5-*O*-methoxypsoralen (bergapten). The ^{1}H NMR data (in $CDCl_3$) was identical with those of reported values [63]. Thus, **12** was identified as bergapten.

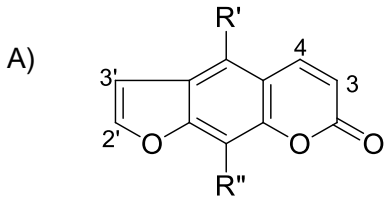

psoralen (**10**) R'=H R"=H
xanthatoxin (**11**) R'=H R"=OCH_3
bergapten (**12**) R'=OCH_3 R"=H

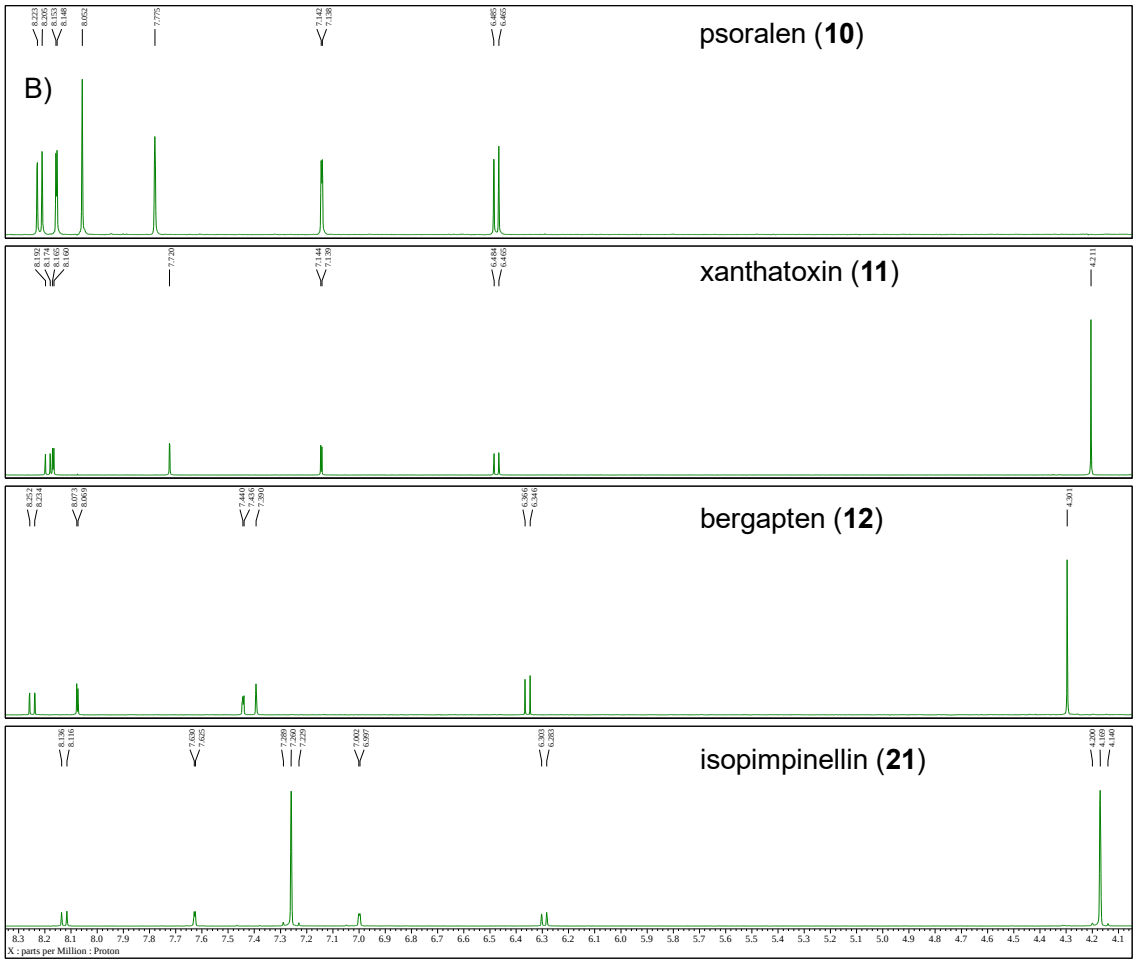

Fig. 1-7 Structures (A) and ^{1}H NMR spectrums (B) of **10**–**12** and **21** in DMSO-d_6.

Table 1-4. ^{1}H NMR data of **10**-**12** (500 MHz)

Position	δ_H (m, *J* Hz) in $CDCl_3$			δ_H (m, *J* Hz) in DMSO-d_6		
	psoralen (**10**)	xanthatoxin (**11**)	bergapten (**12**)	psoralen (**10**)	xanthatoxin (**11**)	bergapten (**12**)
2						
3	6.38 (d, 9.9)	6.38 (d, 9.5)	6.27 (d, 9.5)	6.47 (d, 9.5)	6.47 (d, 9.2)	6.36 (d, 9.5)
4	7.80 (d, 9.9)	7.77 (d, 9.5)	8.15 (d, 9.5)	8.21 (d, 9.5)	8.18 (d, 9.2)	8.24 (d, 9.5)
5	7.68 (s)	7.35 (s)		7.78 (s)	7.72 (s)	
5-OCH_3		4.30 (s)	4.27 (s)			4.30 (s)
6						
8	7.48 (br s)		7.14 (br s)	8.05 (br s)		7.39 (s)
OCH_3					4.21 (s)	
2'	7.69 (d, 2.3)	7.69 (d, 2.3)	7.59 (d, 2.3)	8.15 (d, 2.3)	8.16 (d, 2.3)	8.07 (d, 2.3)
3'	6.83 (d, 2.3)	6.82 (d, 2.3)	7.02 (d, 2.3)	7.13 (d, 2.3)	7.14 (d, 2.3)	7.44 (d, 2.3)

Compound **20** was obtained as colorless needles and its molecular formula was assigned as $C_{17}H_{16}O_5$ based on the $[M+H]^+$ ion peak at *m/z* 301.1079 (calcd. for $C_{17}H_{16}O_5$ 301.1071, Δ+0.8 mmu) in the HR-ESI-MS. The UV spectrum of **20** showed absorption maxima at 222, 268, and 313 nm. The ^{1}H NMR spectrum (in $CDCl_3$) showed two pairs of doublet at δ_H 8.12 (1H, d, *J* = 9.5 Hz, H-4), 6.28 (1H, d, *J* = 9.5 Hz, H-3), 7.62 (1H, d, *J* = 2.3 Hz, H-2′), and 6.99 (1H, d, *J* = 2.3 Hz, H-3′) indicating the presence of the furanocoumarin moiety (Fig. 1-8, Table 1-5). In addition to the furanocoumarin moiety, a methoxy at δ_H 4.17 (3H, s), two methyls at δ_H 1.74 and 1.70 (each 3H, s), a methylene at δ_H 4.85 (2H, d, *J* = 7.3 Hz), and a methine at δ_H 5.60 (1H, t, *J* = 7.3 Hz) were observed. Based on these spectroscopic data, **20** was suggested to be phellopterin. This ^{1}H NMR data was identical with those of reported values [24]. Hence, **20** was identified as phellopterin (Fig. 1-8).

Compound **21** obtained as colorless needles was shown to have the molecular formula $C_{13}H_{10}O_5$ on the basis of HR-ESI-MS data (*m/z* 247.0982, calcd. for $C_{13}H_{10}O_5$ $[M+H]^+$ 247.0901, Δ+8.1 mmu), with one more carbon, two more hydrogens, and one more oxygen than that of **12**. The ^{1}H NMR spectrum (in $CDCl_3$) was similar to those of **10**–**12** (Fig. 1-8). Additional methoxy signal at δ_H 4.17 (6H, s) and an absence of singlet protons indicated that **21** was suggested to be 5,8-*O*-dimethoxypsoralen (isopimpinellin) (Table

1-5). This ^{1}H NMR data was identical with those of reported values [63]. Thus, **21** was identified as isopimpinellin.

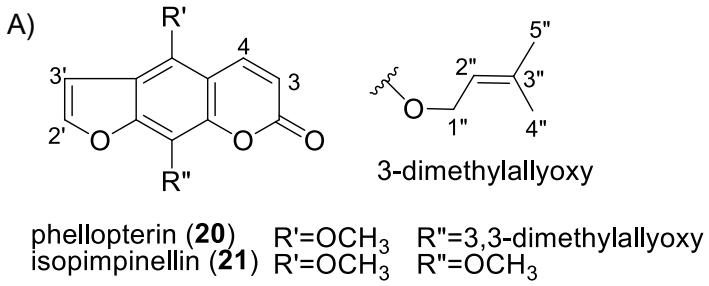

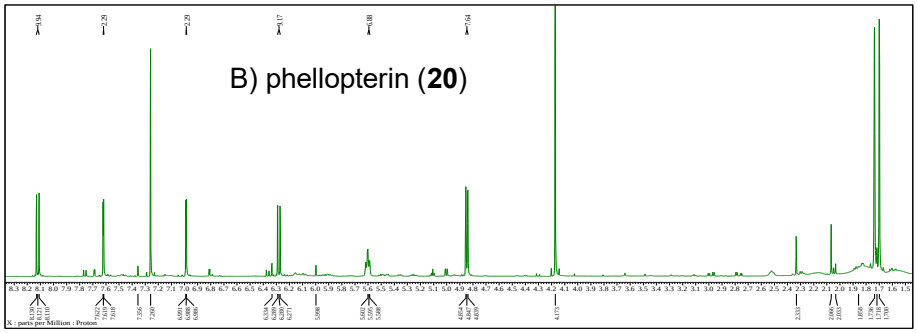

Fig. 1-8. Structures of **20** and **21** (A) and ^{1}H NMR spectrum of **20** (B)

Table 1-5. ^{1}H NMR data of **13**, **16**, **20**, and **21** (500 MHz)

Position	deltoin (**13**) in DMSO-d_6	δ_H (m, *J* Hz) in $CDCl_3$			
		deltoin (**13**)	praeruptorin B (**16**)	phellopterin (**20**)	isopimpinellin (**21**)
2					
3	6.26 (d, 9.5)	6.21 (d, 9.2)	6.22 (d, 9.2)	6.28 (d, 9.5)	6.29 (d, 9.9)
4	7.98 (d, 9.5)	7.59 (d, 9.2)	7.59 (d, 9.2)	8.12 (d, 9.5)	8.13 (d, 9.9)
5	6.89 (s)	6.74 (s)	7.35 (d, 8.4)		
5-OCH_3				4.17 (s)	4.17 (s)
6			6.81 (d, 8.4)		
8	7.54 (s)	7.21 (s)			
OCH_3					4.17 (s)
2'	5.07 (dd, 9.9, 6.9)	5.06 (dd, 9.0, 7.6)		7.62 (d, 2.3)	7.63 (d, 2.3)
3'	3.28 (dd, 16.1, 6.9)	3.26 (dd, 9.0, 6.9)	5.45 (d, 5.0)	6.99 (d, 2.3)	6.99 (d, 2.3)
4'			6.70 (d, 5.0)		
gem-$(CH_3)_2$	1.54, 1.61 (s)	1.60, 1.62 (s)	1.45, 1.49 (s)		
3,3-dimethyl allyoxy-1"				4.85 (d, 7.3)	
2"				5.60 (t, 7.3)	
4"				1.70 (s)	
5"				1.74 (s)	
angeloyl 3"	5.99 (dq, 7.3, 1.5)	5.97 (dq, 6.9, 1.5)	6.11 (dq, 7.5, 1.5)		
4"	1.58 (t-like)	1.67 (t-like)	1.98 (d, 7.5)		
5"	1.81 (dt, 7.3, 1.5)	1.89 (dt, 7.6, 1.5)	1.85 (qui, 1.5)		
3"'			6.02 (dq, 7.5, 1.5)		
4"'			1.95 (d, 7.5)		
5"'			1.82 (qui, 1.5)		

Compound **13** was obtained as colorless prism and its molecular formula was assigned as $C_{19}H_{20}O_5$ based on the $[M+H]^+$ ion peak at *m/z* 329.1400 (calcd. for $C_{19}H_{20}O_5$ 329.1384, Δ+1.6 mmu) in the HR-ESI-MS. The UV spectrum of **8** displayed absorption maxima at 204, 222, and 333 nm indicating the furanocoumarin nucleus. The ESI-MS/MS showed a product ion peaks at *m/z* 248 $[M+H–C_5H_7O]^+$ which is a loss of 82 Da, suggesting that **13** might have an angeloyl group similar with **9**. The ^{1}H NMR spectrum (in DMSO-d_6) showed downfield shifted two methyl signals at δ_H 1.58 (3H, t-like) and 1.81 (3H, dt, J = 7.3, 1.5 Hz), an upfield shifted oxymethine at δ_H 5.07 (1H, dd, J = 9.9, 6.9 Hz), and characteristic oxymethine at δ_H 3.28 (2H, dd, J = 16.1, 6.9 Hz) similar with that of **3** indicated that the angeloyl moiety is linked to quarterenaly carbon at C4′ (Table 1-5, Fig. 1-9). These spectroscopic data suggested that **13** was deltoin. The ^{1}H NMR (in $CDCl_3$) data was identical with those of reported values [7]. Thus, **13** was identified as deltoin.

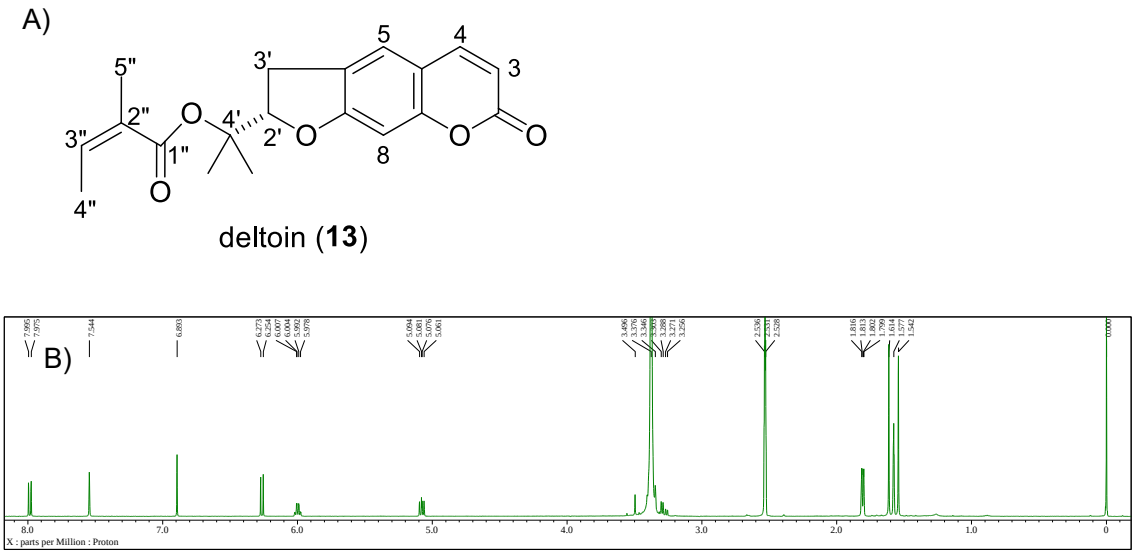

Fig. 1-9. Structure (A) and ^{1}H NMR spectrum (B) of **13**

Compound **16** was obtained as colorless needles and its molecular formula was assigned as $C_{24}H_{26}O_7$ (*m/z* 449.1572 $[M+Na]^+$, calcd. for $C_{24}H_{26}O_7Na$ 449.1571, Δ+0.1 mmu) in the HR-ESI-MS. The UV spectrum of **16** showed absorption maxima at 205 and 325 nm, indicating the coumarin nucleus. In the ^{1}H NMR spectrum (in $CDCl_3$), the pairs of doublet signals at δ_H 6.22 (1H, d, *J* = 9.2 Hz, H-3), 7.59 (1H, d, *J* = 9.2 Hz, H-4), 7.35 (1H, d, *J* = 8.4 Hz, H-5), and 6.81 (1H, d, *J* = 8.4 Hz, H-6) also supported the presence of a C-7 oxygenated coumarin moiety. The ^{1}H NMR spectrum showed two oxygenated methines at δ_H 5.45 (1H, d, *J* = 5.0 Hz, H-3′) and 6.70 (1H, d, *J* = 5.0 Hz, H-4′) with a characteristic splitting pattern and a geminal dimethyl group at δ_H 1.45 and 1.49 (each 3H, s) of dihydropyran-ring (Table 1-5, Fig. 1-10). Two methyls δ_H 1.85 (3H, qui, 1.5) and 1.82 (3H, qui, 1.5), two doublets methyls δ_H 1.95 (3H, d, *J* = 7.5 Hz) and 1.98 (3H, d, *J* = 7.5 Hz), and two doublet quartets methines δ_H 6.02 (1H, dq, *J* = 7.5, 1.5 Hz) and 6.11 (1H, dq, *J* = 7.5, 1.5 Hz) indicated that **16** might have two angeloyl groups. Based on these spectroscopic data, **16** was suggested to be praeruptorin B. This ^{1}H-NMR data was identical with those of reported values [64]. Thus, **16** was identified as praeruptorin B.

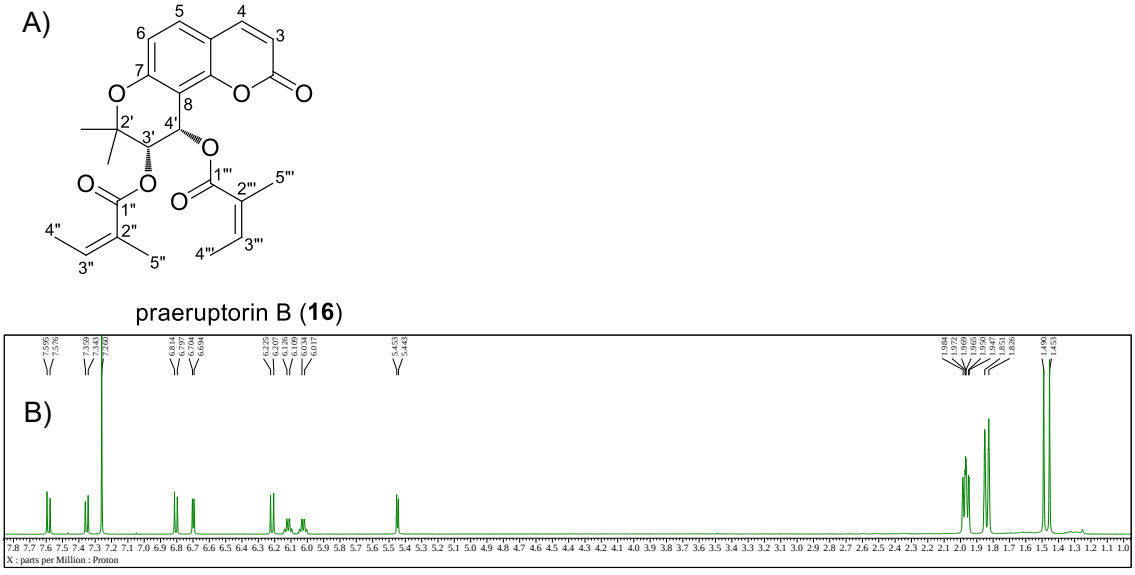

Fig. 1-10. Structure (A) and ^{1}H NMR spectrum (B) of **16**

Compound **15** was obtained as colorless oil and its molecular formula was assigned as $C_{17}H_{24}O$ (*m/z* 245.1927 $[M+H]^+$, calcd. for $C_{17}H_{25}O$ 245.1899, Δ+2.8 mmu) in the HR-ESI-MS. The UV spectrum of **15** showed absorption maxima at 229, 241, 254, 269, and 285 nm. The ^1H NMR (in $CDCl_3$) showed following signals of vinyl group at δ_H 5.24 (1H, dt, *J* = 10.4, 1.2 Hz, Ha-1), 5.46 (1H, dt, *J* = 17.1, 1.2 Hz, Hb-1), and 5.93 (1H, ddd, *J* = 17.1, 10.4, 4.9 Hz, H-2), an oxymethine proton at δ_H 4.91 (1H, d, *J* = 4.9 Hz, H-3) adjacent to the vinyl group, a methine proton at δ_H 3.03 (1H, d, *J* = 6.7 Hz, H-8) adjacent to an olefin group, cis olefin protons at δ_H 5.38 (1H, dtt, *J* = 10.7, 6.7, 1.2 Hz, H-9) and 5.51 (1H, dtt, *J* = 10.7, 7.3, 1.2 Hz, H-10), a methylene proton at δ_H 2.02 (2H, q, *J* = 7.3 Hz, H_2-11) adjacent to the olefin group, five methylene protons at δ_H 1.63 (2H, qui, *J* = 7.3 Hz, H_2-12) and 1.22-1.40 (8H, br s, H_2-13, 14, 15, 16), a terminal methyl group at δ_H 0.88 (3H, t, *J* = 7.3 Hz, H_3-17), and a hydroxy group at δ_H 2.35 (1H, t, *J* = 7.6 Hz, 3-OH) (Fig. 1-11, Table 1-6). The ^{13}C NMR spectrum showed 17 carbon signals indicating a polyacetylene compound. Based on these spectroscopic data **15** was suggested to be panaxynol. This ^1H NMR data was identical with those of reported values [65]. Thus, **15** was identified as panaxynol.

Compound **17** was obtained as colorless oil and was concluded to have the molecular formula $C_{17}H_{24}O_2$ based on the $[M+H]^+$ ion peak at *m/z* 261.2101 (calcd. for $C_{17}H_{25}O_2$ 261.1849) in the HR-ESI-MS. The UV spectrum of **17** showed absorption maxima at 220, 240, 255, 271, and 282 nm, similar with that of **15**. The ^1H NMR spectra (in $CDCl_3$) was also similar to that of **15** and an additional broad singlet at δ_H 1.61 (1H, br s) caused by a hydroxy group at C8 was observed (Fig. 1-11, Table 1-6). The ^{13}C NMR spectrum was also similar to that of **15**, showing 17 carbon signals. Based on this spectroscopic data, **17** was suggested to be falcarindiol. This ^1H NMR data was identical with those of

reported values [65]. Hence, **17** was identified as falcarindiol.

Compound **18** was obtained as colorless oil and its molecular formula was assigned as $C_{17}H_{26}O_2$ based on the $[M+H]^+$ ion peak at *m/z* 263.1996 (calcd. for $C_{17}H_{26}O_2$ 263.2006, Δ–1.0 mmu) in the HR-ESI-MS. The UV spectrum of **18** showed absorption maxima at 214, 240, 253, 267, and 283 nm close to **17** in the HPLC. The ^{1}H NMR (in $CDCl_3$) spectrum showed an oxymethine proton at δ_H 4.17 (2H, dq, *J* = 6.1, 1.2 Hz) adjacent to an olefin group, trans olefin protons at δ_H 6.27 (1H, dd, *J* = 15.9, 6.1 Hz, H-9) and 5.73 (1H, dd, *J* = 15.9, 1.2 Hz, H-8), seven methylenes at δ_H [1.46-1.56 (2H, m), 1.27 (8H, br s), 2.46 (2H, t, *J* = 6.7 Hz), 1.80 (2H, dt, *J* = 6.7, 6.1 Hz)], an oxymethylene at δ_H 3.76 (2H, t, *J* = 6.1 Hz) adjacent to the hydroxy group, and a terminal methyl at δ_H 0.88 (3H, t, *J* = 6.7 Hz) (Fig. 1-11, Table 1-6). The ^{13}C NMR spectrum was also showed 17 carbon signals. Based on these spectroscopic data, **18** was suggested to be virol C. This ^{1}H NMR data was identical with those of reported values [66]. Thus, **18** was identified as virol C and isolated from *S. divaricata* roots for the first time.

Compound **19** was obtained as colorless oil. The ^{1}H NMR (in $CDCl_3$) showed four olefinic methines at δ_H 5.30-5.41 (8H, m), methylene protons of linoleate at δ_H 2.35 (2H, t, *J* = 7.3 Hz), methylene protons between two olefinic bonds at δ_H 2.77 (4H, t, *J* = 6.1 Hz), and methyl protons at δ_H 0.89 (3H, t, *J* = 7.3 Hz) (Table 1-6). The ^{13}C NMR data indicated ester carbonyl carbon at δ_C 173.9 (C1′), glycerol group at δ_C 65.0 (C3), 68.3 (C1), and 71.8 (C2), and four olefinic carbons at δ_C 129.9 (C9′), 127.9 (C10′), 128.0 (C11′), and 130.2 (C13′). The ^{1}H NMR and ^{13}C NMR (in $CDCl_3$) spectrums of **19** were identical with those of glycerolmonolinoleate [6]. Thus, **19** was estimated to be glycerolmonolinoleate.

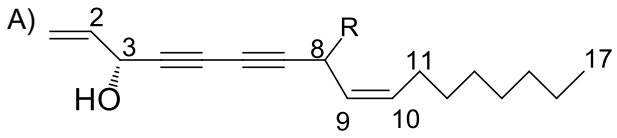

panaxynol (**15**) R=H
falcarindiol (**17**) R=OH

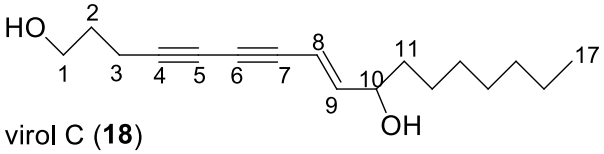

virol C (**18**)

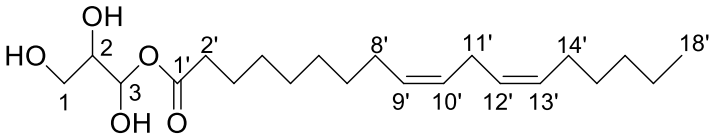

glycerol monolinoleate (**19**)

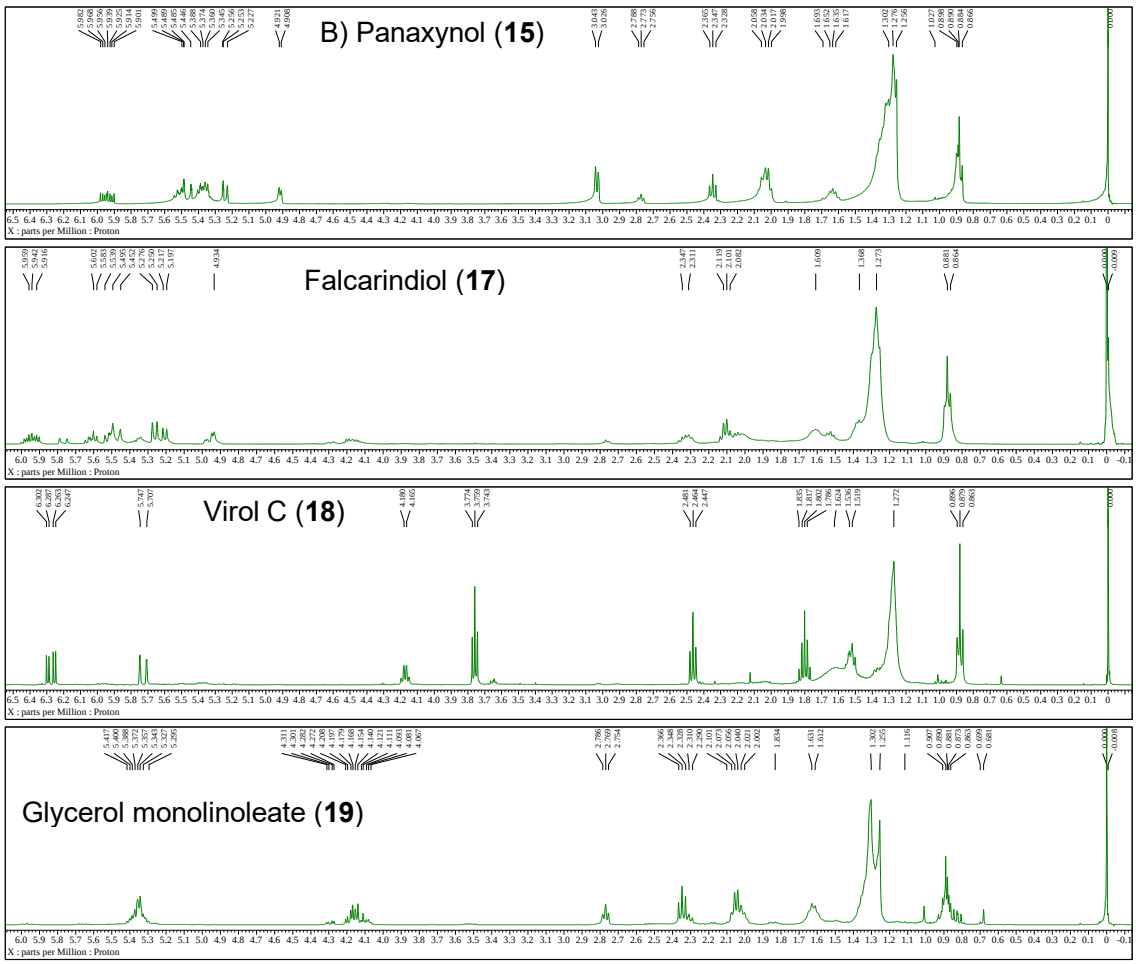

Fig. 1-11. Structures (A) and ^{1}H NMR spectrums (B) of **15**, **17**, **18**, and **19** (in $CDCl_3$)

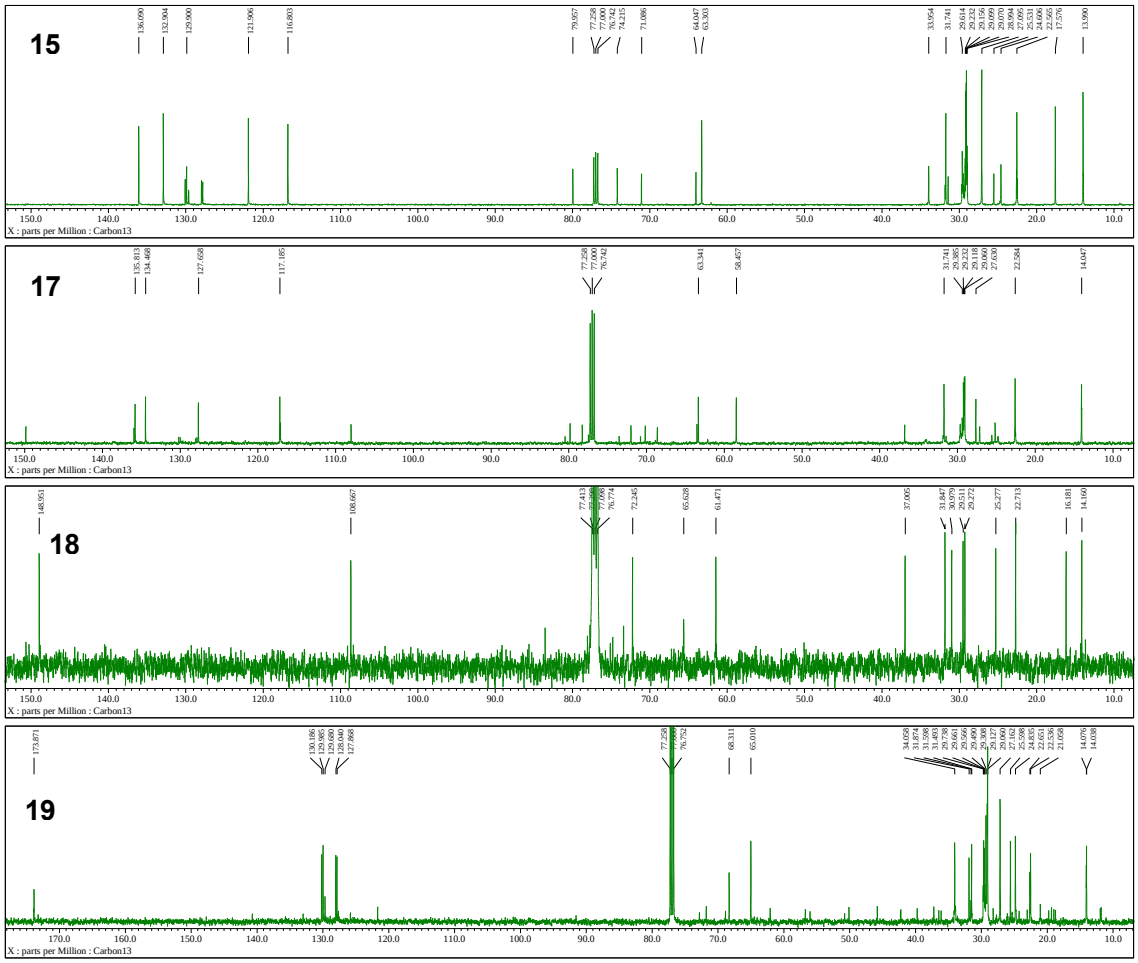

Fig. 1-12 ^{13}C NMR spectrums of **15**, **17**, **18**, and **19** (in $CDCl_3$)

Table 1-6. ^{1}H and ^{13}C NMR data of **15**, **17**, **18**, and **19** (500 MHz)

δ_H (m, *J* Hz) in $CDCl_3$

Position	panaxynol (**15**)	falcarindiol (**17**)	virol C (**18**)	glycerol monolinoleate (**19**)
1 a	5.24 (1H, dt, 10.4, 1.2)	5.26 (1H, dt, 10.4, 1.2)		4.16 (1H, dd, 11.6, 4.3)
b	5.46 (1H, dt, 17.1, 1.2)	5.47 (1H, dt, 17.1, 1.2)	3.76 (2H, t, 6.1)	4.27 (1H, dd, 11.6, 4.3)
2	5.93 (1H, ddd, 17.1, 10.4, 4.9)	5.94 (1H, ddd, 17.1, 10.4, 4.9)	1.80 (2H, dt, 6.7, 6.1)	4.06-4.11 (2H, m)
3 a	4.91 (1H, d, 4.9)	4.94 (1H, d, 4.9)	2.46 (2H, t, 6.7)	3.49-3.56 (2H, m)
b				
8	3.03 (2H, d, 6.7)	5.20 (1H, d, 7.9)	5.73 (1H, dd, 15.9, 1.2)	
9	5.38 (1H, dtt, 10.7, 6.7, 1.2)	5.51 (1H, ddt, 9.8, 3.7, 1.2)	6.27 (1H, dd, 15.9, 6.1)	
10	5.51 (1H, dtt, 10.7, 7.3, 1.2)	5.61 (1H, dtd, 11.0, 7.3, 3.7)	4.17 (1H, dq, 6.1, 1.2)	
11	2.02 (2H, q, 7.3)	2.11 (2H, q, 7.3)	1.46-1.56 (2H, m)	
12	1.63 (2H, qui, 7.3)	1.52 (2H, qui, 7.3)		
13–16	1.22-1.40 (8H, br s)	1.22-1.40 (8H, br s)	1.27 (8H, br s)	
17	0.88 (3H, t, 7.3)	0.88 (3H, t, 6.7)	0.88 (3H, t, 6.7)	
3-OH	2.35 (1H, t, 7.6)	2.32 (1H, t, 7.3)		
8-OH		1.61 (1H, br s)		
2'				2.35 (2H, t-like, 7.3)
3'				1.59-1.66 (2H, m)
8', 11'				2.77 (4H, t, 6.1)
9', 10', 12', 13'				5.30-5.41 (8H, m)
14'–17'				2.00-2.07 (8H, m)
18'				0.89 (3H, t, 7.3)

δc in $CDCl_3$

Position	panaxynol (**15**)	falcarindiol (**17**)	virol C (**18**)	Position	glycerol monolinoleate (**19**)
1	116.8	117.2	61.4	1’	173.9
2	136.1	135.8	30.9	2’	34.1
3	63.3	63.3	16.1	3’	24.8
4	79.9	79.8	83.5	4’	29.7
5	64.0	68.6	65.5	5’	29.6
6	71.0	70.2	74.7	6’	29.3
7	74.2	78.3	73.3	7’	29.1
8	17.6	58.5	108.6	8’	27.16
9	121.9	127.6	148.9	9’	129.9
10	132.9	134.5	72.2	10’	127.9
11	27.1	27.6	36.9	11’	25.6
12	29.1	29.1	29.4	12’	128.0
13	29.1	29.1	31.8	13’	130.2
14	29.2	29.2	29.2	14’	27.16
15	31.7	31.7	25.2	15’	31.9
16	22.6	22.6	22.6	16’	31.5
17	13.9	14.0	14.1	17’	22.5
18				18’	14.0
1’				1	68.3
2’				2	71.8
3’				3	65.0

1.2.2 Structure elucidation of compound **14**

Compound **14** was obtained as a yellow amorphous powder. Its molecular formula was determined to be $C_{24}H_{28}O_{13}$ based on the HR-ESI-MS at *m/z* 525.1616 $[M+H]^+$ (Calcd. for $C_{24}H_{28}O_{13}$ 525.1603, Δ+1.3 mmu). The UV spectra of **14** measured by HPLC-DAD displayed absorption maxima at 209, 229, 250, 257, and 297 nm similar to that of **5** and **6**. ESI-MS/MS analysis showed a pseudomolecular ion peak at *m/z* 525 $[M+H]^+$, and product ion peaks at *m/z* 439 $[M+H–C_3H_2O_3]^+$ and *m/z* 277 $[M+H–C_3H_2O_3–C_6H_{10}O_5]^+$, indicating the sequential loss of one malonyl and one glucosyl moieties (Fig. 1-13). The ^1H and ^{13}C NMR spectra of **14** indicated a similar structure to those of **5** except for hydroxy group at C-6″ (Fig. 1-13). The ^1H and ^{13}C NMR showed additional signals ascribed to malonyl methylene [δ_H 3.09 (s, 2H) and δ_C 45.3] and carboxyl and ester carbonyl carbon at [δ_C 169.0 (2C)] (Table 1-7, Fig. 1-14). Downfield shifted methylene at C-6″ [δ_H 4.09 (dd, *J* = 12.1, 6.8 Hz), δ_H 4.23 (dd, *J* = 12.1, 2.0 Hz), and δ_C 63.9] indicated that additional malonyl group is linked to C-6″ and this was also confirmed by HMBC correlation from H-6″and H-2‴ to C-3‴ (Fig. 1-15). Anomeric proton δ_H 4.32 (d, *J* = 7.6 Hz) with large coupling constants indicated the presence of β-glucopyranose moiety. Based on these spectroscopic data, **14** was elucidated as 3'-*O*-(6"-*O*-malonyl)-glucosylhamaudol, a new natural compound. However, as **14** was an unstable compound, the specific rotation data were not acquired, and its stereochemistry was not investigated.

A. MS spectrum of **14** B. MS/MS spectrum of **14**

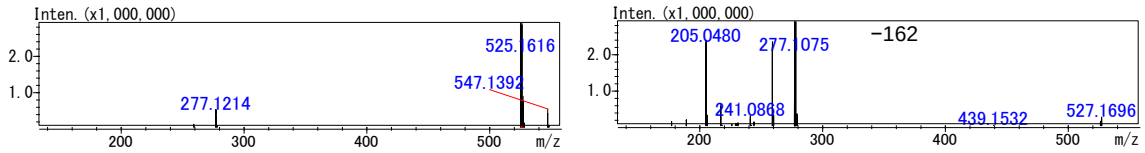

Fig. 1-13. MS (A) and MS/MS (B) spectrum of **14** in positive ionization mode.

a. ^{1}H NMR spectrums of **14** and **5**

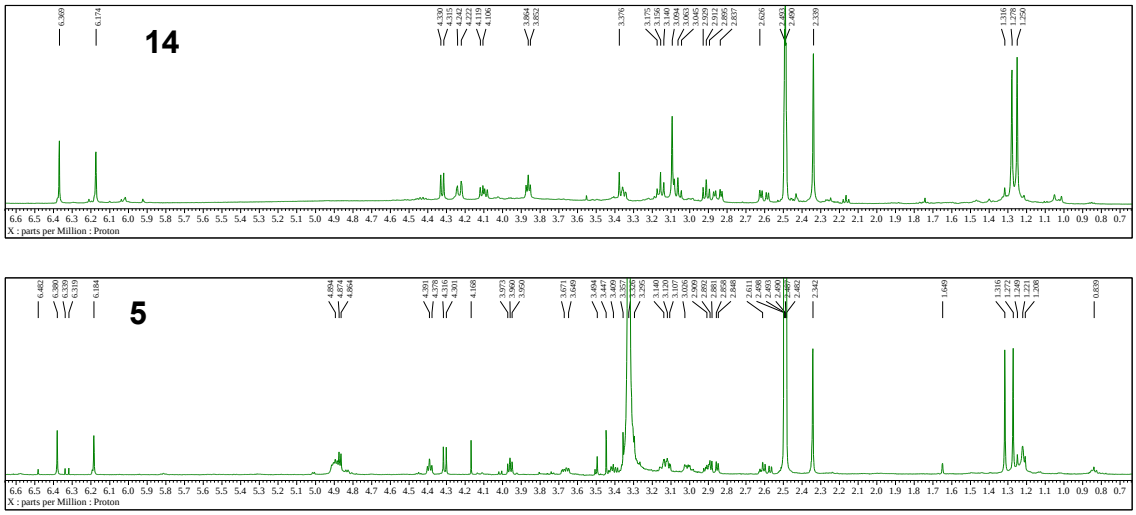

b. ^{13}C NMR spectrum of **14**

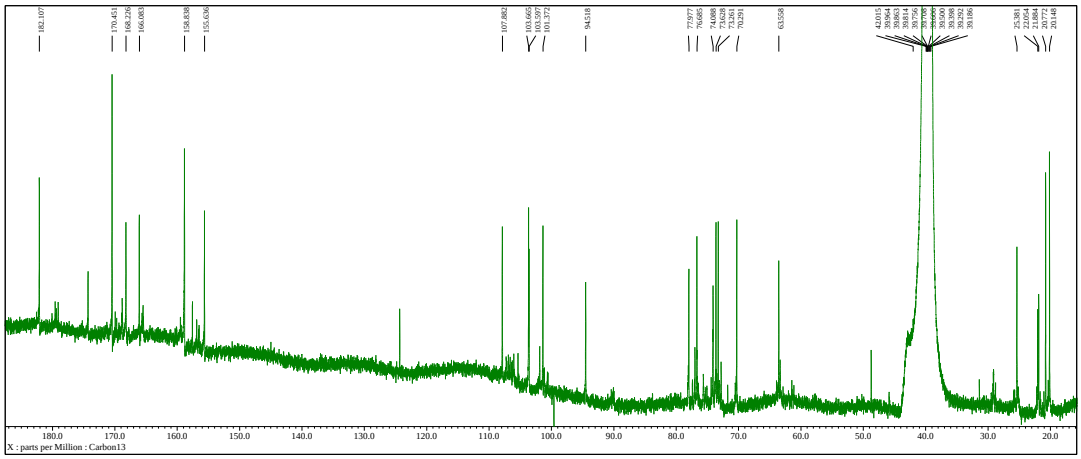

c. HMBC correlation of **14**

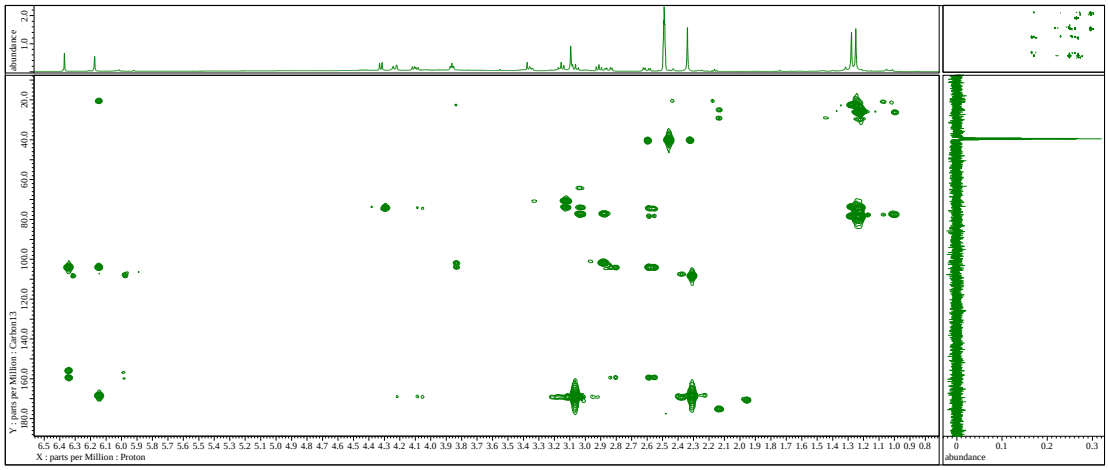

Fig. 1-14. ^{1}H (a), ^{13}C NMR (b), HMBC correlation (c) spectrums of **14** (in DMSO-d_6).

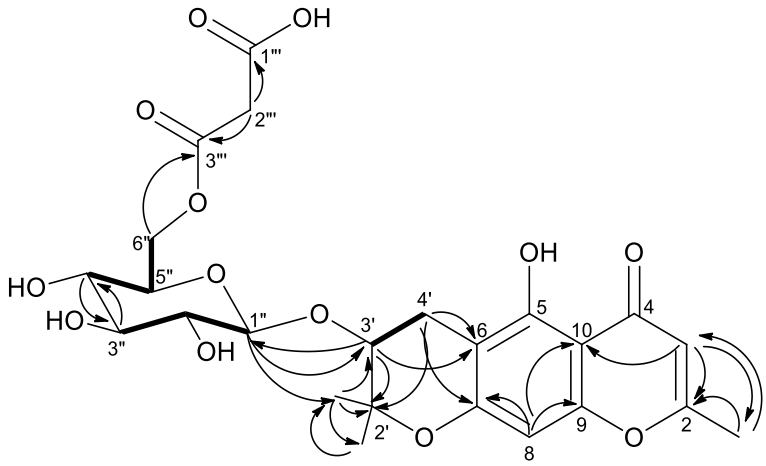

Fig. 1-15. HMBC (arrows) and COSY (bold) correlations in **14**.

Table 1-7. 1D and 2D NMR data for **14**

Position	δ_H [a] (mult, *J* Hz)			δ_C [a]			HMBC
	5	QMG [b]	**14**	**5** [c] [2]	QMG [b]	**14**	**14**
2				167.9		168.6	
3	6.19 (s)		6.17 (s)	107.7		108.3	C11, C10, C2
4				181.9		182.5	
5				158.8		166.5	
6				103.4		104.1	
7				158.7		159.2	
8	6.39 (s)		6.37 (s)	94.3		94.9	C10, C9, C7
9				155.5		156.0	
10				103.5		103.9	
5-OH	13.20 (s)						
11	2.33 (s, 3H)		2.34 (s, 3H)	20.0		20.5	C3, C2
2'						78.4	
3'	3.97 (t, 5.4)		3.87 (t, 5.4)	72.7		74.5	C-1", C6
4' a	2.61 (dd, 5.4, 17.4)		2.60 (dd, 5.4, 17.6)	21.5		22.3	C-3', C-2', C6, C7
b	2.87 (dd, 5.4, 17.4)		2.85 (dd, 5.4, 17.6)				C6, C7
2'-gem-$(CH_3)_2$	1.33 (s, 3H)		1.25 (s, 3H)	21.7		22.5	C2'-1
	1.29 (s, 3H)		1.28 (s, 3H)	25.3		25.8	C2'-2, C-3', C-4'
1"	4.31 (d, 7.8)	5.36 (d-like, 6.1)	4.32 (d, 7.6)	100.6	101.0	101.8	C-3'
2", 3", 4"-OH	4.87 (m)						
2"		3.46-3.16 (m)	3.36 (m)	73.4	73.9	73.6	
3"	3.14 (m)	3.46-3.17 (m)	3.17 (t, 9.2)	76.9	76.2	77.1	C-4", C-5"
4"	3.02 (dd, 5.4)	3.46-3.18 (m)	3.06 (t, 9.2)	70.3	69.5	70.2	C-6", C-2", C-3"
5"		3.46-3.19 (m)	2.91 (t, 8.4)	76.9	73.9	73.4	C-3", C-1"
6"-OH	4.36 (t, 6.0)						
6" a	3.67 (m)	3.99 (dd, 11.8, 5.8)	4.09 (dd, 6.8, 12.1)	61.4	63.6	63.9	C-5", C-1"'
b	3.41 (m)	4.20 (d, 11.8)	4.23 (dd, 2.0, 12.1)				C-1"'
1"'					166.7	169.0	
2"'		3.09 (s, 2H)	3.09 (s, 2H)		41.2	45.3	C-3"'
3"'					167.8	169.0	

[1]H NMR and HMBC data were acquired in DMSO-d_6 using 500 MHz NMR spectrometer.
[13]C NMR data was acquired in DMSO-d_6 using 800 MHz NMR spectrometer.
[a]: δ_H and δc of **14** were reported in ppm relative to DMSO-d_6 at δ_H 2.49 and δc 39.5, respectively.
[b]: δ_H and δc data for 6-*O*-malonyl-glucose moiety of quercetin 3-*O*-(6"-*O*-malonyl)-glucoside (QMG) [67].
[c]: δc data of sec-*O*-glucosylhamaudol [6].

1.3 Summary of chapter 1

Totally, 21 compounds including one new compound **14** were isolated from MeOH extract of SR sample C9 by means of chromatography. Twenty known compounds were identified as prim-*O*-glucosylcimifugin (**1**) [7], cimifugin (**2**) [7], 4′-*O*-β-D-glucosyl-5-*O*-methylvisamminol (**3**) [7], 5-*O*-methylvisamminol (**4**) [7], sec-*O*-glucosylhamaudol (**5**) [7], psoralen (**10**) [63], xanthatoxin (**11**) [63], bergapten (**12**) [63], hamaudol (**6**) [7], 3′-*O*-acetylhamaudol (**7**) [7], ledebouriellol (**8**) [7], deltoin (**13**) [7], 3′-*O*-angeloylhamaudol (**9**) [7], panaxynol (**15**) [65], praeruptorin B (**16**) [64], falcarindiol (**17**) [65], virol C (**18**) [66], glycerol monolinoleate (**19**) [6], phellopterin (**20**) [68], and isopimpinellin (**21**) [63] by spectroscopic analysis as well as by comparison of their MS and ^{1}H NMR data with values reported in the literatures. Structure of compound **14** was elucidated as 3'-*O*-(6"-*O*-malonyl)-glucosylhamaudol by spectroscopic analysis.

Chapter 2. Metabolomic profiling of *S. divaricata* roots from Mongolia by LC-IT-TOF-MS/MS

In this chapter, aiming to inspect comprehensive chemical profiles of *S. divaricata* roots from Mongolia, to assess chemical differences between Mongolian *S. divaricata* roots and Chinese SR and to identify characteristic compounds affecting in geographical variation, metabolomic profiling of *S. divaricata* roots from Mongolia and Chinese SR samples based on LC-IT-TOF-MS combined with multivariate statistical analysis was conducted.

2.1 Materials and methods

2.1.1 Plant materials

2.1.1.1 Field investigation in Mongolia

Sixty-six plant specimens of *S. divaricata* were collected from the eastern part of Mongolia, including Khentii and Dornod provinces (provs.) during the field investigation from 2015 to 2019 (Fig. 2-1a, Table 2-1a). Eight batches of SR samples and 2 plant specimens were obtained from China (Table 2-1b). All plant specimens were authenticated by Prof. Katsuko Komatsu (Institute of Natural Medicines, University of Toyama, Japan), and voucher specimens were deposited at the Museum of Materia Medica, Institute of Natural Medicine, University of Toyama, Japan (TMPW).

2.1.1.2 Sampling of *S. divaricata* roots

The underground parts of plant specimens varied in shape and size depending on their growing conditions. To clarify the chemical variations concerned with aspects such as

growing region, flowering or not, and root parts, all specimens as well as SR samples were divided into the following categories:

1) Flowering or non-flowering variations: 17 flowering specimens and 17 non-flowering specimens, as well as 9 specimens without aerial parts (Fig. 2-1b).

2) Root parts: as the shape and the length of roots were varied, the roots of all specimens and SR samples were cut into portions according to the following rules (Fig. 2-1c):

(i) Length of the roots < 30 cm: Upper and lower parts (sometimes middle parts) were separated in equal length.

(ii) Length of the roots > 30 cm: The parts of A, B, C, etc. (each 10 cm in length) were separated from the base.

(iii) 2 or more new roots formed on the old root: New roots of B1, B2, B3, etc. were separated from the old root.

(iv) Roots that branch at the lower part: The rootlets of R1 and R2 were separated from the upper part of the root.

3) Regional variations: 9 different locations from the eastern part of Mongolia, including 5 locations in Khentii prov. and 4 in Dornod prov. (Fig. 2-1a).

According to the above classification method, 173 individual samples were obtained from the roots of 66 Mongolian plant specimens, and 19 individual samples were obtained from 2 Chinese plant specimens and 8 batches of SR samples (3 batches composed of cut pieces were counted as 2 individual samples).

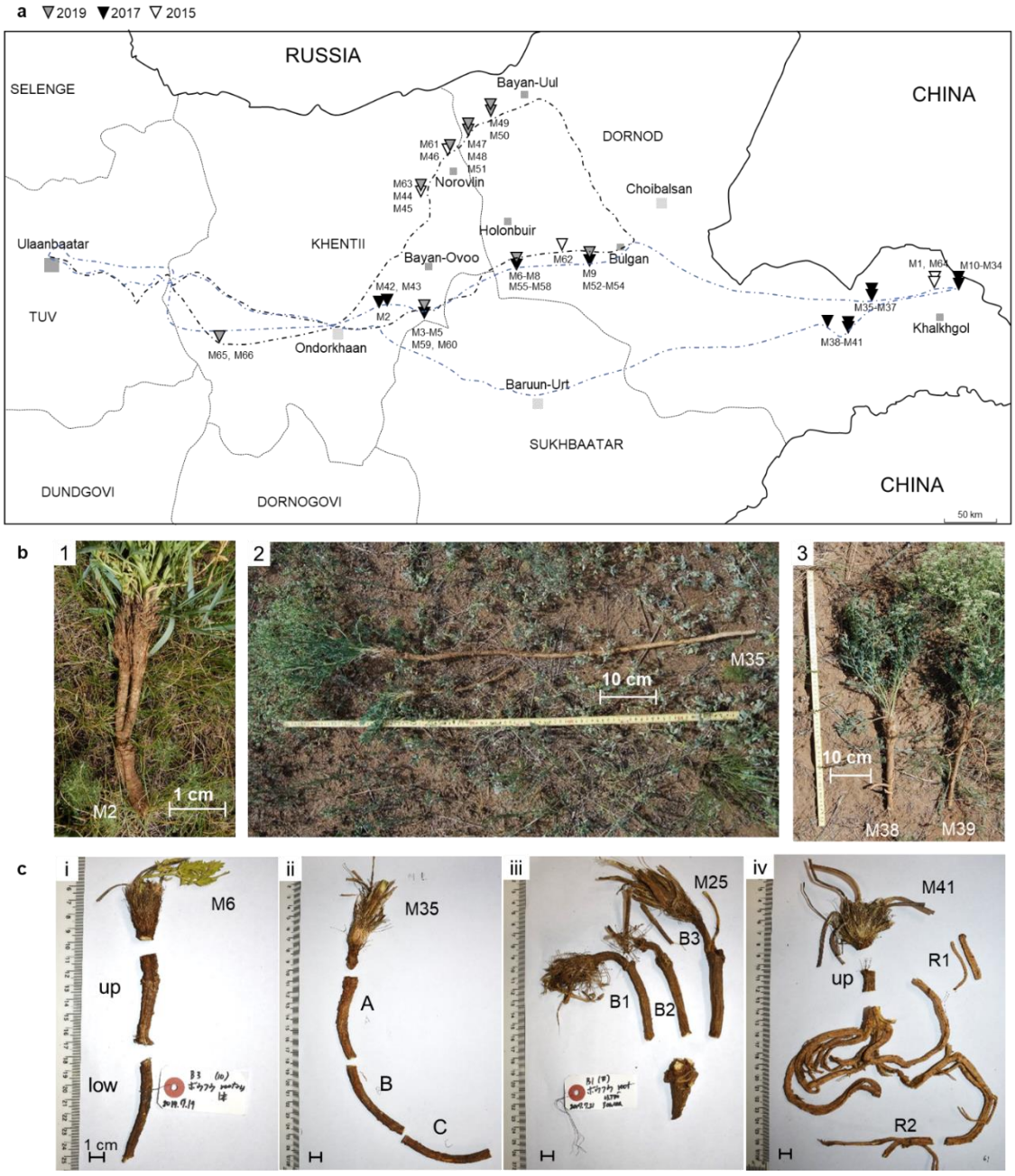

Fig. 2-1 Information on plant specimens from Mongolia. **a**. Field investigation of *Saposhnikovia divaricata* in Mongolia: the dotted line in blue and black color shows the route of the field investigation in 2017 and 2019, respectively; **b**. Shape of underground parts: (1) newly formed roots on the old root; (2) a long root 75 cm in length; (3) 2 types of root from flowering (M39) and non-flowering plants (M38); **c**. Methods for division: (i) roots not greater than 30 cm in length were divided into two halves and were labeled upper and lower parts; (ii) roots greater than 30 cm in length were divided approximately every 10 cm and were labeled A, B, C, etc. from the base; (iii) 2 or more newly formed roots on the old root were labeled B1, B2, B3, etc.; (iv) roots branched at the lower part, 2 rootlets labeled R1 and R2, and upper part of the root were selected.

Table 2-1. List of plant specimens from Mongolia (A) and SR samples and plant specimens from China (B)

A)

LC-MS [a]	HPLC [a]	qHNMR [a]	No.	Field No.[b]	Date	Latitude/ Longitude [c]	Altitude (m) [c]	Locality	Type [d]	Parts[e]	Length (cm)	Diameter (cm) [f]
			M1	JB1502	2015.09.23	-	-	Khalkhgol, Dornod prov.	F/NB	up, low	26	1
			M2	MIII005	2017.07.19	N47.28832 E111.11837	1266	Ondorkhaan, Khentii prov.	F/B	up, B1, B2	17.5	1.6
			M3	MIII008	〃	N47.37760 E111.79312	1120	Bayan-Ovoo, Khentii prov.	F/NB	up, mid, low	26	1.1
			M4	MIII009	〃	〃	1120	〃	F/NB	up, mid, low	22	0.9
			M5	MIII010	〃	〃	1120	〃	F/NB	up, low	16	1.1
			M6	MIII011	〃	N47.80784 E113.00900	1036	Holonbuir, Khentii prov.	F/NB	up, mid, low	19.5	1.5
			M7	H1	〃	N47.91732 E112.96032	-	〃	-/NB	up, low	19	1.4
			M8	H2	〃	〃	-	〃	-/NB	up, low	18	1.5
			M9	MIII012	〃	N47.83350 E113.95940	901	Bulgan, Dornod prov.	F/NB	up, mid, low	23	1.2
			M10	MII019	2017.07.20	N47.62913 E118.48016	759	Khalkhgol, Dornod prov.	NF/NB	up, mid, low	24.5	1.6
			M11	MII020	〃	〃	759	〃	F/NB	up	10	0.9
			M12	Y1	〃	-	-	〃	-/NB	up, mid, low	21	1
			M13	Y2	〃	-	-	〃	-/NB	B1, B2	18	1
			M14	Y3	〃	-	-	〃	-/NB	up, low	16	1.2
			M15	K1	〃	-	-	〃	-/NB	up, low	20	1.1
			M16	K2	〃	-	-	〃	-/NB	up, mid, low	25	1.3
			M17	K3	〃	-	-	〃	-/NB	up, low	15.8	1.7
			M18	C	〃	-	-	〃	-/NB	up, low	14	0.8
			M19	MIII022	2017.07.21	N47.62626 E118.53384	755	〃	F/NB	up, low	22	1
			M20	MIII023	〃	〃	755	〃	F/NB	up, low	19	1.3
			M21	MIII024	〃	〃	755	〃	NF/NB	up, low	24	0.9
			M22	MIII025	〃	〃	755	〃	NF/NB	up, low	24	1.6
			M23	MIII027	〃	〃	755	〃	NF/NB	up, low	20	0.9
			M24	MIII028	〃	〃	755	〃	NF/B	up, B1, B2	17	1.1
			M25	MIII031	〃	〃	755	〃	F/B	up, B1- B3	20	2.1
			M26	MIII033	〃	〃	755	〃	F/B	up, mid, low, B1-B3	20	1.1
			M27	MIII034	〃	〃	755	〃	NF/B	up, low, B1	20	1.5
			M28	MIII036	〃	〃	755	〃	NF/B	up, mid, low, B1-B3	18	1.2
			M29	MIII037	〃	〃	755	〃	NF/B	up, mid, low, B1	30	1
			M30	MIII039	〃	〃	755	〃	F/B	up, B1- B6	19	1.6
			M31	MIII042	〃	N47.59197 E118.42325	734	〃	NF/B	up, B1-B3	18	2.8
			M32	MIII043	〃	N47.62626 E118.53384	755	〃	F/NB	up, low	25	1
			M33	MIII044	〃	〃	755	〃	NF/B	up, B1-B3	21	1.6
			M34	MIII046	〃	〃	755	〃	NF/B	up, low	19	0.7
			M35	MIII049	2017.07.22	N47.52941 E117.67292	653	〃	F/NB	A-I	75	1.2
			M36	MIII050	〃	〃	653	〃	NF/B	up, low	21	0.8
			M37	MIII051	〃	〃	653	〃	NF/B	up, B1, B2	23	0.7
			M38	MIII053	〃	N47.28708 E117.27450	651	Tamsagbulag, Dornod prov.	NF/NB	up, low	25	1.4
			M39	MIII054	〃	〃	651	〃	F/B	up, mid, low, B1-B2	28	1.7
			M40	MIII055	〃	〃	651	〃	NF/NB	up, low, B1	22	0.9
			M41	MIII061	〃	N47.32263 E117.00775	670	〃	NF/R	up, R1, R2	15	0.7
			M42	MIII071	2017.07.23	N47.29372 E111.15959	1200	Ondorkhaan, Khentii prov.	F/NB	A-D	40.5	1.2
			M43	MIII072	〃	〃	1200	〃	NF/B	up, low	18	0.9

LC-MS [a]	HPLC [a]	qHNMR [a]	No.	Field No.[b]	Date	Latitude/ Longitude [c]	Altitude (m) [c]	Locality	Type [d]	Parts [e]	Length (cm)	Diameter [f] (cm)
			M44	MIV017	2019.07.22	N48 27.001 E111 44.363	1239	Norovlin, Khentii prov.	F	up, low	24	10
			M45	MIV019	〃	〃	〃	〃	F	up, low	28	12
			M46	MIV025	2019.07.23	N48 48.668 E112 06.593	1108	〃	F	up, low	21	12
			M47	MIV030	2019.07.23	N48 58.707 E112 22.020	1037	Bayan-Uul, Dornod prov.	F	up, low	23	13.5
			M48	MIV033	〃	〃	〃	〃	F	up	16	8
			M49	MIV039	〃	N49 08.980 E112 39.457	1029	〃	F	up	14	9.5
			M50	MIV041	〃	〃	〃	〃	F	up	15	8
			M51	MIV049	〃	〃	〃	〃	F	up	16	8
			M52	MIV098	2019.07.24	N47 55.157 E113 57.641	923	Bulgan, Dornod prov.	F	up, low	20	10
			M53	MIV099	〃	〃	〃	〃	F	up	13	13
			M54	MIV102	〃	〃	〃	〃	F	up, low	22	13
			M55	MIV105	2019.07.24	N47 49.738 E113 00.313	1002	Holonbuir, Dornod prov.	F	up, low	18	13.5
			M56	MIV106	〃	〃	〃	〃	F	up	16	12
			M57	MIV109	〃	〃	〃	〃	F	up	17	10
			M58	MIV110	〃	〃	〃	〃	F	up, mid, low	36	18
			M59	MIV112	2019.07.24	N47 26.868 E111 46.660	1088	Bayan-Ovoo, Khentii prov.	F	up, low	30	13
			M60	MIV114	〃	〃	〃	〃	F	up, mid, low	30	10
			M61	MII060	2015.07.22	N48 50.404 E112 09.538	1003	Norovlin, Khentii prov.	F	up, low	12	12
			M62	MII100	2015.07.25	N47 58.938 E113 35.467	830	Bulgan, Dornod prov.	F	up, mid, low	29.5	12
			M63	JB1501	2015.09.21	N48 26.922 E111 44.388	1155	Norovlin, Khentii prov.	F	up, low	11	9
			M64	JB1506	2015.09.26	-	-	Khalkhgol, Dornod prov.	F	up, low	17	12
			M65	MIV136	2019.07.25	N47 08.990 E108 42.293	1305	Kherlem Bayan-Ulaan field,	-	up, low	19	12
			M66	MIV137	〃	〃	〃	Khentii prov.	-	up, low	14	7.5

B)

LC-MS [a]	HPLC [a]	qHNMR [a]	No.	Type [g]	TMPW No.	Date	Production area [h]	Market	Part	Length [i] (cm)	Diameter [i, f] (cm)
			C1	W	Cn076	2012.07.20	Inner Mongolia Autonomous Region	Inner Mongolia Autonomous Region	up	13	1.5
			C2	W	Cn262	2012.08.04	〃	〃	up, mid, low	28.5	1.2
			C3	-	21596	2002.09.17	-	Anguo, Hebei Prov.	up, low	20	1
			C4	C	21601	〃	-	〃	up, mid, low	28	1
			C5	W	21602	〃	-	〃	up, low	20	1.1
			C6	-	24482	2005.10.25	-	Shenyang, Liaoning Prov.	piece	-	-
			C7	W	27840	2012.07.19	Dorbod Mongol Autonomous County, Heilongjiang Prov.	Dorbod Mongol Autonomous County, Heilongjiang Prov.	up, mid, low	34	1
			C8	W	27846	2012.07.20	Inner Mongolia Autonomous Region	Arun Banner, Inner Mongolia Autonomous Region	up, low	25	1.6
			C9	W	28814	〃	〃	Osaka, Japan	piece	-	-
			C10	C	28813	2016.10.18	Hebei Prov.	〃	〃	-	-

[a] Specimens and SR samples used each method are shown in grey;
[b] Specimens without aerial part were obtained from local government (H, C) or collector (Y, K);
[c] Latitude/longitude and altitude are not clear (-);
[d] Specimens are in flowering (F) or non-flowering (NF);
[e] Flowering specimens (F) or non-flowering specimens (F); roots were branched at the lower part (R); 2 or more newly occurred root was observed (B) or not observed (NB) on the old root;
[f] Diameter was measured at the thickest position of the root;
[g] SR sample derived from cultivated (C) or wild (W) plant; other samples had no information (−);
[h] Production area was not clear (-);
[i] Length and diameter were not clear (-);

2.1.2 Sample preparation for LC-IT-TOF-MS analysis

Plant specimens and SR samples were pulverized into fine powders of about 70 mesh. For the preliminary analysis that is comparing 8 Chinese SR samples and 2 plant specimens and 7 Mongolian plant specimens, 10 mg of each sample was extracted with 2 mL of MeOH in an ultrasonic bath at room temperature for 30 min, and then centrifuged at 3000×g for 2 min. The supernatant solution was diluted with ultrapure water to 1:1 (*v*/*v*), and the resultant solution was filtered through a 0.2 μm membrane filter prior to use. Sample solutions were analyzed with gradient elution system I [0–4 min at 20% solvent B (MeCN containing 0.1% FA), 4–69 min at 20–80% B, and 69–70 min at 80–100% B].

For comparing all 43 plant specimens from Mongolia by a validated method, 100 mg of pulverized sample was extracted with 20 mL of 70% MeOH in an ultrasonic bath at room temperature for 30 min, and then centrifuged at 2580×g for 5 min. The supernatant solution was diluted with ultrapure water to 1:1 (*v*/*v*), and the resultant solution was filtered through a 0.2 μm membrane filter prior to use. Sample solutions were analyzed with gradient elution system II [0–5 min at 20% B, 5–15 min at 20–25% B, 15–30 min at 25% B, 30–40 min at 25–40% B, 40–90 min at 40–80% B, and 90–91 min at 80–100% B].

2.1.3 Method validation for LC-IT-TOF-MS analysis

The LC-MS method was validated for the repeatability, stability, and reproducibility obtained with the gradient elution system II. The intra- and inter-day precisions were evaluated by triplicate injections of representative sample solutions of SR sample (C9) and upper and lower parts of plant specimen (M1) within a day and on 3 consecutive days. Variations were expressed by the relative standard deviation (RSD) of the peak area for

each analyte.

2.1.4 Statistical analysis

The profiling solution (Shimadzu, Kyoto, Japan) was used to convert all raw data (t_R 3–60 min for gradient system I or t_R 3–85 min for gradient system II) from LC-MS analysis into the data matrix for subsequent import to Microsoft Excel. Then, the data matrix was imported to SIMCA 14.0 (Umetrics, Umea, Sweden) for mean centering and Pareto scaling before multivariate analysis.

All data were expressed as mean and standard deviation (SD). The differences between 2 independent groups were analyzed by the Students *t*-test and *p* value of $p<0.05$ was regarded as statistically significant.

2.2 Results

2.2.1 Optimization of extraction and chromatographic condition

Three parameters were considered based on the previous study [69]: extraction solvent, extraction duration, and the amount of solvent in the sample preparation procedure. MeOH and 70% MeOH were tested as the extraction solvents, sonication with 30 min or 60 min was investigated as extraction methods, and 20 vs. 25 mL solvents were tested. The results indicated that sonication with 70% MeOH allowed for better extraction than was achieved with others. Extraction duration and solvents amount did not exhibit significant differences between 30 or 60 min and 20 vs. 25 mL, respectively. Finally, sonication with 25 mL of 70% MeOH at room temperature for 30 min was selected as the conditions used to prepare the sample solution for LC-MS analysis.

Three analytical parameters were optimized to achieve good peak resolutions and desirable separations: gradient system, mobile phase modifier, and column oven

temperature. Initially, the gradient system was optimized from the simple gradient elution method I to establish the combined isocratic and gradient method II. Peak of P11 was overlapped with a minor peak during linear gradient elution from 20–80% of solvent B; these overlapping peaks could be effectively separated by insertion of the isocratic 25% B step at 15–30 min in gradient system II, at the cost of an extra 27 min analysis. Next, the mobile phase modifiers formic acid vs. acetic acid were considered: 0.1% formic acid was selected because it enhanced the intensity of adducted molecular ions $[M+HCOO]^-$ and protonated molecular ions $[M+H]^+$ in the MS. The column temperature was also optimized to achieve a better resolution: 4 oven temperature, 25°C, 30°C, 35°C, and 40°C. Increased column temperatures up to 40°C decreased analysis time and two peaks (**5** and **14**) were overlapped with other minor peaks. When the column temperature was controlled at 30°C, a good resolution of these peaks was obtained (Fig. 2-2).

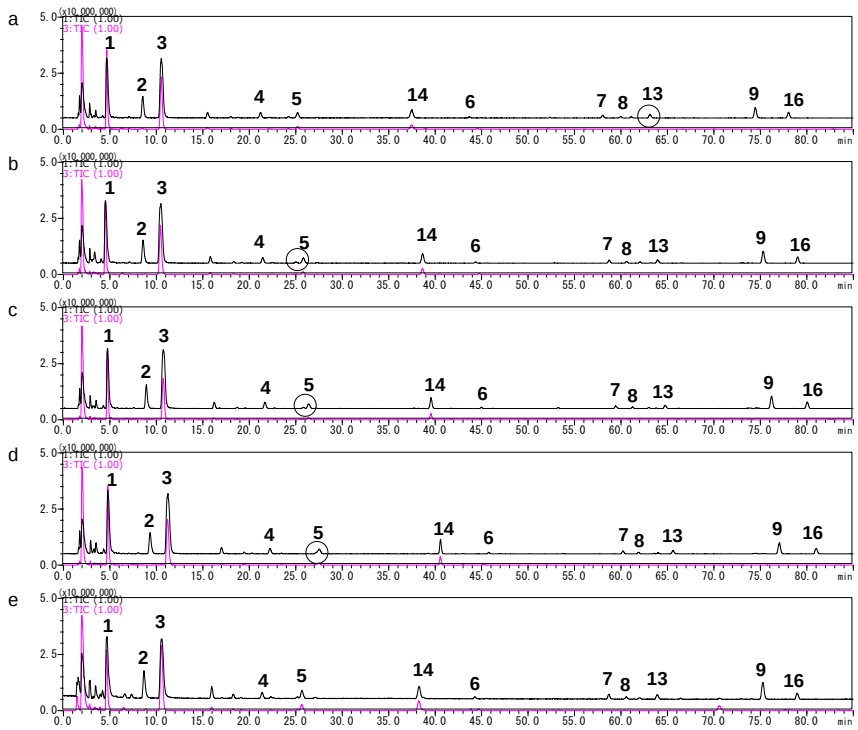

Fig. 2-2 Total ion chromatography (TIC) of the 70% MeOH extract of SR sample C9 at different column temperatures in positive (upper) and negative (lower) ionization modes:

at 40℃ (a), 35℃ (b), 30℃ (c), and 25℃ (d) with mobile phase modifier 0.1% formic acid; at 35℃ with mobile phase modifier 0.1 % acetic acid (e) with gradient elution system II. Numerals indicate respective compounds in Fig. 2-5.

2.2.2 Method validation for LC-IT-TOF-MS analysis

The repeatability, stability, and reproducibility of the chromatographic method were determined in intra- and inter-day (n=3) precisions. As summarized in Table 2-2, the RSD values for intra- and inter-day analyses were 0.4–6.8% and 0.7–8.6%, respectively. This result indicated that the precision was sufficient to proceed with multivariate statistical analysis.

Table 2-2. Intra-day and inter-day precisions for LC-IT-TOF-MS analysis

Compounds	intra-day precision* (RSD, %)			inter-day precision* (RSD, %)		
	Sample**			Sample**		
	C9 (wild)	M1 (upper part)	M1 (lower parts)	C9 (wild)	M1 (upper part)	M1 (lower part)
1	1.5	2.2	1.3	1.7	2.2	3.5
2	0.8	4.6	1.3	4.4	6.8	8.6
3	1.3	1.5	0.4	2.8	3.4	2.9
4	1.7	2.7	4.9	3.9	2.6	3.4
5	1.0	4.2	2.8	8.2	8.2	5.4
9	2.2	6.8	2.4	0.7	0.7	2.8

*: Intra- and inter-day precisions were determined as RSD value (%) of peak area in triplicate injection within a day or 3 consecutive days.
**: C9: SR sample from China; M1: Mongolian specimen.

2.2.3 Characterization of metabolites by LC-IT-TOF-MS

For LC-MS profiling, Chinese SR sample C9 obtained from Tochimoto Tenkaido (Osaka, Japan) was used to identify metabolites. Chopped roots (1450 g) were extracted 3 times with MeOH at room temperature for 24 h to yield 360 g of MeOH extract. Then, a portion of MeOH extract (140 g) was suspended in water and subsequently partitioned with EtOAc and *n*-BuOH to give the EtOAc layer, *n*-BuOH layer, and water residue with yields of 26.3, 11.3, and 97.1 g, respectively. The EtOAc layer contained more abundantly and numerous constituents than the other fractions, whereas the *n*-BuOH layer mainly contained the major chromones (Fig. 2-3). From the EtOAc layers, 30 compounds,

including 13 chromones and 17 coumarins, were characterized and tentatively identified by comparing precursor ion values, product ion values, and UV spectra with related literature findings [9,30,70] (Fig. 2-4, Table 2-3). Their chemical structures are shown in Fig. 2-5. Among them, 17 compounds were unambiguously identified as prim-*O*-glucosylcimifugin (**1**), cimifugin (**2**), 4′-*O*-β-D-glucosyl-5-*O*-methylvisamminol (**3**), 5-*O*-methylvisamminol (**4**), sec-*O*-glucosylhamaudol (**5**), psoralen (**10**), xanthatoxin (**11**), bergapten (**12**), hamaudol (**6**), 3′-*O*-acetylhamaudol (**7**), ledebouriellol (**8**), deltoin (**13**), 3'-*O*-(6"-*O*-malonyl)-glucosylhamaudol (**14**), 3′-*O*-angeloylhamaudol (**9**), isopimpinellin (**21**), praeruptorin B (**16**), and phellopterin (**20**) by comparing LC-MS/MS and UV data of reference standard compounds (see Chapter 1).

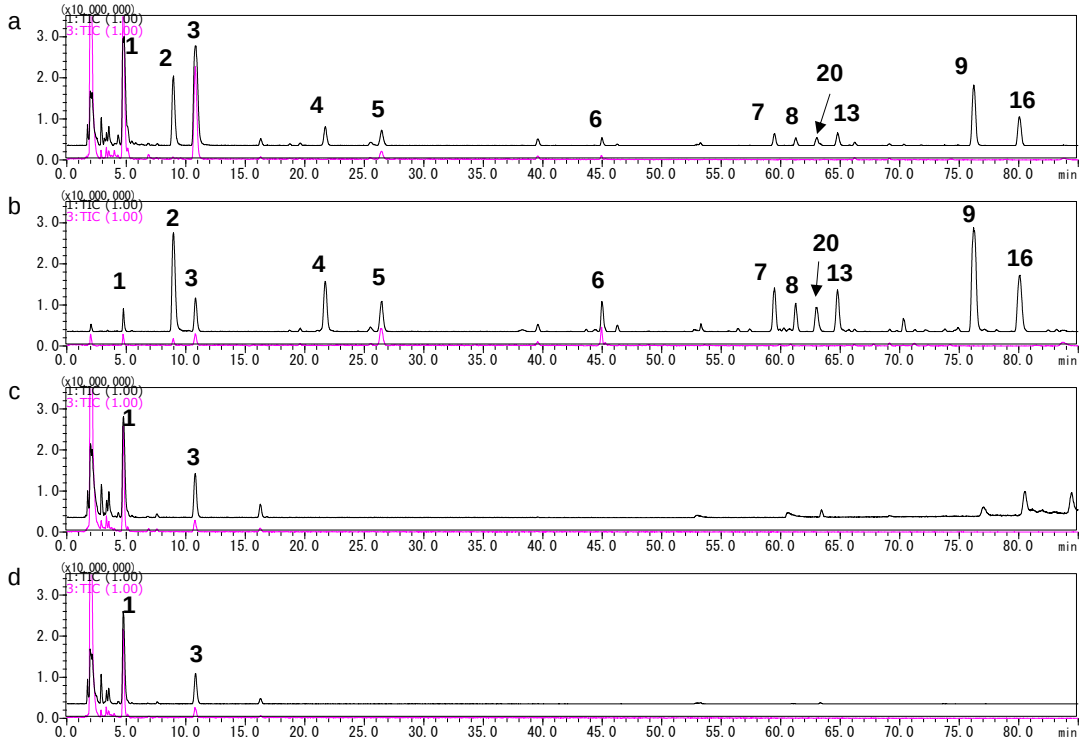

Fig. 2-3 TIC for the MeOH extract and all layers of SR sample C9 in positive (upper) and negative (lower) ionization modes. MeOH extract (a), EtOAc layer (b), *n*-BuOH layer (c), and water residue (d) were analyzed by LC-MS with gradient elution system I. Numerals indicate respective compounds in Fig. 2-5.

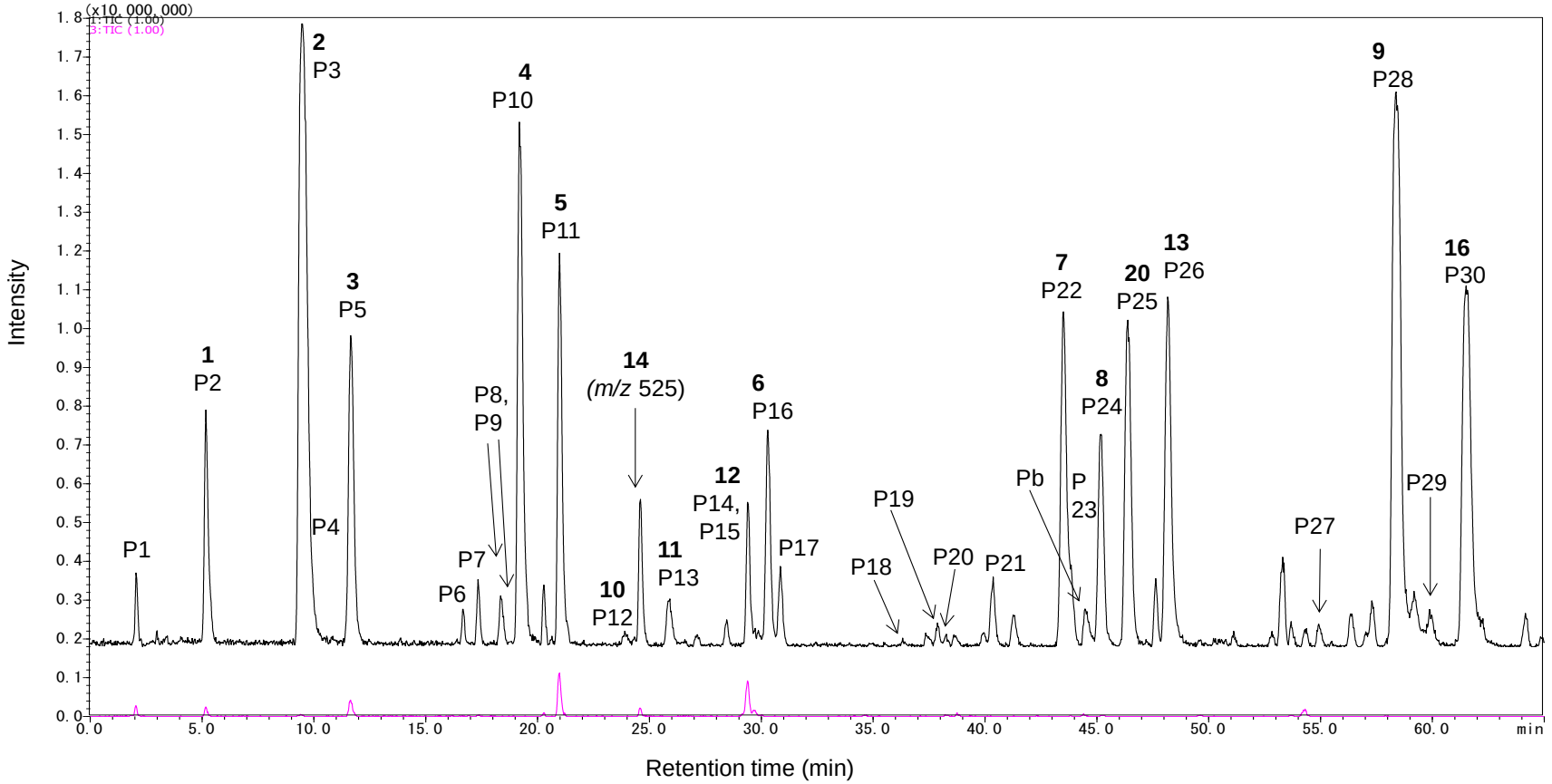

Fig. 2-4 TIC for EtOAc layer of SR sample C9 in positive (upper) and negative (lower) ionization modes. The details of characterized compounds (P1–P30) are summarized in Table 2-3. Pb: the peak also detected in the blank sample (only solvent).

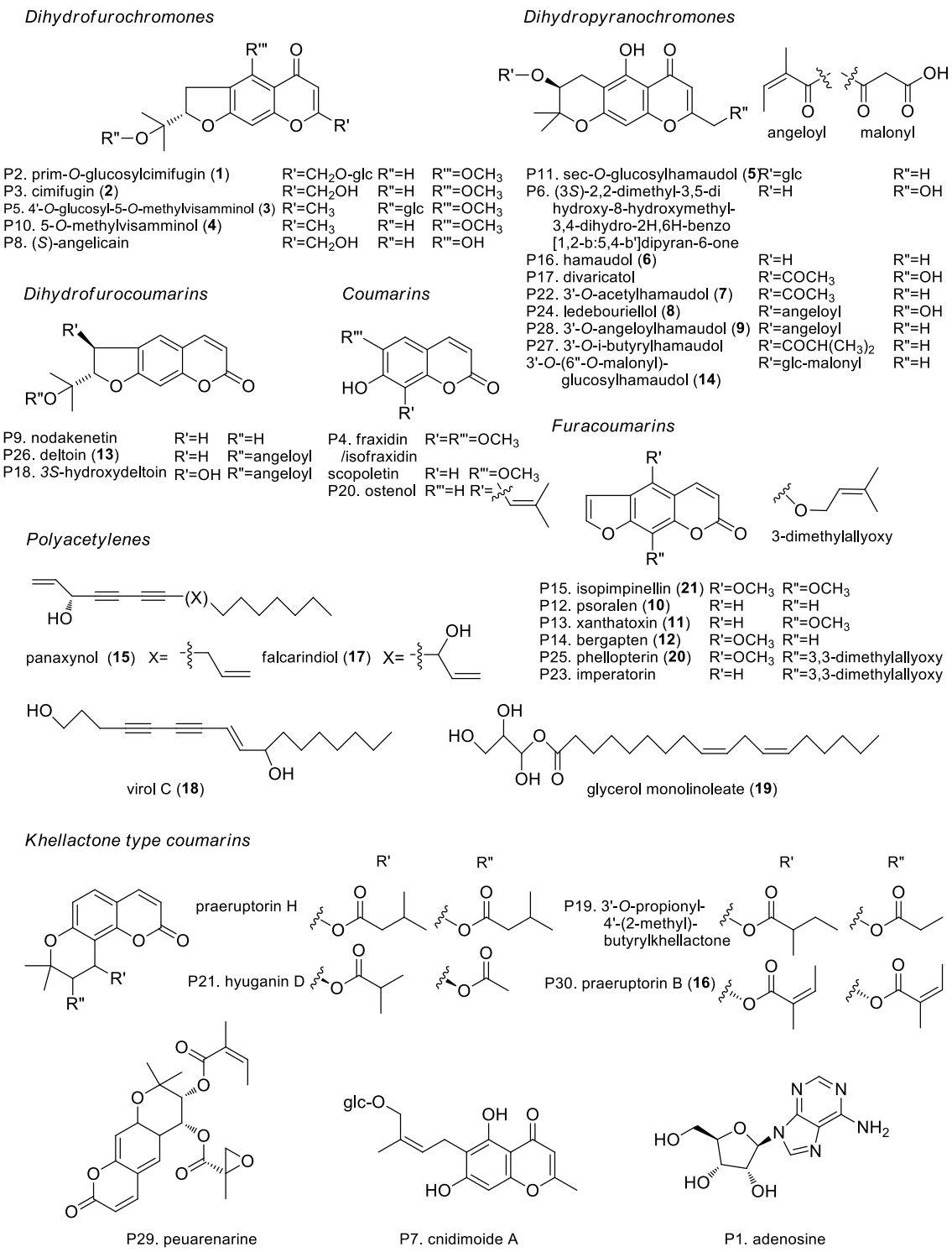

Fig. 2-5 Chemical structures of compounds characterized and identified in SR. The compounds with bold numbers were isolated and identified from SR. The other compounds were characterized and tentatively identified by LC-MS/MS.

Table 2-3. LC-IT-TOF-MS/MS data of compounds identified in SR sample

Chemical group**	Peak No.	t_R min	$[M+H]^+$ *m/z*	Error mDa	$[M+Na]^+$ *m/z*	Error mDa	$[M+HCOO]^-$ *m/z*	Error mDa	λmax nm	Molecular formula	Identification	Fragment ion MS/MS *m/z* (positive ionization mode)
	P1	2.07	268.1042	0.2					258, 325	$C_{10}H_{13}N_5O_4$	adenosine	136.0619
Chr	P2*	5.17	469.1716	1.2	491.1527	0.3	513.1583	-3.1	248, 300	$C_{22}H_{28}O_{11}$	prim-*O*-glucosylcimifugin (**1**)	307.1232, 289.1119, 259.0630, 235.0635, 205.0547
Chr	P3*	9.39	307.1185	0.9	329.1003	0.7			213, 246, 298	$C_{16}H_{18}0_6$	cimifugin (**2**)	289.1102, 259.0609, 235.0618, 221.0464, 193.0564
Cou[a]	P4	9.86	223.0856	-3.7					254, 310	$C_{11}H_{10}O_5$	fraxidin/isofraxidin	
Chr	P5*	11.64	453.1762	0.7	475.1584	0.9	497.1654	-1.1	203, 294	$C_{22}H_{28}O_{10}$	4'-*O*-glucosyl-5-*O*-methylvisamminol (**3**)	291.1264, 273.1162, 243.0669, 219.0677, 205.0520
Chr	P6	16.65	293.1076	5.6					208, 254, 294	$C_{15}H_{16}O_6$	(3*S*)-2,2-dimethyl-3,5-dihydroxy-8-hydroxymethyl-3,4-dihydro-2*H*,6*H*-benzo[1,2-*b*:5,4-*b*']dipyran-6-one	
Cou	P7	17.39	439.1627	2.8	461.1370	-4.8	483.1489	-1.9	207, 255, 300	$C_{21}H_{26}O_{10}$	cnidimoside A	277.1030
Chr	P8	18.40	293.1040	2.0					207, 258, 325	$C_{15}H_{16}O_6$	angelicain	275.0932, 233.0252, 221.0505
Cou	P9*	18.54	247.0982	1.7						$C_{14}H_{14}O_4$	nodakenetin	
Chr	P10*	19.21	291.1230	0.3	313.1065	1.9			211, 294	$C_{16}H_{18}O_5$	5-*O*-methylvisamminol (**4**)	273.1198, 243.0660, 219.0681, 205.0519, 189.0581
Chr	P11*	20.98	439.1617	1.8	461.1460	4.2	483.1475	-3.3	210, 250, 257, 298	$C_{21}H_{26}O_{10}$	sec-*O*-glucosylhamaudol (**5**)	277.1110, 259.1023, 217.0630, 205.0521, 193.0551
Cou	P12*	23.99	187.0394	0.4					211, 246, 294, 325	$C_{11}H_6O_3$	psoralen (**10**)	
Cou	P13*	25.83	217.0525	3.0					216, 248, 263, 303	$C_{12}H_8O_4$	xanthatoxin (**11**)	202.0386, 185.0229
Cou	P14*	29.22	217.0474	2.2					268, 313	$C_{12}H_8O_4$	bergapten (**12**)	202.2222
Cou	P15	29.87	247.0652	5.1						$C_{13}H_{10}O_5$	isopimpinellin (**21**)	
Chr	P16*	30.32	277.1077	0.6					215, 250, 257, 297	$C_{15}H_{16}O_5$	hamaudol (**6**)	259.0994, 241.0853, 231.0849, 217.0501, 205.0511
Cou	P17	30.86	335.1161	3.6					218, 250, 258, 299	$C_{17}H_{18}O_7$	divaricatol	275.0944, 247.0929, 233.0473, 205.0518
Cou	P18	36.35	345.1283	-5.0					220, 325	$C_{19}H_{20}O_6$	3'-*S*-hydroxydeltoin	245.1669, 217.0843
Cou	P19	37.94			425.1406	2.3				$C_{21}H_{22}O_8$	3'-propionyl-4'-(2-methyl) butyrylkhellactone	
Cou	P20	38.13	231.1091	7.5						$C_{14}H_{14}O_3$	ostenol	175.0572
Cou	P21	40.39			397.0730	2.3				$C_{20}H_{22}O_7$	hyuganin D	269.9954, 254.9943
Chr	P22*	43.45	319.1190	1.4					221, 250, 258, 295	$C_{17}H_{18}O_6$	3'-*O*-acetylhamaudol (**7**)	259.0989, 241.0923, 231.1029, 217.0547, 205.0552
Cou	P23	43.82	271.0992	2.7						$C_{16}H_{14}O_4$	imperatorin	
Chr	P24*	45.12	375.1445	0.7					221, 250, 259, 297	$C_{20}H_{22}O_7$	ledebouriellol (**8**)	275.0953, 247.0969, 233.0507, 221.0531, 205.0475
Cou	P25*	46.33	301.1079	0.8	323.0918	2.8			222, 268, 313	$C_{17}H_{16}O_5$	phellopterin (**20**)	233.0482, 218.0339
Cou	P26*	48.22	329.1400	1.8					222, 334	$C_{19}H_{20}O_5$	deltoin (**13**)	248.1026, 229.0845, 230.0934, 212.0654
Chr	P27	54.97	347.1566	7.7						$C_{19}H_{22}O_6$	3'-*O*-*i*-butyrylhamaudol	259.0987, 217.0424
Chr	P28*	58.41	359.1487	-0.2					223, 250, 257, 295	$C_{20}H_{22}O_6$	3'-*O*-angeloylhamaudol (**9**)	259.0986, 241.0897, 231.1000, 217.0529, 205.0508
Cou	P29	60.19			465.1543	2.3				$C_{24}H_{26}O_8$	peuarenarine	
Cou	P30*	61.59			449.1572	-0.6			223, 325	$C_{24}H_{26}O_7$	praeruptorin B (**16**)	444.2013, 327.1294, 227.0734

*: Compounds corresponding to the peaks were identified by comparing with reference standard compounds;

**: 13 Chromones (Chr), 17 coumarins (Cou), and a nucleoside (P1) were characterized in SR sample; a: peak P4, containing 2 coumarins, was overlapped with peak P3;

2.2.4 Preliminary analysis for the comparison between Mongolian *S. divaricata* roots and Chinese SR

For a comparison between Mongolian *S. divaricata* roots and Chinese SR, representative 7 plant specimens from 5 different locations of Mongolia were selected and analyzed together with 8 SR samples as well as 2 plant specimens from China by LC-MS with the gradient elution system I. Total ion chromatograms (TIC) for representative samples are shown in Fig. 2-6.

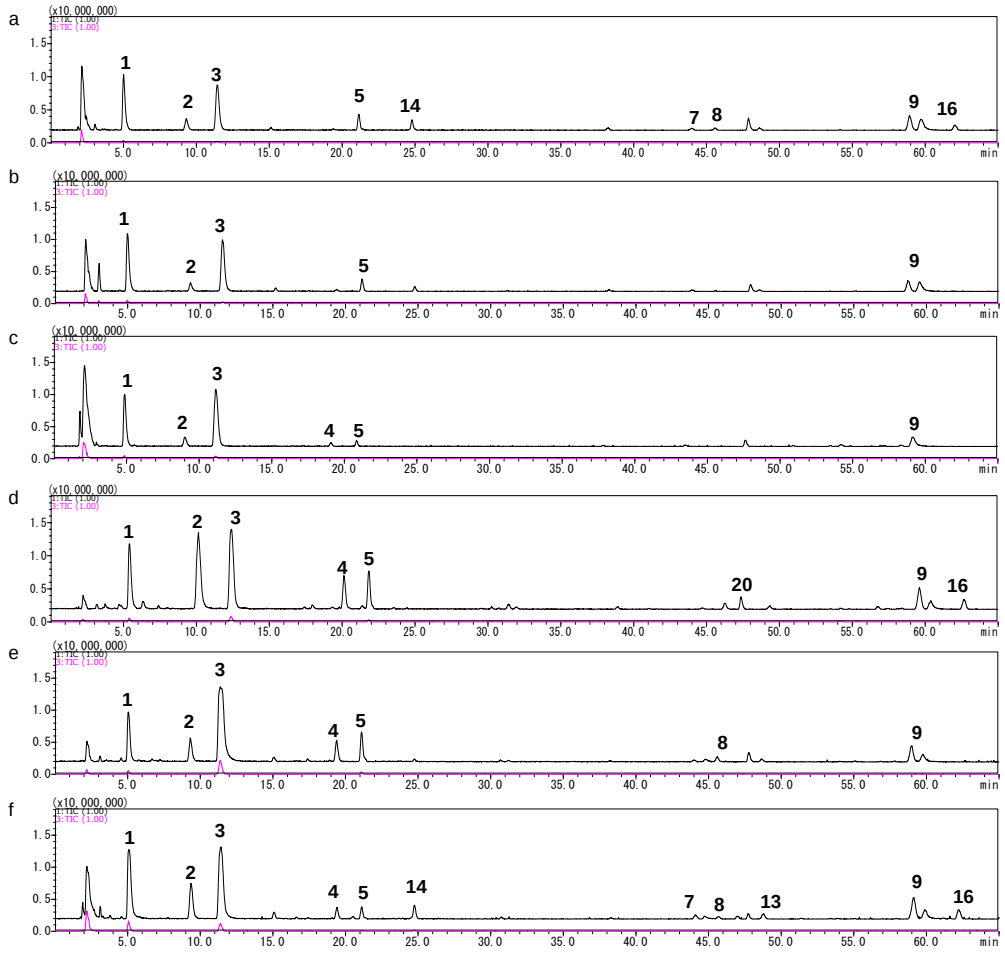

Fig. 2-6 TIC for MeOH extracts of representative SR samples and plant specimens from China in positive (upper) and negative (lower) ionization modes. MeOH extracts of upper parts of the roots were analyzed with gradient elution system I. (a), (b) plant specimens C1 and C2, respectively; (c)–(f) SR samples C4, C5, C7, and C9, respectively. Numerals indicate respective compounds in Fig. 2-5.

All plant specimens and SR samples exhibited similar LC-MS profiles to each other. Sixteen compounds were identified in both MeOH extracts of Mongolian and Chinese *S. divaricata* roots (Table 2-3). When touching upon peak areas of each compound, some differences were shown between the wild and cultivated types of Chinese SR samples. The wild type of SR contained relatively larger amounts of constituents than the cultivated type. When comparing the peak areas of main dihydrofurochromones **1**–**4** and dihydropyranochromones **5** and **9** in the extracted ion chromatogram (EIC) (Fig. 2-7), the peak areas of **1** and **9** were significantly higher in Mongolian plant specimens than in Chinese specimens and SR samples ($p<0.05$, Table 2-4). Obviously, the peak areas of **2**, **3** and **4** in Chinese SR samples, C3 and C5, were higher than others. Although the variation among samples was observed, the peak areas of other compounds were similar in Mongolian specimens, Chinese specimens, and SR samples.

Subsequently, to clarify the differences between them and to identify the primary contributors, multivariate statistical analysis, PCA and OPLS-DA were carried out for LC-MS data of 9 specimens and SR samples. The PCA results were similar to those of OPLS-DA. All specimens and SR sample were separated into two main groups, Chinese and Mongolian. The overall goodness of fit (R^2Y=0.829) and overall cross-validation coefficient (Q^2Y=0.754) demonstrated that the predictability of the model was good (Fig. 2-8A). As shown in Fig. 2-8B, the loading scatter plot of OPLS-DA indicated **2** and **4** as potential contributors to the Chinese group. On the other hand, **1**, **3**, **9**, and **14** contributed most to the Mongolian group. The compound **14** was a new compound, and its structure was elucidated as 3'-*O*-(6"-*O*-malonyl)-glucosylhamaudol (see Chapter 1).

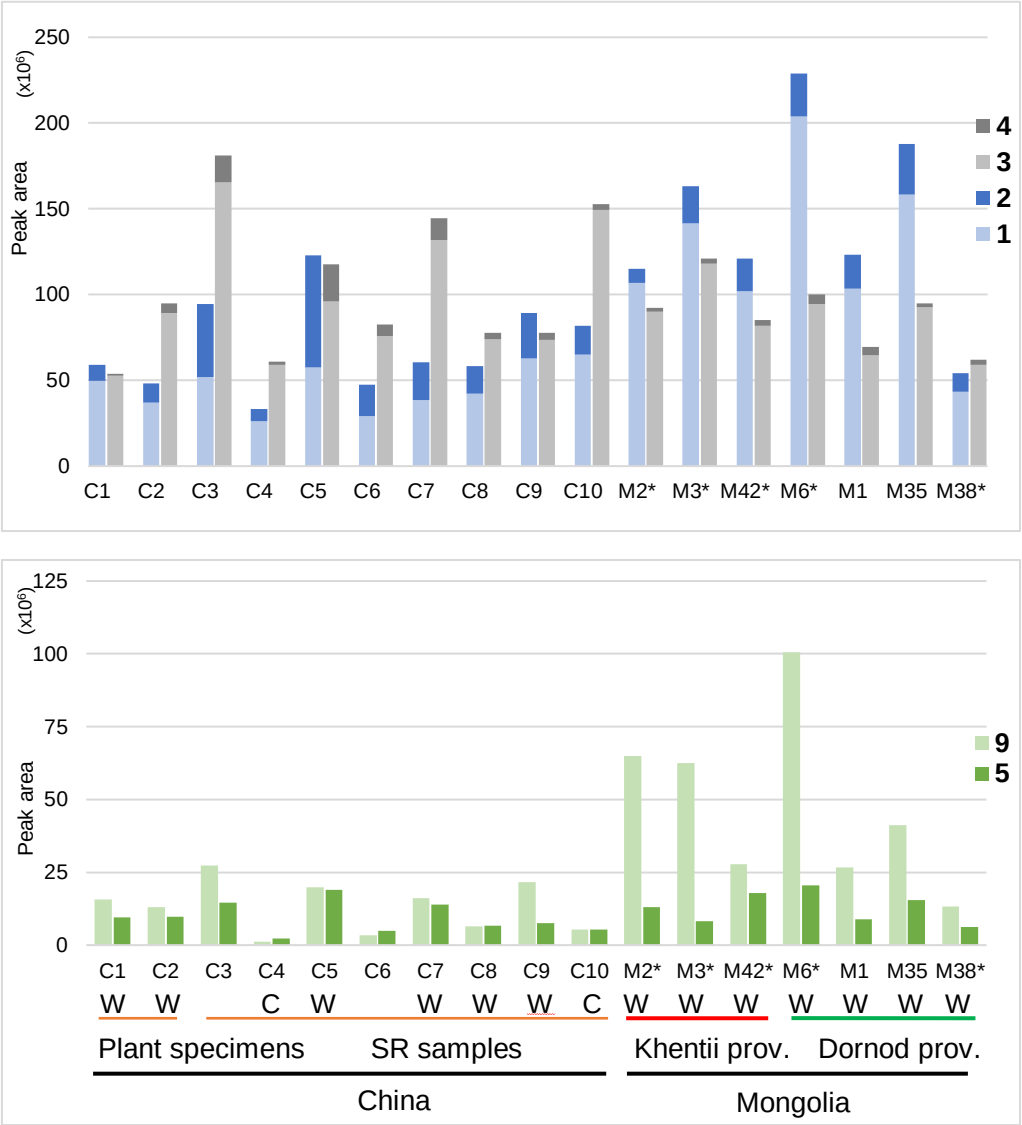

Fig. 2-7. The peak areas of main chromones (a) **1**–**4** and (b) **5** and **9** in 8 SR samples as well as 2 plant specimens from China and 7 flowering specimens from Mongolia. The peak areas are shown as the means of the divided root parts in extracted ion chromatogram (EIC) that analyzed with gradient elution system I (n=3; *: n=1). W: wild type of SR; C: cultivated type of SR. Numerals indicate respective compounds in Fig. 2-5.

Table 2-4. Comparison of **1** and **9** between Chinese and Mongolian group.

Compound	Mean of peak area (mAU)		p value
	Chinese group	Mongolian group	
1	45.9×10^6	122.9×10^6	0.002
9	12.9×10^6	45.5×10^6	0.014

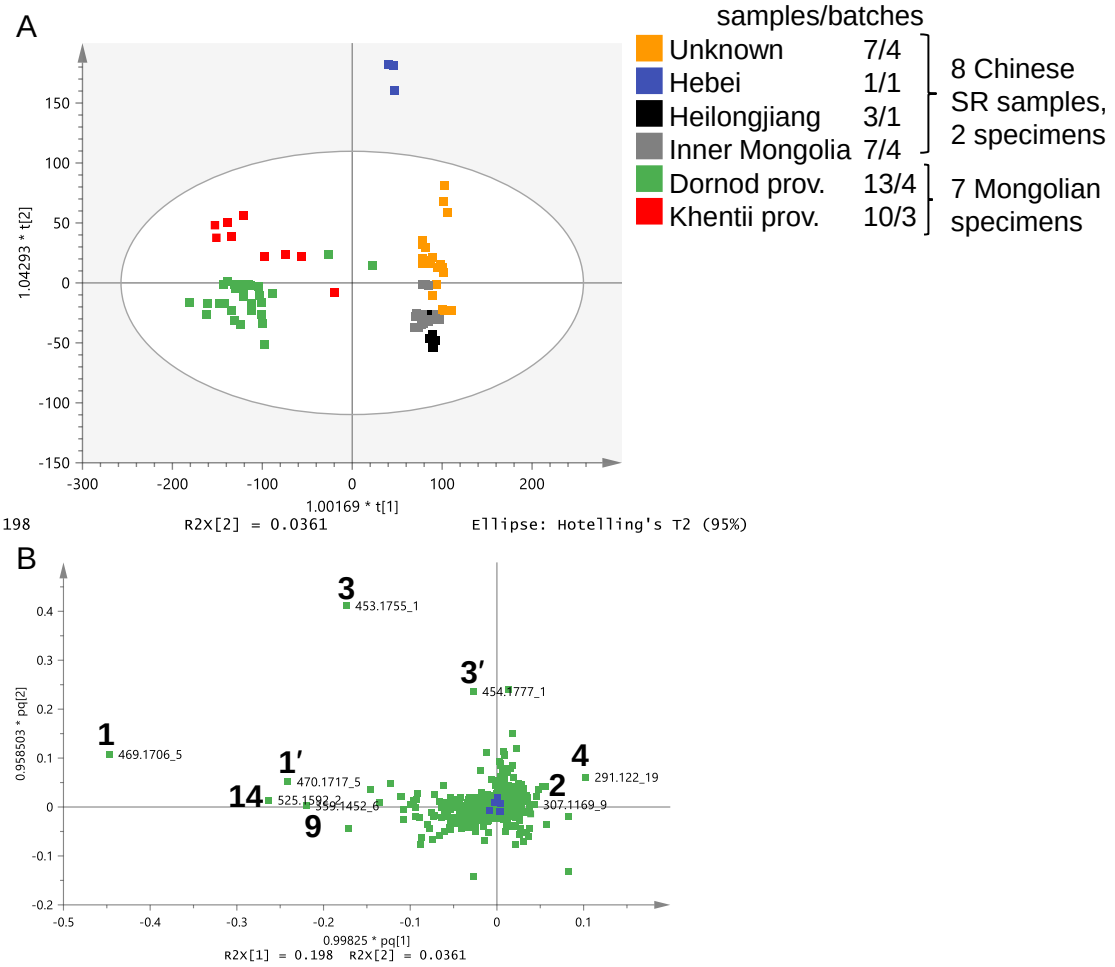

Fig. 2-8. Orthogonal partial least squares-discriminant analysis (OPLS-DA) for the SR samples and plant specimens from China and specimens from Mongolia. (A) score scatter plot and (B) loading scatter plot. The LC-MS data set was same with Fig. 2-7. Numerals indicate respective compounds in Fig. 2-5. **1**' and **3**' indicate isotopic ion $[M+H+1]^+$ of the respective compounds.

2.2.5 Multivariate analysis based on LC-IT-TOF-MS data

OPLS-DA was conducted to clarify variation on root parts, flowering or non-flowering, and regions using 43 plant specimens collected from six different regions of Mongolia in 2017.

First, the differences in the root parts in the chemical profile in SR was demonstrated. The OPLS-DA based on LC-MS data of 40 specimens of upper root parts and 31 specimens of lower root parts (R^2Y=0.676, Q^2Y=0.533) indicated that the upper and lower parts of the roots tended to separate into two groups (Fig. 2-9A). The S-plot of OPLS-DA revealed that **3** had more influence on discrimination of the lower parts of the roots, while **8**, **9**, and **14** were likely to have more contribution for separation of the upper parts of the roots (Fig. 2-9B).

Second, the differences between flowering and non-flowering specimens was found, using 8 flowering specimens and 11 non-flowering specimens, both growing in grassland. As shown in Fig. 2-9C, the loading scatter plot of the OPLS-DA for the 2 groups showed good separation (R^2Y = 0.983and Q^2Y = 0.763). The S-plot of the OPLS-DA indicated that **1** discriminated the specimens that were flowering, and the unidentified compound with *m/z* 358 was frequently found in non-flowering specimens (Fig. 2-9D).

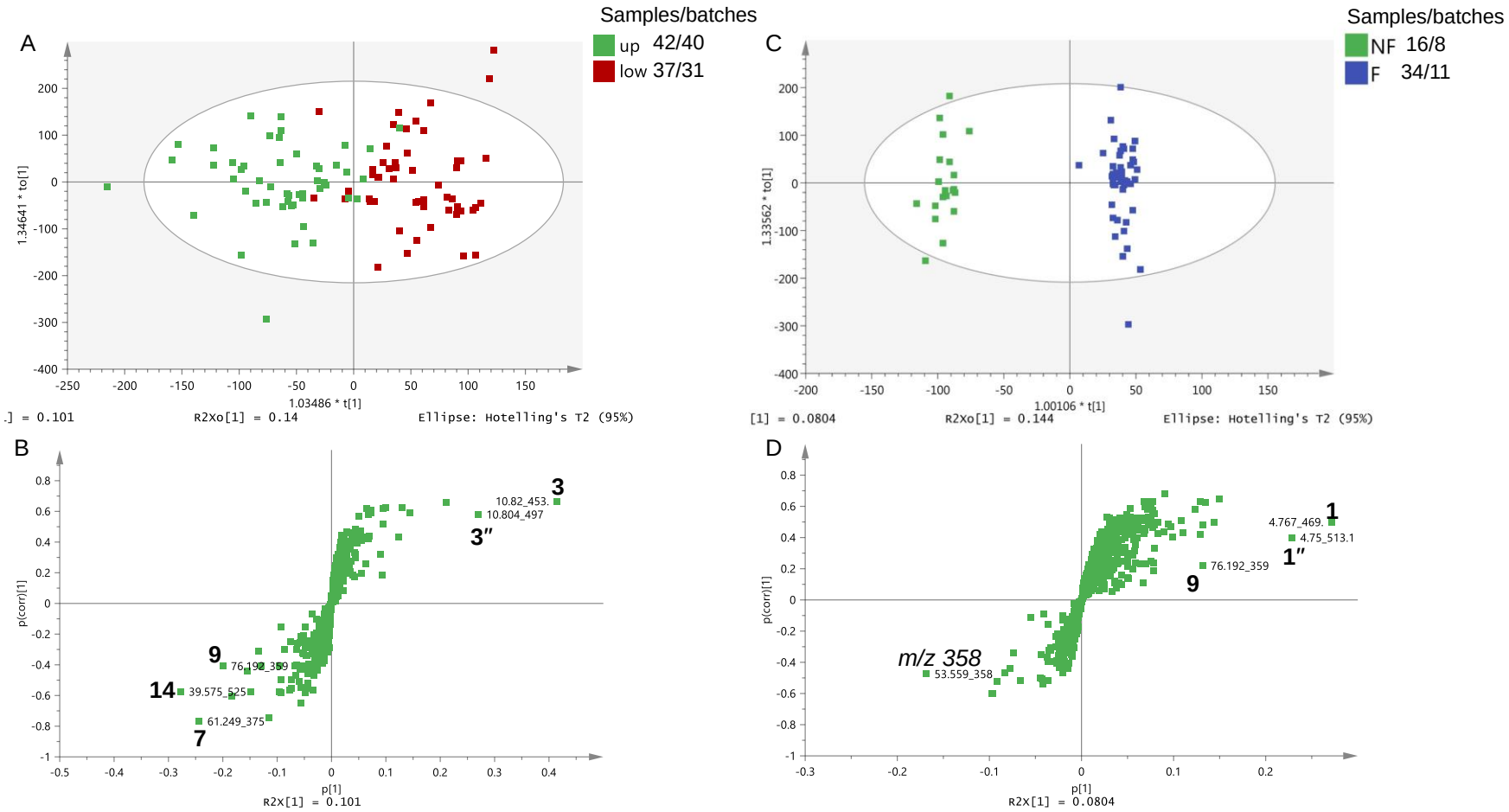

Fig. 2-9. OPLS-DA for elucidating the difference among root parts (A: score scatter plot, B: S-plot) and that between flowering or non-flowering specimens (C: score scatter plot, D: S-plot). Numerals indicate respective compounds in Fig. 2-5. **1**" and **3**" indicate $[M+HCOO]^-$ of the respective compounds.

Finally, the variation among growing regions of Mongolian specimens was estimated and discriminatory markers for group separation was clarified using OPLS-DA based on the LC-MS data of 31 specimens collected in 2017, which have single or straight root. Most of the specimens from cropland (except M32) and 3 specimens from grassland (M24, M39, M41) that have new roots on the old root or branched roots were excluded. The score scatter plot of the OPLS-DA indicated that all specimens were characterized by their growing regions ($R^2Y = 0.821$, $Q^2Y = 0.536$, Fig. 2-10). The loading scatter plot of the OPLS-DA indicated that **1**–**3** were most relevant to the specimens from the far eastern part of Mongolia, Khalkhgol and Tamsagbulag; **6**, **7**, **9**, and **16** were most abundant in the specimens from the eastern part, Holonbuir; **6** was recognized as a marker compound for the specimens from Bulgan; **14** may be used as a discriminatory marker for the specimens from the central eastern part of Mongolia, particularly Ondorkhaan and Bayan-Ovoo. Since the specimens from Holonbuir and Bulgan were characterized by **6**, **7**, **9**, and **16** besides **14**, they were discriminated from the specimens of Ondorkhaan and Bayan-Ovoo.

2.2.6 Relative quantification of compounds by LC-IT-TOF-MS

LC-MS profiles of Mongolian specimens showed similarity in the composition of peaks, as well as those of upper, middle, and lower parts of the root (Fig. 2-11 1u, 1m, and 1l). Sixteen common peaks (**1**–**14**, **16**, **20**) were observed and identified in the LC-MS chromatograms of all specimens except for 3 specimens from the Tamsagbulag (M39–M41), Dornod prov., which had the unidentified peak with *m/z* 358 at t_R 53 min (Fig. 2-11 2d). Furthermore, **14** was frequently observed in the specimens from Mongolia (Fig. 2-11 2a – 2e). Peaks of **6**, **7**, **9**, and **16** were higher in the specimen from Holonbuir, Dornod prov. (Fig. 2-11 2b). When comparing the root parts within one root, the peak

area of **3** was higher in the lower parts of the roots, while that of **14** tended to be higher in the upper parts of the roots.

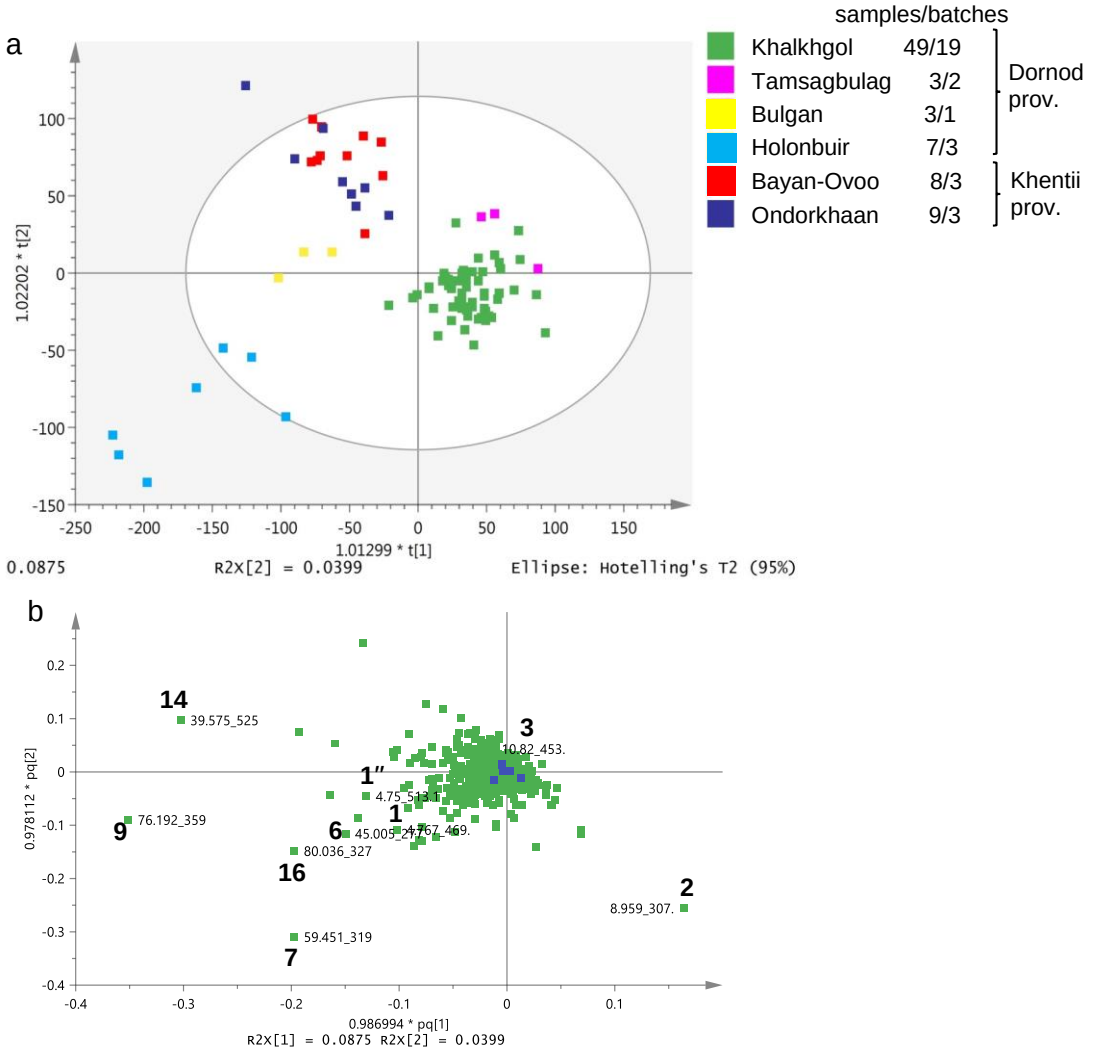

Fig. 2-10. OPLS-DA for the specimens from different regions of Mongolia. (a) score scatter plot and (b) loading scatter plot. Numerals indicate respective compounds in Fig. 2-5. **1**" indicates $[M+HCOO]^-$ of **1**.

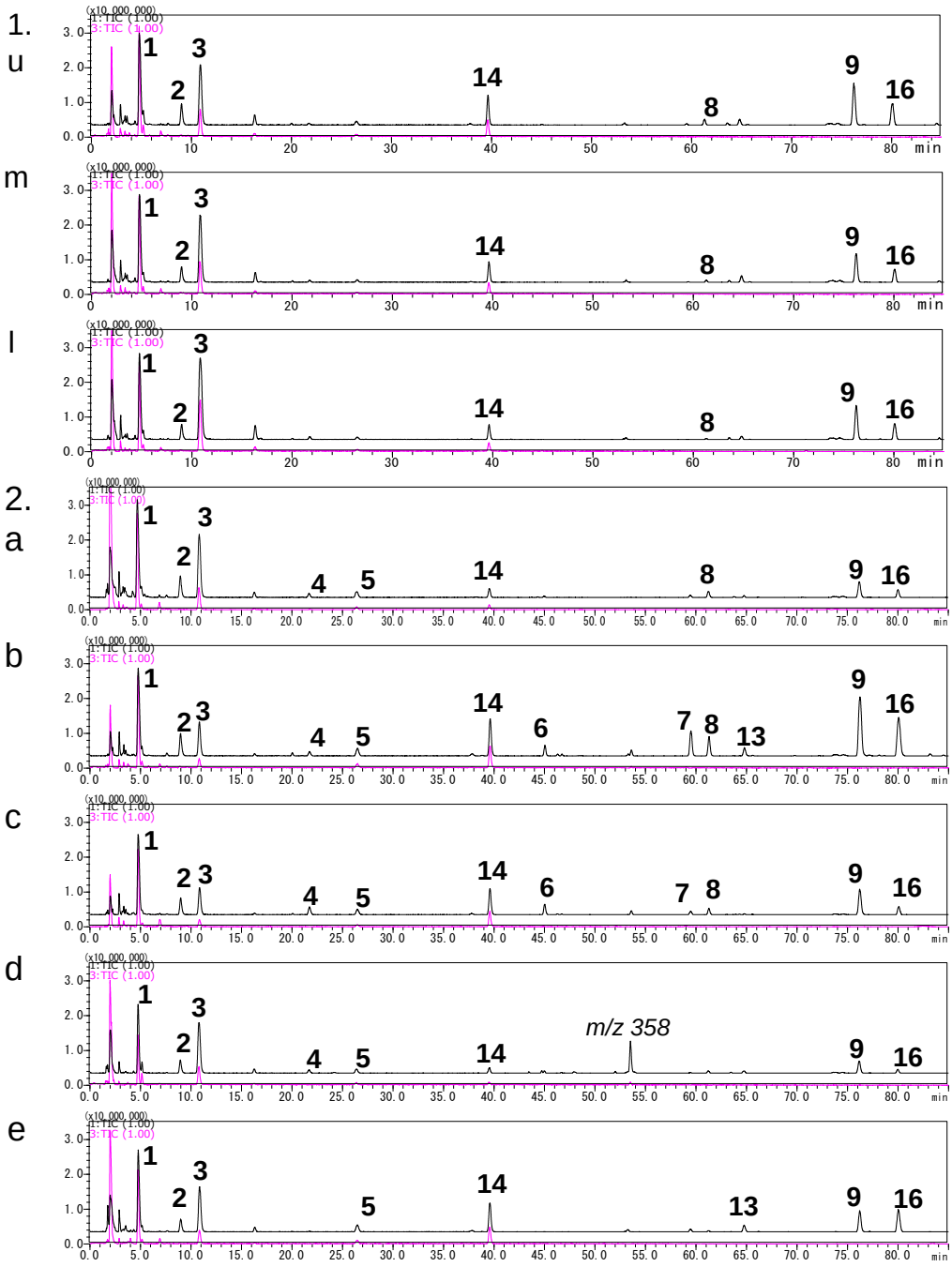

Fig. 2-11. TIC of 70% MeOH extracts of representative plant specimens from each region of Mongolia in positive (upper) and negative (lower) ionization modes. 1) M3 from Bayan-Ovoo, Khentii prov., upper (u), middle (m), and lower (l) parts of the root. 2) upper parts of M1 from Khalkhgol, Dornod prov. (a); M6 from Holonbuir, Dornod prov. (b); M9 from Bulgan, Dornod prov. (c); M41 from Tamsagbulag, Dornod prov. (d); M43 from Ondorkhaan, Khentii prov (e). Numerals indicate respective compounds in Fig. 2-5.

The peak areas in EIC of dihydrofurochromones **1**–**4** and dihydropyranochromones **5** and **9** are shown as the means of the divided root parts in Fig. 2-12. The result indicated that the peak area of each chromone was also extremely variable depending on the growing region and flowering or not. Mongolian specimens generally contained a large amount of **1** and **9**. The peak area of **9** was markedly higher in the specimens from Holonbuir, and those of **1** and **3** were tended to be higher in the specimens from Khalkhgol. While, the peak areas of **2** and **4** varied among all specimens, and this variation might be attributable to the growing stage rather than the growing region. These results were strongly consistent with that of OPLS-DA (Fig. 2-10).

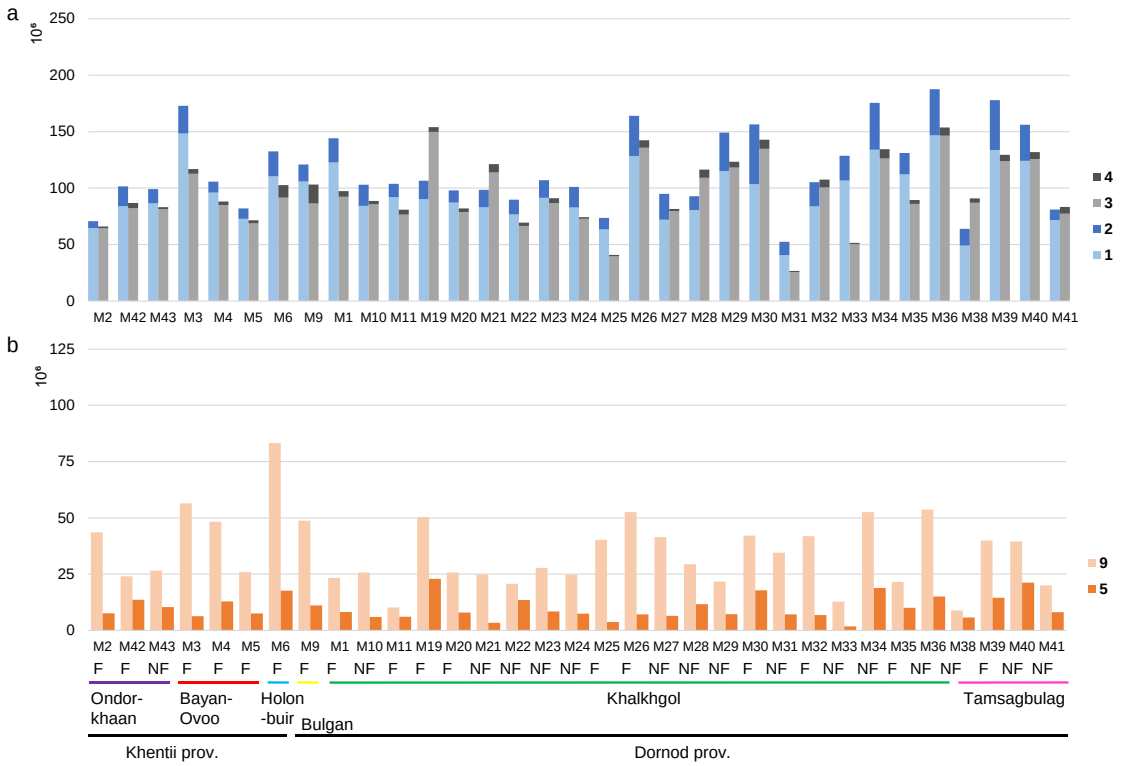

Fig. 2-12. The peak areas of main chromones (a) **1**–**4** and (b) **5** and **9** in all plant specimens except for specimens obtained from local government and collector (H, Y, K, C) from different regions of Mongolia. The peak areas are shown as the means of the divided root parts in EIC that analyzed with gradient elution system II. F: flowering specimens; NF: non-flowering specimens. Numerals indicate respective compounds in Fig. 2-5.

2.3 Discussion

Metabolomic profiling of *S. divaricata* roots from Mongolia using LC-IT-TOF-MS analysis was investigated for the first time and revealed that all Mongolian specimens showed similar LC-MS profiles to the Chinese SR samples. Based on the LC-MS data of all specimens from Mongolia, multivariate statistical analysis, PCA and OPLS-DA, was performed. The OPLS-DA revealed that Mongolian specimens could be discriminated from the Chinese SR samples by the abundance of chromones **1**, **9**, and **14** which was identified as 3'-*O*-(6"-*O*-malonyl)-glucosylhamaudol, a new natural compound. Moreover, the OPLS-DA of flowering and non-flowering specimens from Mongolia revealed that **1** contributed most to the flowering specimens, while an unidentified peak with *m/z* 358 contributed to the non-flowering specimens. However, this peak could not be identified due to low amount of sample materials.

As mentioned above, it was revealed that **1** contributed most to the flowering specimens. However, as shown in Fig. 2-12a, a markedly higher amount of **1** was observed in several non-bolting and non-flowering specimens from Khalkhgol (M29, M34, M36, M40). Since these specimens had single thick root or newly formed roots on the old root, they may have grown more than 2 years. Thus, it was indicated that whether the flowering or non-flowering at the mature stage has no relevance to the contents of constituents. In the case of Mongolian wild plants, the aerial parts of the plant freeze and fall in the winter season, and then new roots grow on the old root in next spring. Probably in the first year, the plant will not be bolting (no flower), but the root becomes mature. For this reason, the contents of the constituents in the root can increase even in a non-flowering plant. It was suggested that one of the most important factors that influence the quality of SR might be the number of growing years. A detailed study on the variation of

chemical components associated with the growing year as well as the season will be necessary.

Relative quantification of main dihydrofurochromones (**1**–**4**) and dihydropyranochromones (**5**, **9**) revealed that the specimens from Khalkhgol and Tamsagbulag contained high amounts of major chromones (**1**–**3**) although the variation among the specimens was observed (Fig. 2-12). However, some specimens (M25, M31) collected in the cropland in Khalkhgol showed remarkably lower contents (Fig. 2-12a). The difference in the shape and hardness of the root were observed between specimens from cropland and those from grassland. The specimen from grassland had a hard, straight, and single root, while the specimen from cropland had soft and curved root with newly formed roots on the top. In particular, the specimen M31, which contained lower amounts of chromones, had more than 10 newly formed thin roots on the old root (Fig. 2-13). Therefore, the specimens from grassland were thought to be suitable for the crude drug SR to avoid SR with low content of main chromones. From this viewpoint, the high-performance cultivation method including grassland cultivation in suitable areas, followed by the best harvest season determined on the basis of the experiment, sometimes combined with wild plant collection, should be developed.

Fig. 2-13. Mongolian specimen M31.

2.4 Summary of chapter 2

Metabolomic profiling of *S. divaricata* roots obtained from different regions of Mongolia was conducted by LC-IT-TOF-MS/MS combined with multivariate statistical analysis. Forty-three plant specimens from Mongolia together with 8 SR samples and 2 plant specimens from China were investigated and characterized by the differences of growing regions, root parts, and flowering or not. Among 30 compounds tentatively identified by LC-MS/MS, 16 compounds were identified in both Mongolian specimens and Chinese SR samples and plant specimens. LC-MS profiles of Mongolian specimens were similar to the Chinese SR samples and plant specimens. The OPLS-DA revealed that Mongolian specimens were distinguished from Chinese SR by abundance of **1**. Moreover, Mongolian specimens could be discriminated by their growing regions based on the content of 8 chromones. The total content of dihydrofurochromones **1**–**3** was relatively higher in the specimens from Khalkhgol in the far eastern part of Mongolia, while the contents of **6**, **7**, **9**, and **16** were higher in those from Holonbuir in the eastern part. The new chromone **14** was the discriminatory marker for the specimens from the central eastern part, particularly Ondorkhaan and Bayan-Ovoo. Based on this research, *S.divaricata* roots from Mongolia have potential new sources of SR, particularly those from the far eastern part of Mongolia, Khalkhgol, possessed a superior property such as higher contents of major chromones **1**–**3**.

Chapter 3. Quantification of metabolites in *S. divaricata* roots from Mongolia by HPLC-DAD and qHNMR

In the chapter 3, HPLC-DAD method was developed and validated for characterization and quantification of 9 chromones and 4 coumarins in 44 Mongolian *S. divaricata* specimens and 8 SR sample and 2 plant specimens from China (Table 2-1). Among Mongolian specimens, 19 specimens were newly collected from northeastern part of Mongolia in 2019. Subsequently, OPLS-DA was performed on HPLC data of Mongolian specimens to clarify geographical variation. Finally, ^{1}H NMR analysis was conducted to characterize metabolites such as sugars and polyacetylenes as well as chromones and coumarins, besides qHNMR analysis were carried out to determine the levels of sucrose and polyacetylenes including **15** and to develop the rapid quantification method of main chromones (**1**–**3**).

3.1 Methods

3.1.1 Purity determination of reference compounds by qHNMR

Reference compounds were prepared by the isolation of MeOH extract of SR sample C9 (see chapter 1). 1–2 mg of reference compounds was accurately weighed by ultramicro balance (Sartorius, Germany) and dissolved in 0.7–1.0 mL of DMSO-d_6 containing 0.5 mg/mL DSS-d_6 (internal calibrant; IC). A portion of each standard solution (0.6 mL) was transferred into an NMR tube.

To determine the purities of compounds **1**–**13**, the signals selected from the reference compounds were used for determining the purity based on the integral value referred to the signal at δ_H 0.00 ppm of DSS-d_6.

The purity (P) was calculated using the following equation:

$$P[\%] = \frac{N_{IC} \cdot I_t \cdot M_t \cdot C_{IC}}{N_t \cdot I_{IC} \cdot M_{IC} \cdot C_t} \cdot P_{IC}$$

N and I are the numbers of protons of the selected signal and the integral: M, C, and P are the molecular weight, concentration (mg/mL), and the purities of the target analyte (t) or internal calibrant (IC), respectively.

3.1.2 Preparation of standard and sample solutions for HPLC-DAD analysis

All 13 reference compounds (1 mg) were weighed accurately and dissolved in 1 mL MeOH individually. These stock solutions were mixed and diluted to appropriate concentrations to prepare the mixed standard solutions and then used to make the calibration curves.

A powdered sample (100 mg) of each plant specimen and SR sample was sonicated with 13 mL of 70% MeOH in the ultrasonication bath at room temperature for 30 min. The extract was centrifuged at 2580×g for 10 min and the supernatant solution was collected into a 25 mL volumetric flask. Then another 12 mL of 70% MeOH was added to the residue and extracted. The supernatant solutions were combined and adjusted to 25 mL with 70% MeOH. Finally, 0.2 mL of the resultant solution was filtered through a 0.2 μm membrane filter prior to use. Sample solutions were analyzed with gradient elution system II.

3.1.3 Method validation for HPLC-DAD analysis

The calibration curves were obtained by integrated peak areas against the concentration of each analyte in the mixed standard solutions at seven different levels. The limit of detection (LOD) and limit of quantification (LOQ) were determined at the

signal-to-noise ratio (*S/N*) of 3 and 10, respectively. The precision was evaluated by the intra- and inter-day analysis to determine the repeatability, stability, and reproducibility of the method. For the intra- and inter-day precision tests, sample solutions of the SR samples (C9, C10) and the specimen (M1) were prepared and injected in triplicate within a day and on three consecutive days, respectively. Variations were expressed by the relative standard deviation (RSD) of the peak area. A recovery test was carried out to evaluate the accuracy of the extraction and the analytical method. The same amount of each standard solution was added to the crude powder of SR sample C9 and then extracted and analyzed using the HPLC method. The recovery rate was calculated using the following equation:

$$R(\%) = \frac{(measured\ amount - original\ amount)}{spiked\ amount} \times 100\%$$

3.1.4 Quantification of compounds by qHNMR

The extract obtained from the HPLC method was lyophilized for 24 hrs and the extract amount was measured. Then, approximately 10 mg of the extracts were accurately weighed and dissolved in 0.7–1.0 mL of DMSO-d_6 containing 0.5 mg/mL DSS-d_6 (IC). After centrifugation at 3000 × g for five mins, 0.6 mL of sample solution was transferred into the NMR tube for further analysis.

To determine the content of **1**–**3** in the extracts, the signals (H-3) at δ_H 6.33, 6.09, and 5.99 of **1**, **2**, and **3** (including **4**) were used for the quantification based on the integral value referred to the signal at δ_H 0.00 ppm of DSS-d_6.

The content (%) was calculated using the following equation:

$$\text{Content}\ [\%] = \frac{N_{IC} \cdot I_t \cdot M_t \cdot W_{ex} \cdot C_{IC}}{N_t \cdot I_{IC} \cdot M_{IC} \cdot W_S \cdot C_{ex}} \cdot P_{IC}$$

N and I are the numbers of protons of the selected signal and the integral: M, W, C, and P are the molecular weight, weighted mass (mg), concentrations (mg/mL), and the purity of the target analyte (t), internal calibrant (IC), extract (ex), or sample powder (S), as indicated.

As the H-3 signal at δ_H 5.99 was mostly due to **3**, the content of **3** was calculated by using the molecular weight of **3**.

3.1.5 Statistical analysis

The data matrix of the peak areas of all compounds was normalized using the Z-score transformation before the multivariate statistical analysis. Principal component analysis (PCA) and orthogonal partial least squares-discriminant analysis (OPLS-DA) were performed on SIMCA 14.0 (Umetrics, Sweden)

The contents were expressed as mean and standard deviation (SD). The differences between 2 independent groups were analyzed by the Students *t*-test. The level of statistical significance was set as $p<0.01$.

3.2 Results

3.2.1 Optimization of extraction

The sample preparation and chromatographic method used in the LC-MS analysis were supposed to employ for HPLC analysis. However, when evaluating the recovery rate of extraction, the recovery rate of each compound in the extracts was not sufficient. Among 1, 2, and 3-time extraction considered, 2-time extraction was selected since it showed a similar efficacy as 3-time extraction. As a result, 2-time extraction with 70% MeOH has led to a 2.1–7.6% higher yield than 1-time extraction.

3.2.2 Purity determination of reference compounds by qHNMR

The purities of the 13 reference compounds were determined by qHNMR, using DSS-d_6 as an internal calibrant. The qHNMR spectra of all reference compounds are shown in the Appendix (Fig. S1). The purities of 13 compounds ranged from 60.94 to 99.06% (Table 3-1).

Table 3-1. The purity of reference compounds determined by qHNMR.

Compound name	Molecular formula	Molecular mass	Selected signal* δ_H (mult.)	Purity (%)	RSD (%)
prim-*O*-glucosylcimifugin (**1**)	$C_{22}H_{28}O_{11}$	468.45	6.68 (s)	75.81	1.44
cimifugin (**2**)	$C_{16}H_{18}O_6$	306.31	3.85 (s)	73.22	3.72
4'-*O*-glucosyl-5-*O*-methylvisamminol (**3**)	$C_{22}H_{28}O_{10}$	452.45	3.84 (s)	89.76	1.54
5-*O*-methylvisamminol (**4**)	$C_{16}H_{18}O_5$	290.31	2.29 (s)	62.35	1.55
sec-*O*-glucosylhamaudol (**5**)	$C_{21}H_{26}O_{10}$	438.42	2.38 (s)	60.94	1.09
hamaudol (**6**)	$C_{15}H_{16}O_5$	276.28	2.38 (s)	80.34	1.46
3'-*O*-acetylhamaudol (**7**)	$C_{17}H_{18}O_6$	318.32	6.47 (s)	97.01	1.16
ledebouriellol (**8**)	$C_{20}H_{22}O_7$	374.38	4.43 (d)	86.50	1.85
3'-*O*-angeloylhamaudol (**9**)	$C_{20}H_{22}O_6$	358.38	6.49 (s)	99.06	1.86
psoralen (**10**)	$C_{11}H_6O_3$	186.16	7.77 (s)	91.95	1.33
xanthatoxin (**11**)	$C_{12}H_8O_4$	216.19	4.21 (s)	99.06	0.69
bergapten (**12**)	$C_{12}H_8O_4$	216.19	4.30 (s)	95.75	1.78
deltoin (**13**)	$C_{19}H_{20}O_5$	328.36	7.54 (s)	95.43	0.74

qHNMR data was acquired in DMSO-d_6 using 500 MHz NMR spectrometer.
*: δ_H was reported in ppm relative to DSS-d_6 at δ_H 0.00.

3.2.3 Method validation for HPLC-DAD analysis

The HPLC method was validated by evaluating its linearity, LOD, LOQ, precision, repeatability, stability, and accuracy. As shown in Table 3-2, the correlation coefficient (R^2) of each compound was greater than 0.9995, indicating good linearity. The LOD and LOQ were in the range of 0.04–0.12 μg/mL and 0.07–0.24 μg/mL, respectively. The intra- and inter-day precisions (RSD) were less than 1.99% and 4.90%, respectively (Table 3-3). The average recovery rate of the 13 compounds was 87.6–99.1% and the RSD values were less than 6.7% (Table 3-4). These results proved that the developed HPLC method to be suitable for the quantification of the 13 compounds in the extracts.

Table 3-2. Linear regression data of compounds

Compounds	LOD[a] (μg/mL)	LOQ[b] (μg/mL)	r^{2} [c]	Regression equation	Linear range (μg/mL)
prim-*O*-glucosylcimifugin (**1**)	0.04	0.07	0.9995	y = 19789x + 6805.3	0.07-151.62
cimifugin (**2**)	0.04	0.07	0.9999	y = 36895x + 977.77	0.07-18.31
4'-*O*-glucosyl-5-*O*-methylvisamminol (**3**)	0.04	0.09	0.9997	y = 25902x - 6670.2	0.09-89.76
5-*O*-methylvisamminol (**4**)	0.06	0.13	0.9998	y = 20890x - 720.95	0.12-15.59
sec-*O*-glucosylhamaudol (**5**)	0.12	0.24	0.9997	y = 14320x + 31.125	0.24-15.24
hamaudol (**6**)	0.04	0.08	0.9999	y = 51357x + 257.74	0.08-10.04
3'-*O*-acetylhamaudol (**7**)	0.05	0.09	0.9999	y = 46047x - 791.59	0.09-6.06
ledebouriellol (**8**)	0.04	0.08	0.9999	y = 39309x - 232.85	0.04-2.70
3'-*O*-angeloylhamaudol (**9**)	0.05	0.10	0.9999	y = 41415x + 596.3	0.10-12.38
psoralen (**10**)	0.04	0.09	1.0000	y = 46410x - 280.37	0.09-11.49
xanthatoxin (**11**)	0.05	0.10	0.9998	y = 59392x - 1167.9	0.05-3.10
bergapten (**12**)	0.05	0.10	0.9999	y = 63536x + 2652.1	0.10-6.13
deltoin (**13**)	0.09	0.19	0.9999	y = 9588.3x - 235.5	0.19-11.93

[a]: Limit of detection
[b]: Limit of quantification
[c]: Correlation coefficient

Table 3-3. Intra- and inter-day precision of SR samples (C9, C10) and Mongolian *S. divaricata* roots (M1) for each compound (n=3)

Compounds	Intra-day precision* (RSD, %)				Inter-day precision* (RSD, %)			
	C9 (wild)	C10 (cult.)	M1 (upper part)	M1 (lower part)	C9 (wild)	C10 (cult.)	M1 (upper part)	M1 (lower part)
prim-*O*-glucosylcimifugin (**1**)	0.47	0.05	0.03	0.13	0.44	0.63	0.91	1.10
cimifugin (**2**)	0.27	0.03	0.62	0.74	0.16	0.98	1.07	3.54
4'-*O*-glucosyl-5-*O*-methylvisamminol (**3**)	0.42	0.24	0.32	0.42	0.38	1.04	0.94	0.81
5-*O*-methylvisamminol (**4**)	0.57	1.19	0.80	1.02	1.48	1.96	2.97	1.62
sec-*O*-glucosylhamaudol (**5**)	0.98	1.99	0.87	1.24	4.43	4.02	3.32	4.75
hamaudol (**6**)	0.48	1.43	0.81	1.13	0.49	3.33	2.53	0.51
3'-*O*-acetylhamaudol (**7**)	1.60	1.04	1.79	0.22	1.37	4.22	0.79	1.20
ledebouriellol (**8**)	1.41	nd	0.60	0.64	2.90	nd	2.16	3.32
3'-*O*-angeloylhamaudol (**9**)	0.26	0.31	0.42	0.31	0.38	2.91	1.24	1.51
psoralen (**10**)	1.66	1.18	1.39	0.22	1.70	0.55	2.48	2.70
xanthatoxin (**11**)	0.73	0.67	0.51	1.56	1.02	3.80	1.79	4.90
bergapten (**12**)	1.43	1.06	0.65	1.36	1.85	4.09	1.78	0.66
deltoin (**13**)	0.71	nd	nd	nd	1.98	nd	nd	nd

*: Intra- and inter-day precisions were determined as RSD value (%) of peak area in triplicate injection within a day or 3 consecutive days.
nd: not detected

Table 3-4. Recovery rate of the compounds

Compounds	Original amount (μg/100 mg)	Spiked amount (μg)	Measured amount (μg/100 mg)	Recovery rate (%)	RSD (%)	n*
prim-*O*-glucosylcimifugin (**1**)	1013.98	951.00	1847.42	87.6	0.1	2
cimifugin (**2**)	117.47	124.50	235.94	95.2	0.4	3
4'-*O*-glucosyl-5-*O*-methylvisamminol (**3**)	554.78	572.00	1121.42	99.1	6.7	3
5-*O*-methylvisamminol (**4**)	19.00	11.17	30.05	98.9	2.1	2
sec-*O*-glucosylhamaudol (**5**)	148.04	95.09	229.82	86.0	3.1	2
hamaudol (**6**)	11.72	3.61	15.28	98.7	1.0	2
3'-*O*-acetylhamaudol (**7**)	14.15	4.23	18.09	93.2	0.5	2
ledebouriellol (**8**)	4.32	2.33	6.57	96.5	1.0	3
3'-*O*-angeloylhamaudol (**9**)	61.25	58.35	118.78	98.6	5.5	3
psoralen (**10**)	10.79	9.88	20.52	98.5	2.1	3
xanthatoxin (**11**)	5.01	8.05	12.57	93.9	5.4	3
bergapten (**12**)	3.41	4.08	7.35	96.6	2.4	3
deltoin (**13**)	14.46	7.04	21.13	94.7	0.9	3

*: Replicate of recovery test.

3.2.4 Quantification of compounds by HPLC-DAD

The simultaneous determination of 13 compounds, including 9 chromones and 4 coumarins, was conducted for the 44 *S. divaricata* specimens from different regions of Mongolia and for the 2 plant specimens and 8 SR samples from China. HPLC chromatograms of the mixed standard solution and representative specimens are shown in Fig. 3-1 and 13 compounds were detected sequentially as **1** (5.0 min), **2** (9.0 min), **3** (11.0 min), **4** (22.0 min), **5** (26.4 min), **10** (31.3 min), **11** (36.5 min), **12** (43.5 min), **6** (45.0 min), **7** (59.0 min), **8** (61.5 min), **13** (64.7 min), and **9** (76.0 min). The contents of the 13 compounds in the divided root parts of every specimen and SR sample are listed in Table S1, and the mean values of the divided root parts are shown in Fig. 3-2. Concerning dihydrofurochromones, all *S. divaricata* specimens from Mongolia contained **1** (3.98–20.79 mg/g) and **3** (1.06–6.68 mg/g), and their total amount (5.04–25.06 mg/g) exceeded the criterion (2.4 mg/g) assigned in the CP. The content of **1** in the Mongolian specimens was significantly higher than in the Chinese specimens and SR samples (Table 3-5). Among the Mongolian specimens, those from Norovlin contained a higher amount of **1** (9.18–16.22 mg/g) and **3** (2.60−6.68 mg/g) (Fig. 3-2a), and the specimen M51 from Bayan-Uul showed the highest value of **1** (20.79 mg/g) (Fig. 3-2a). Two specimens M63 and M64 were collected after the fruiting period and contained a remarkably higher amount of **2** (2.61 and 2.97 mg/g, respectively) (Figs. 3-1 b, c, 3-2 b).

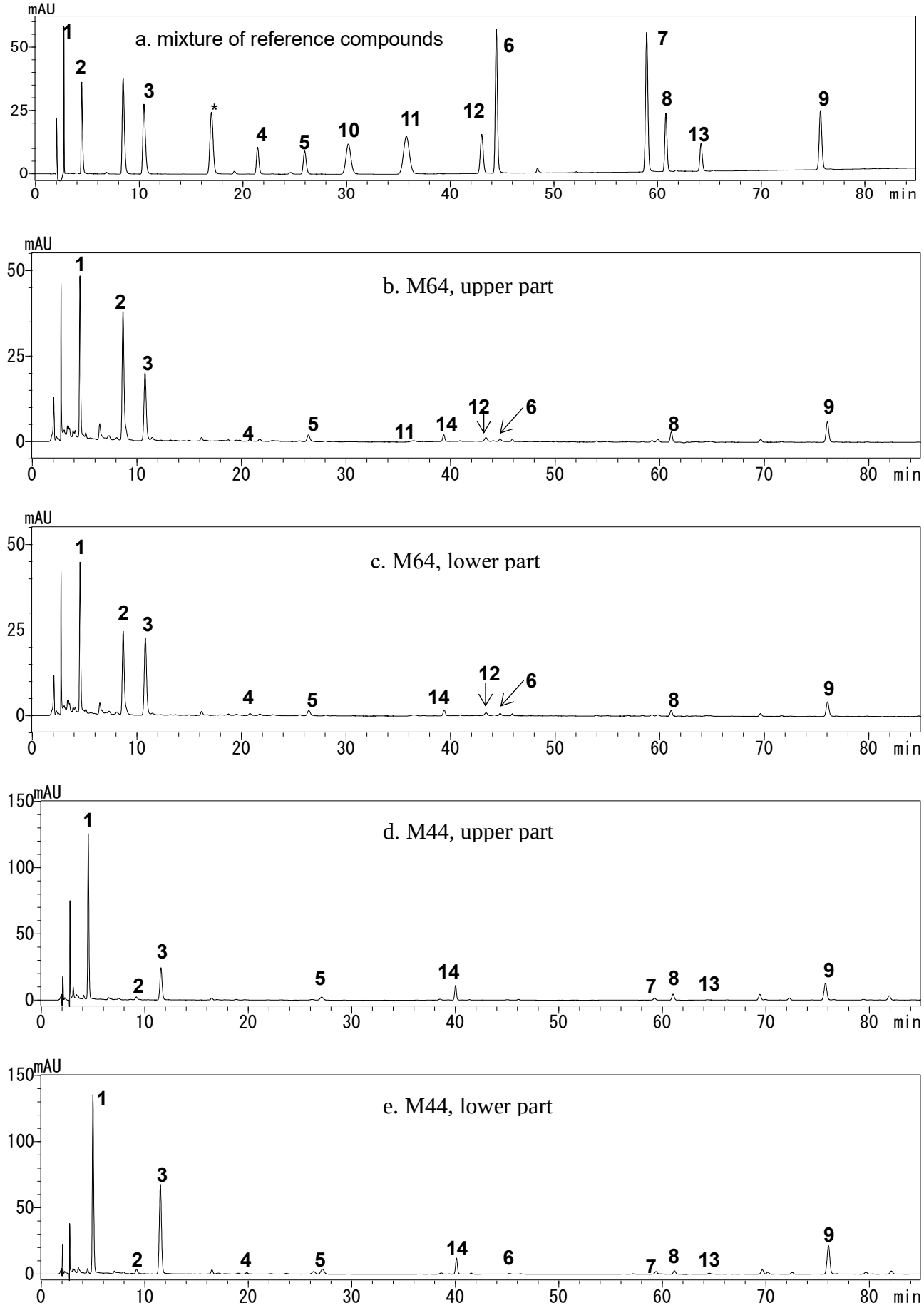

Fig. 3-1. Continued. The HPLC chromatograms of the mixture of reference compounds (a) and representative specimens from Mongolia at 254 nm. 70% MeOH extract of M64, upper (b) and lower (c) part of the root from Khalkhgol; M44, upper (d) and lower (e) part of the root from Norovlin. Numerals indicate the respective compounds in Fig. 2-5.

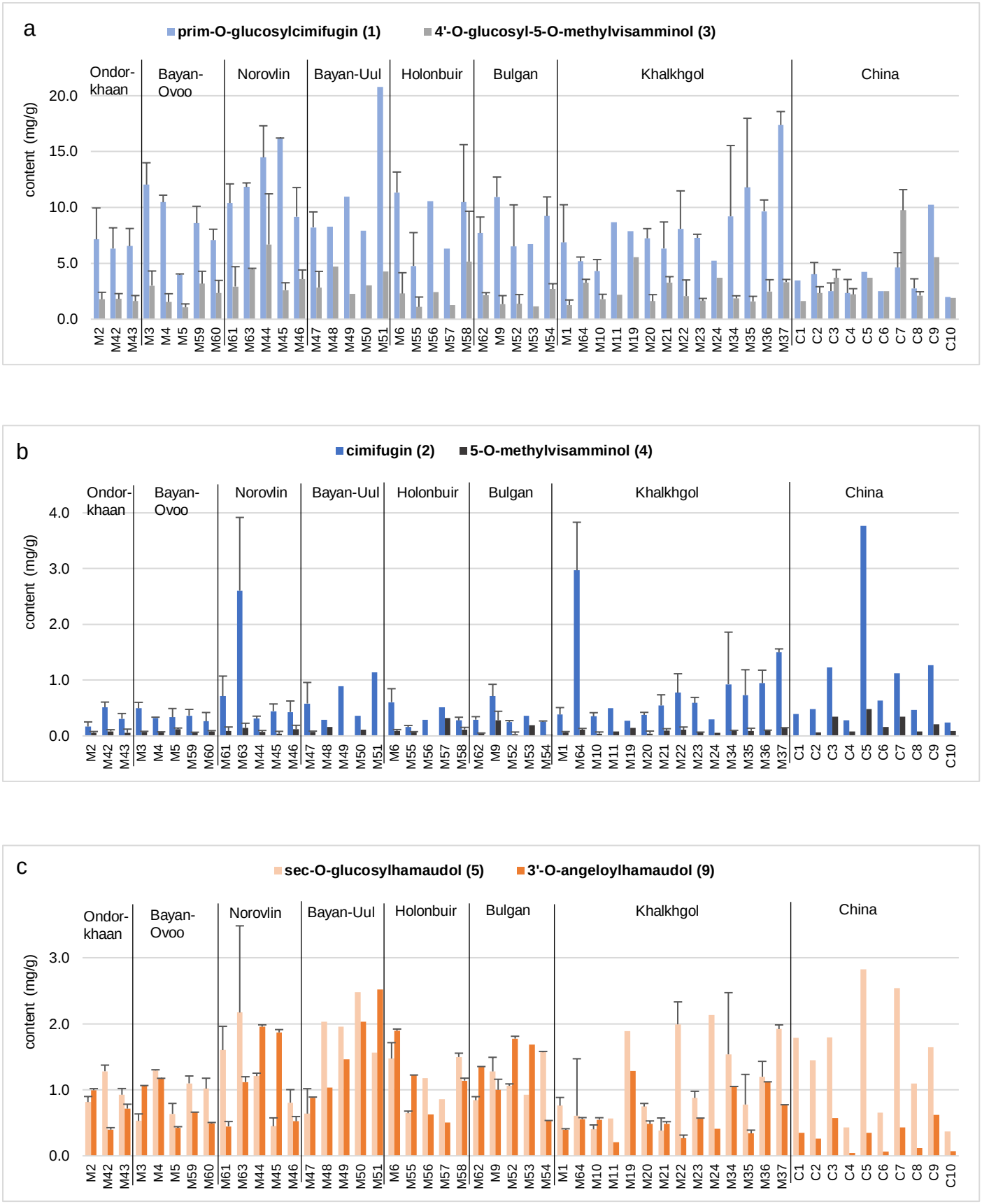

Fig. 3-2. The contents of dihydrofurochromones (**1**–**4**), dihydropyranochromones (**5**–**9**), and coumarins (**10**–**13**). The content was expressed as the mean of divided root parts and standard deviation (SD).

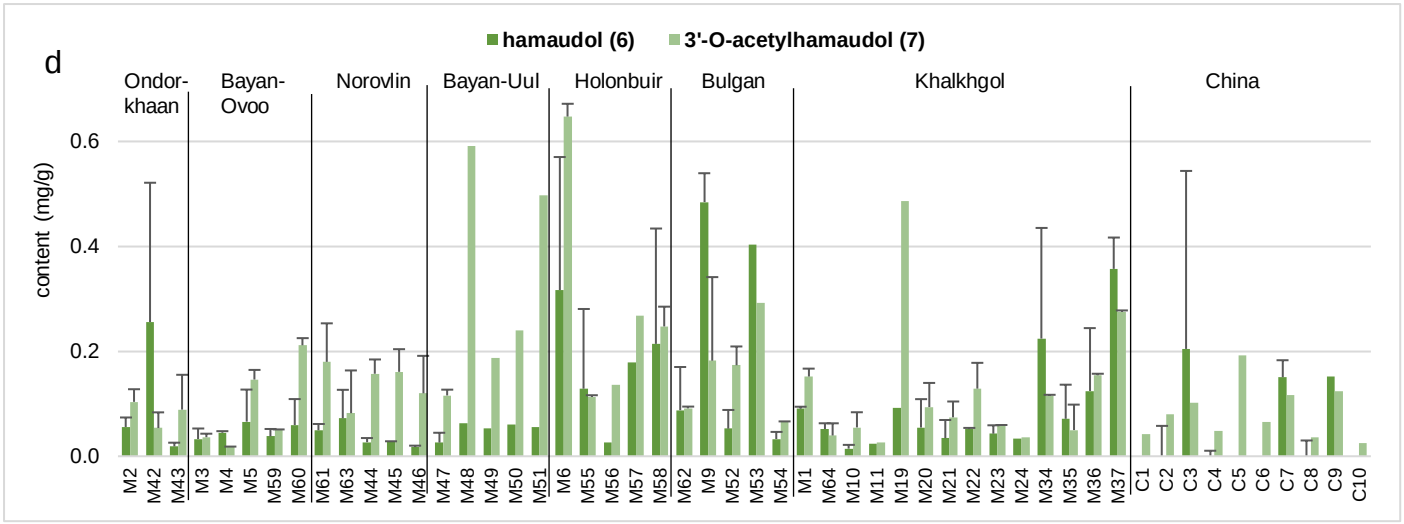

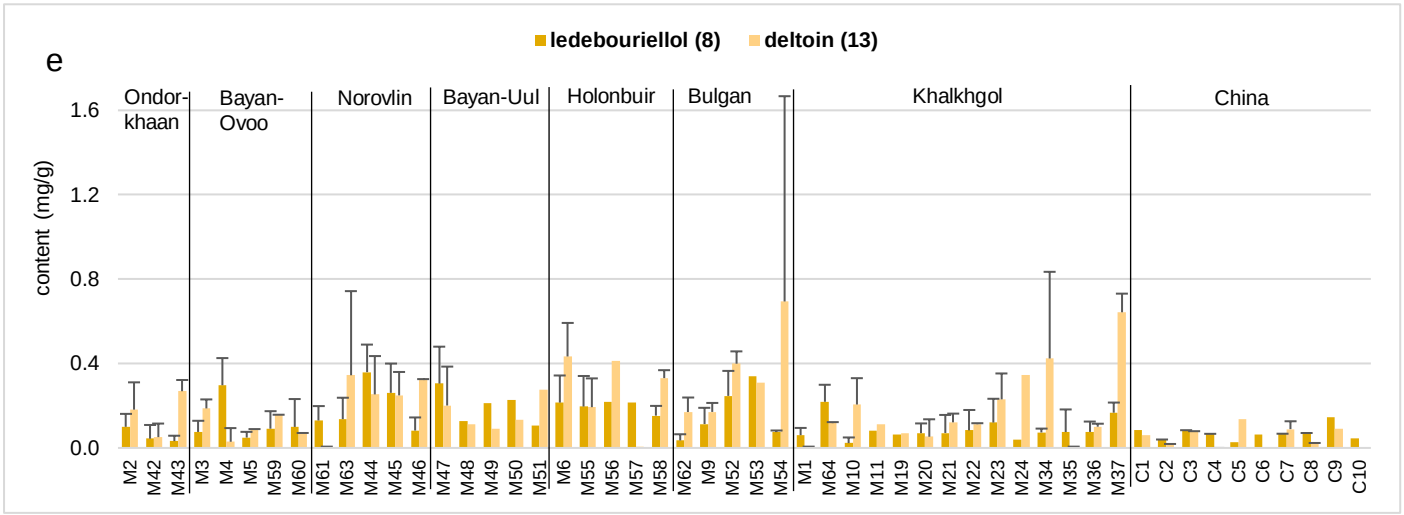

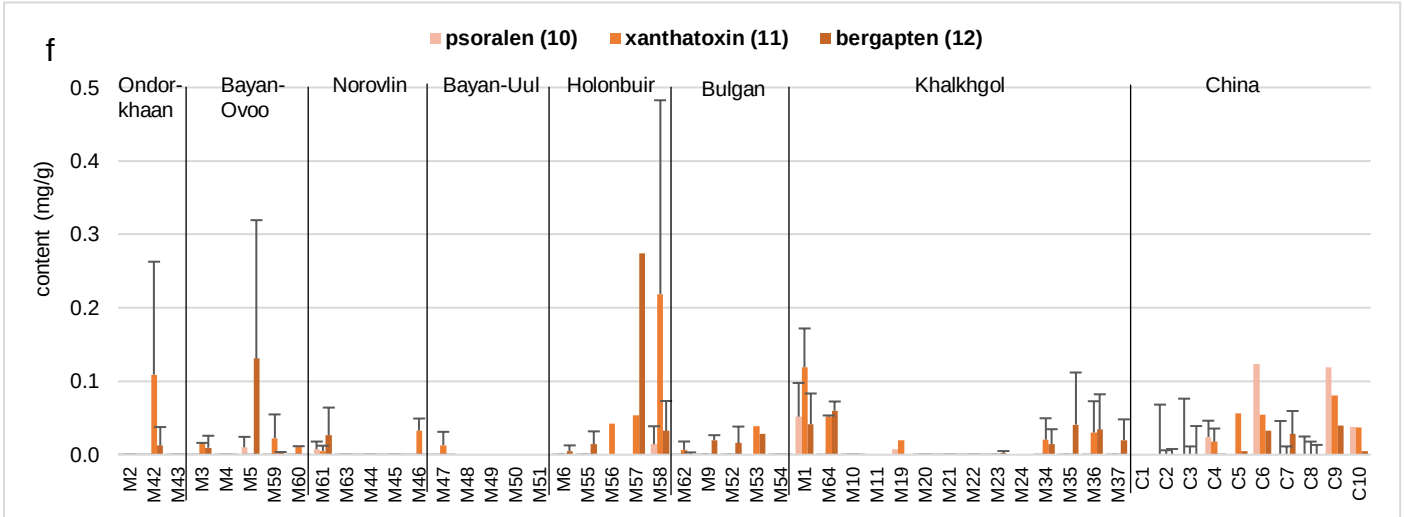

Fig. 3-2 continued.

Concerning dihydropyranochromones, the contents of **7**–**9** were significantly higher in the Mongolian specimens than in the Chinese specimens and SR samples (Table 3-5). However, the variation among samples was observed. The contents of **5** and **9** were relatively higher in the specimens from Bayan-Uul (0.64–2.48 mg/g and 0.88–2.52 mg/g, respectively) (Fig. 3-2c). The content of **6** was highest in the specimen M9 from Bulgan (0.48 mg/g), while the content of **7** was highest in the specimen M6 from Holonbuir (0.65 mg/g) (Fig. 3-2d). The specimens from Holonbuir and Bayan-Uul contained a higher amount of **8** (0.11–0.31 mg/g) and the specimen M44 from Norovlin contained highest (0.36 mg/g) (Figs. 3-2e, 3-1 d, e). Dihydrofurocoumarin **13** was also significantly higher in the specimens from Mongolia than in the Chinese SR (Table 3-5). The highest content of **13** was found in the specimens from Bulgan (0.17–0.69 mg/g) (Fig. 3-2e). Although coumarins were not detected or trace amounts in several samples, the contents exceeding 0.2 mg/g were observed in the specimens M57 and M58 from Holonbuir (Fig. 3-2f).

Table 3-5. Comparison of the contents of compounds (mg/g) between Mongolian and Chinese groups.

Compounds	Mongolian group (n=42)	Chinese group (n=10)	p-value
prim-*O*-glucosylcimifugin (**1**)	9.05±3.48	3.87±2.41	0.00002*
cimifugin (**2**)	0.60±0.57	0.99±1.05	0.29
4'-*O*-glucosyl-5-*O*-methylvisamminol (**3**)	2.63±1.29	3.54±2.48	0.29
5-*O*-methylvisamminol (**4**)	0.09±0.06	0.18±0.16	0.10
sec-*O*-glucosylhamaudol (**5**)	1.18±0.55	1.46±0.84	0.34
hamaudol (**6**)	0.10±0.11	0.05±0.08	0.13
3'-*O*-acetylhamaudol (**7**)	0.17±0.15	0.08±0.05	0.005*
ledebouriellol (**8**)	0.14±0.09	0.07±0.03	0.0003*
3'-*O*-angeloylhamaudol (**9**)	0.95±0.56	0.29±0.05	0.0000004*
psoralen (**10**)	0.002±0.008	0.03±0.05	0.11
xanthatoxin (**11**)	0.02±0.04	0.02±0.03	0.65
bergapten (**12**)	0.02±0.05	0.01±0.02	0.30
deltoin (**13**)	0.21±0.16	0.05±0.21	0.000002*

The contents are expressed as mean±SD.

Mongolian and Chinese groups were compared using Student's *t* test. *p<0.01

The regional variation was analyzed by comparing the levels of total dihydrofurochromones (TFC, **1**–**4**), total dihydropyranochromones (TPC, **5**–**9**), and total coumarins (TC, **10**–**13**) (Fig. 3-3). As a result, the specimens from Norovlin and Bayan-Uul had the highest level of TFC exhibiting mean values of 17.07 mg/g and 14.77 mg/g, respectively. Besides, the level of TFC was lower in the specimens from Ondorkhaan, showing a mean value of 8.82 mg/g. The variation of TFC was higher in the specimens from Khalkhgol (5.59–23.41 mg/g) and Holonbuir (3.37–26.12 mg/g), thus some outliers were observed (Fig. 3-3a). The specimens from Bayan-Uul showed a higher level of TPC (1.86–5.04 mg/g) (Fig 3-3b). The level of TC was higher in the specimens from Holonbuir (0.12–0.88 mg/g), but some outliers were observed (Fig. 3-3c).

Concerning the Chinese SR samples, the cultivated type of SR samples (C4, C10) contained a lower amount of chromones (**1**–**9**) than the wild types (Fig. 3-2, Table S1). Among the wild type of samples, C9, C5, and C7 had a large amount of **1** (10.26 mg/g), **2** (3.77 mg/g), and **3** (9.75 mg/g), respectively, compared with other SR samples and they contained a higher amount of **5**.

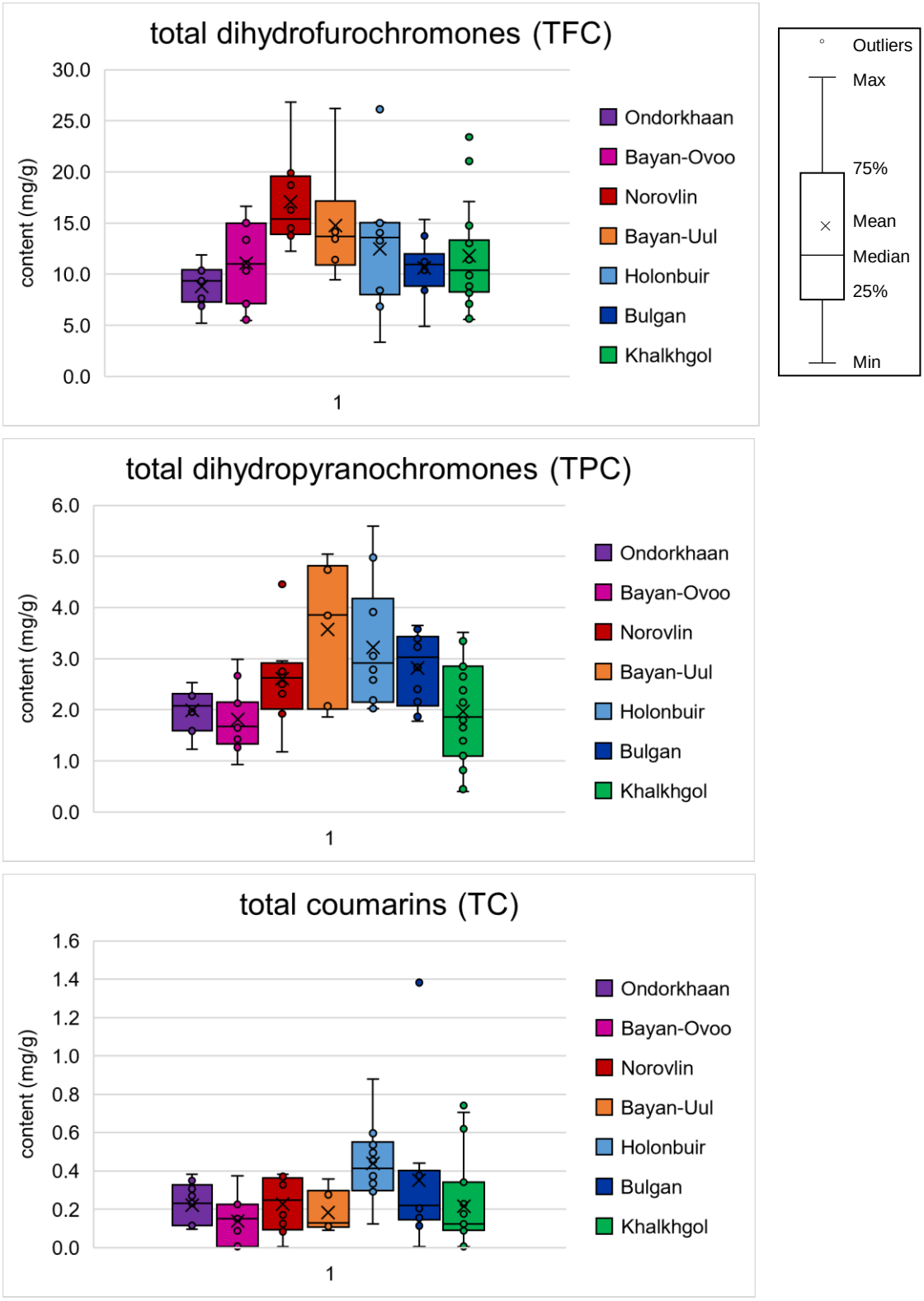

Fig. 3-3. Boxplots of the levels of TFC (a), TPC (b), and TC (c) in the Mongolian *S. divaricata* specimens collected from different regions.

3.2.5 Multivariate analysis based on HPLC-DAD data

The data matrix of peak areas of the compounds (**1**–**14**) was normalized by the Z-score transformation prior to the multivariate statistical analysis. PCA was carried out for 42 plant specimens (except for 2 specimens; M65, M66) collected in the seven different regions of Mongolia. However, a clear separation was not observed (data not shown). Then OPLS-DA was performed on 39 plant specimens except for 3 specimens (M1, M63, M64), which were collected after the fruiting period. The OPLS-DA had better performance with parameters of R^2=0.76 and Q^2=0.27 based on cross-validation. In association with the score and loading scatter plots (Fig. 3-4), the correlation matrix of compounds and regions is used (Table 3-6). The results indicated that the Mongolian specimens could be roughly separated into three groups based on their growing regions. Group 1 was composed of the specimens from Norovlin and Bayan-Uul, in which the specimens from Norovlin showed weak positive correlations with **1**, **3**, and **8**, while those from Bayan-Uul displayed weak positive correlations with **5**, **7**, **8**, and **9**, and moderate positive correlation with **14**. Group 2, consisting of the specimens from Holonbuir, was likely to include those from Bulgan. Here, the specimens from Holonbuir showed weak positive correlations with **6**–**8** and **10**–**12**, while those from Bulgan showed a weak positive correlation with **13**. Group 3 included the specimens from Khalkhgol and they showed a weak positive correlation with **2** and weak negative correlations with **8**, **9**, and **14**. The specimens from Ondorkhaan and Bayan-Ovoo tended to be included in the Khalkhgol group.

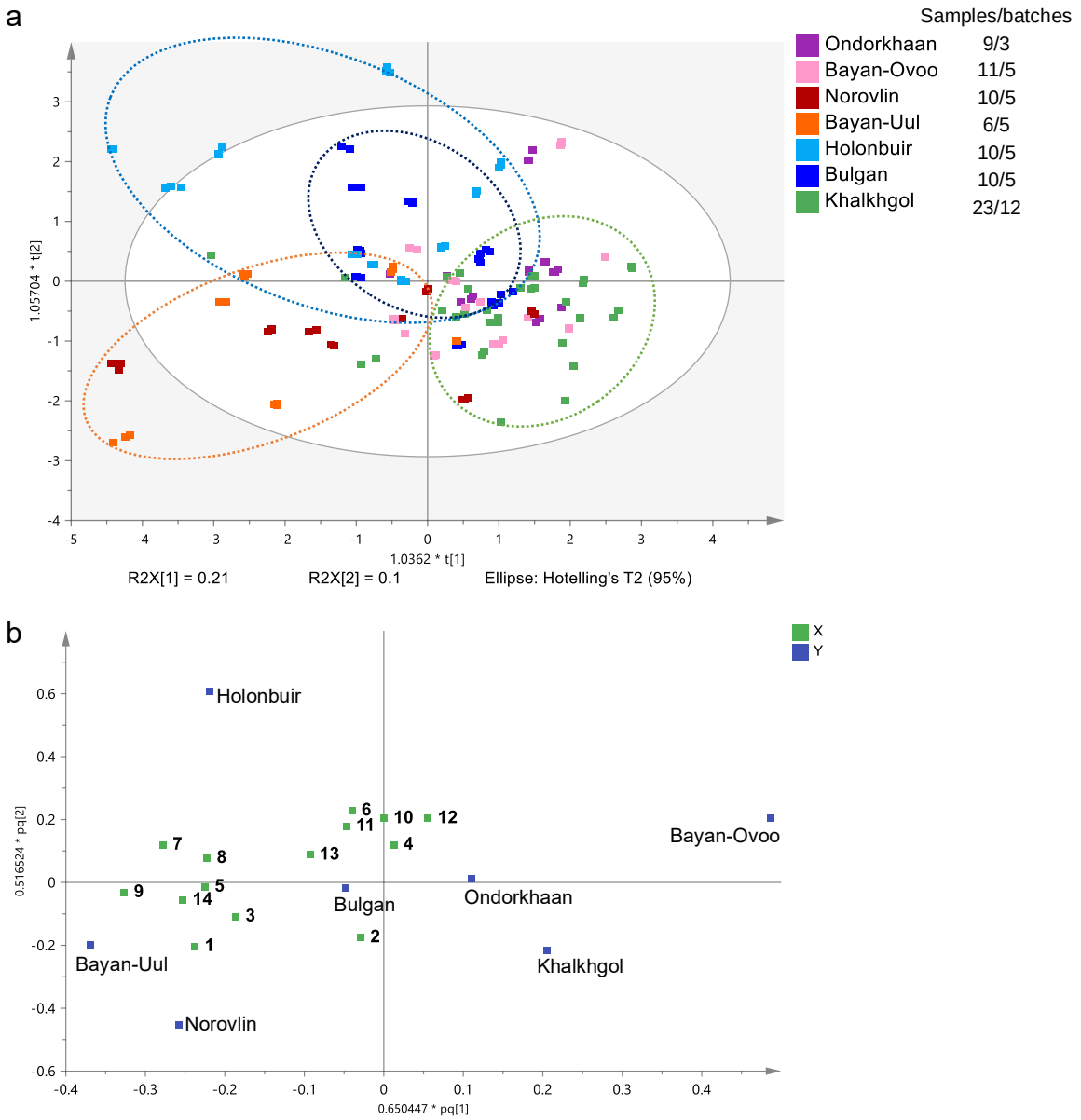

Fig. 3-4. OPLS-DA of Mongolian *S. divaricata* specimens collected from different regions. Score scatter plot (a) and loading scatter plot (b). X indicates the compounds shown in Fig. 2-5 (green) and Y indicates the response variables to each region (blue).

Table 3-6. The correlation matrix of determined compounds and regions.

Compounds	Regions						
	Ondor khaan	Bayan-Ovoo	Norovlin	Bayan-Uul	Holonbuir	Bulgan	Khalkhgol
prim-*O*-glucosylcimifugin (**1**)	-0.2407	-0.0278	0.3385	0.1642	0.0145	-0.0653	-0.1144
cimifugin (**2**)	-0.1109	-0.1350	0.0205	0.1757	-0.1460	-0.1455	0.3194
4'-*O*-glucosyl-5-*O*-methylvisamminol (**3**)	-0.1728	-0.1000	0.3449	0.1484	0.0790	-0.1548	-0.0778
5-*O*-methylvisamminol (**4**)	-0.1007	-0.0099	-0.0240	-0.0585	0.1594	0.0655	-0.0530
sec-*O*-glucosylhamaudol (**5**)	-0.0362	-0.2118	-0.0349	0.3162	0.0722	0.0163	-0.0745
hamaudol (**6**)	0.1071	-0.1646	-0.1959	-0.1450	0.2483	0.1674	-0.0670
3'-*O*-acetylhamaudol (**7**)	-0.2168	-0.1390	-0.0253	0.2690	0.3803	-0.0845	-0.1491
ledebouriellol (**8**)	-0.2796	-0.0102	0.2528	0.2335	0.2338	-0.0473	-0.2947
3'-*O*-angeloylhamaudol (**9**)	-0.2419	-0.1531	0.1429	0.2823	0.1740	0.1675	-0.2979
psoralen (**10**)	-0.0764	0.0726	0.0098	-0.0679	0.2304	-0.0922	-0.0808
xanthatoxin (**11**)	0.1727	-0.0868	-0.0753	-0.0822	0.2978	-0.1105	-0.1128
bergapten (**12**)	-0.0833	0.1432	-0.0915	-0.1268	0.2522	-0.0502	-0.0727
deltoin (**13**)	-0.1206	-0.1971	-0.0209	-0.0725	0.1694	0.2433	-0.0427
3'-*O*-(6''-*O*-malonyl)-glucosylhamaudol (**14**)	0.0553	-0.1151	0.0595	0.4707	-0.0032	0.0525	-0.3748

3.2.6 Characterization of metabolites by ^{1}H NMR analysis

The signals of metabolites in ^{1}H NMR spectra of the extracts were assigned by comparison with those of reference compounds (Table 3-7). Due to the similarity in their structure, the signals from the compounds overlapped with each other. Therefore, most of the compounds in the extracts were tentatively identified and assigned using the specimen M64, which shows clear signals of chromones due to a trace amount of sugars and a higher amount of chromones (Fig. 3-5). For dihydrofurochromones (**1**–**4**): δ_H 1.17–1.29 (each s, *gem*-$(CH_3)_2$), 2.29 (s, H_3-11), 3.84–3.85 (s, 5-OCH_3), 4.35–4.68 (d, J = 6 or 15 Hz, 11-H_2), 4.34–4.74 (t, J = 6 or 9 Hz, H-2′), 5.99–6.33 (s, H-3), 6.66–6.69 (s, H-8). For dihydropyranochromones (**5**–**9**): δ_H 1.26–1.38 (each s, *gem*-$(CH_3)_2$), 2.38–2.39 (s, H_3-12), 2.50–2.91 (dd, J = ca 17.0 and ca 5.0 Hz, H_a-4′), 2.80–3.01 (dd, J = ca 17.0 and ca 5.0 Hz, H_b-4′), 6.22–6.29 (s, H-3), 6.40–6.49 (s, H-8). Further, H-3″of the angeloyl moiety of **8** and **9** at C-3′ position was observed at δ_H 6.15 (dq, J = 7, 1.5 Hz), while the methyl groups of C-4″ and C-5″ were observed at δ_H 1.79 (dd, J = 7, 1.5 Hz) and 1.83 (t, J = 1.3 Hz), respectively. Moreover, the anomeric proton signals of 3 chromone glucosides (**1**, **3**, and **5**) were observed at δ_H 4.31–4.44 ppm (d, J = 8 Hz, H-1″). For coumarins (**10**–**13**), the signals at 7.98–8.24 (d, J = 10 Hz, H-4), δ 6.89–8.05 (s, H-5), 7.39-7.78 (s, H-8), 8.07-8.16 (d, J = 2 Hz, H-2′) were assigned and methyl groups (C-4″ and C-5″) of the angeloyl moiety of **13** were weakly observed at δ 1.57 (dt, J = 7, 1.5 Hz) and 1.81 (t, J = 1.5 Hz).

Table 3-7. Assignment of protonic signals of reference compounds

Compounds	δ_H (mult.)*
prim-*O*-glucosylcimifugin (**1**)	6.33 (1H, s, H-3), 3.85 (3H, s, 5-OCH_3), 6.68 (1H, s, H-8), 4.74 (1H, t, *J* = 9.0 Hz, H-2'), 3.26 (2H, q, *J* = 3.8 Hz, H-3'), 1.17, 1.18 (3H each, s, *gem*-$(CH_3)_2$), 4.68 (1H, d, *J* = 15.0 Hz, Hb-11), 4.54 (1H, d, *J* = 15.0 Hz, Ha-11), 4.31 (1H, d, *J* = 7.9 Hz, H-1"), 3.04-3.11 (2H, m, H-2", 3"), 3.15-3.19 (2H, m, H-4", 5"), 3.44-3.49 (1H, m, Ha-6"), 3.68-3.72 (1H, m, Hb-6"), 4.57 (1H, t, *J* = 5.8 Hz, 6"-OH), 4.98 (1H, d, *J* = 5.4 Hz, 2"-OH), 5.04 (1H, d, *J* = 4.8 Hz, 3"-OH), 5.32 (1H, d, *J* = 4.9 Hz, 4"-OH)
cimifugin (**2**)	6.09 (1H, s, H-3), 3.85 (3H, s, 5-OCH_3), 6.66 (1H, s, H-8), 4.73 (1H, t, *J* = 8.5 Hz, H-2'), 3.27 (2H, q, *J* = 4.0 Hz, H-3'), 1.17, 1.18 (3H each, s, *gem*-$(CH_3)_2$), 4.35 (2H, d, *J* = 6.0 Hz, H_2-11), 5.71 (1H, d, *J* = 6.0 Hz, 11-OH)
4'-*O*-glucosyl-5-*O*-methylvisamminol (**3**)	5.99 (1H, s, H-3), 3.84 (3H, s, 5-OCH_3), 6.69 (1H, s, H-8), 4.34 (1H, t, *J* = 5.7 Hz, H-2'), 3.26 (2H, dd, *J* = 9.5, 16.1 Hz, H-3'), 1.27, 1.29 (3H each, s, *gem*-$(CH_3)_2$), 2.29 (3H, s, H_3-11), 4.44 (1H, d, *J* = 7.8 Hz, H-1"), 2.87-2.91 (1H, m, H-2"), 3.02-3.09 (2H, m, H-3", 4"), 3.13-3.19 (1H, m, H-5"), 3.41-3.44 (2H, m, H-6"), 4.84-4.91 (3H, m, 2", 3", 4"-OH), 4.33 (1H, t, *J* = 5.4 Hz, 6"-OH)
5-*O*-methylvisamminol (**4**)	5.99 (1H, s, H-3), 3.84 (3H, s, 5-OCH_3), 6.69 (1H, s, H-8), 4.73 (1H, t, *J* = 8.3 Hz, H-2'), 3.24 (2H, dd, *J* = 4.5, 9.0 Hz, H-3'), 1.17, 1.18 (3H each, s, *gem*-$(CH_3)_2$), 2.29 (3H, s, H_3-11)
sec-*O*-glucosylhamaudol (**5**)	6.23 (1H, s, H-3), 6.42 (1H, s, H-8), 2.38 (3H, s, H_3-11), 13.24 (1H, s, 5-OH), 4.00 (1H, t, *J* = 5.8 Hz, H-3'), 1.31, 1.36 (3H each, s, *gem*-$(CH_3)_2$), 2.63 (1H, dd, *J* = 6.5, 17.1 Hz, Hb-4'), 2.91 (1H, dd, *J* = 5.3, 17.1 Hz, Ha-4'), 4.35 (1H, d, *J* = 7.8 Hz, H-1"), 2.93-2.97 (1H, m, H-2"), 3.02-3.07 (1H, m, H-3"), 3.14-3.18 (2H, m, H-4", 5"), 3.44-3.79 (1H, m, Ha-6"), 3.69-3.72 (1H, m, Hb-6"), 4.42 (1H, t, *J* = 6.0 Hz, 6"-OH), 4.91-4.95 (3H, m, 2", 3", 4"-OH)
hamaudol (**6**)	6.22 (1H, s, H-3), 6.40 (1H, s, H-8), 2.38 (3H, s, H_3-11), 13.20 (1H, s, 5-OH), 3.73 (1H, t, *J* = 6.3 Hz, H-3'), 5.29 (1H, d, *J* = 4.3 Hz, 3'-OH), 1.26, 1.32 (3H each, s, *gem*-$(CH_3)_2$), 2.50 (1H, dd, *J* = 6.8, 17.1 Hz, Hb-4'), 2.80 (1H, dd, *J* = 5.3, 17.1 Hz, Ha-4')
3'-*O*-acetylhamaudol (**7**)	6.24 (1H, s, H-3), 6.47 (1H, s, H-8), 2.39 (3H, s, H_3-11), 13.24 (1H, s, 5-OH), 5.10 (1H, t, *J* = 4.5 Hz, H-3'), 2.04 (1H, s, 3'-OH), 1.31, 1.35 (3H each, s, *gem*-$(CH_3)_2$), 2.69 (1H, dd, *J* = 3.8, 17.7 Hz, Hb-4'), 2 95 (1H, dd, *J* = 4.8, 17.7 Hz, Ha-4')
ledebouriellol (**8**)	6.29 (1H, s, H-3), 6.49 (1H, s, H-8), 13.19 (1H, s, 5-OH), 5.86 (1H, t, *J* = 5.5 Hz, H-3'), 1.35, 1.38 (3H each, s, *gem*-$(CH_3)_2$), 2.75 (1H, dd, *J* = 3.8, 17.7 Hz, Hb-4'), 3.01 (1H, dd, *J* = 4.5, 17.7 Hz, Ha-4'), 4.43 (2H, d, *J* = 5.0 Hz, H_2-11), 5.19 (1H, t, *J* = 4.3 Hz, 11-OH), angeloyl: 1.79 (3H, t, *J* = 1.3 Hz, H_3-5"), 1.83 (3H, dd, *J* = 1.3, 7.3 Hz, H_3-4"), 6.15 (1H, dq, *J* = 1.0, 7.0 Hz, H-3")
3'-*O*-angeloylhamaudol (**9**)	6.24 (1H, s, H-3), 6.49 (1H, s, H-8), 2.39 (3H, s, H_3-11), 13.24 (1H, s, 5-OH), 5.18 (1H, t, *J* = 4.3 Hz, H-3'), 1.35, 1.38 (3H each, s, *gem*-$(CH_3)_2$), 2.74 (1H, dd, *J* = 3.8, 17.7 Hz, Hb-4'), 3.00 (1H, dd, *J* = 4.8, 17.7 Hz, Ha-4'), angeloyl: 1.79 (3H,t, *J* = 1.3 Hz, H_3-5"), 1.83 (3H, dq, *J* = 1.5, 7.3 Hz, H_3-4"), 6.15 (1H, dq, *J* = 1.3, 7.3 Hz, H-3")
psoralen (**10**)	6.47 (1H, d, *J* = 9.5 Hz, H-3), 8.21 (1H, d, *J* = 9.5 Hz, H-4), 8.05 (1H, s, H-5), 7.78 (1H, s, H-8), 8.15 (1H, d, *J* = 2.0 Hz, H-2'), 7.13 (1H, d, *J* = 2.3 Hz, H-3')
xanthatoxin (**11**)	6.47 (1H, d, *J* = 9.5 Hz, H-3), 8.18 (1H, d, *J* = 9.5 Hz, H-4), 7.72 (1H, s, H-5), 4.21 (3H, s, 8-OCH_3), 8.16 (1H, d, *J* = 2.0 Hz, H-2'), 7.14 (1H, d, *J* = 2.0 Hz, H-3')
bergapten (**12**)	6.36 (1H, d, *J* = 9.8 Hz, H-3), 8.24 (1H, d, *J* = 9.8 Hz, H-4), 7.39 (1H, s, H-8), 4.30 (3H, s, 5-OCH_3), 8.07 (1H, d, *J* = 2.5 Hz, H-2'), 7.42 (1H, d, *J* = 2.3 Hz, H-3')
deltoin (**13**)	6.26 (1H, d, *J* = 9.5 Hz, H-3), 7.98 (1H, d, *J* = 9.5 Hz, H-4), 6.89 (1H, s, H-5), 7.54 (1H, s, H-8), 5.07 (1H, dd, *J* = 7.0, 9.8 Hz, H-2'), 3.28 (1H, dd, *J* = 7.0, 16.3 Hz, H-3'), 1.54, 1.61 (3H each, s, gem-$(CH_3)_2$), angeloyl: 1.57 (3H,t, *J* = 1.5 Hz, H_3-5"), 1.81 (3H, dt, *J* = 1.5, 7.3 Hz, H_3-4"), 6.00 (1H, dq, *J* = 1.5, 7.3 Hz, H-3")
3'-*O*-glucosyl-6"-*O*-malonyl-hamaudol (**14**)	6.17 (1H, s, H-3), 6.37 (1H, s, H-8), 2.34 (3H, s, H_3-11), 3.87 (1H, t, *J* = 5.7 Hz, H-3'), 1.25, 1.28 (3H each, s, *gem*-$(CH_3)_2$), 2.60 (1H, dd, *J* = 6.1, 16.8 Hz, Hb-4'), 2.85 (1H, dd, *J* = 5.4, 17.6 Hz, Ha-4'), 4.32 (1H, d, *J* = 7.6 Hz, H-1"), 2.91 (1H, t, *J* = 8.4 Hz, H-5"), 3.06 (1H, t, *J* = 9.2 Hz, H-4"), 3.17 (1H, t, *J* = 8.4 Hz, H-3"), 3.36 (1H, m, H-2"), 4.09 (1H, dd, *J* = 6.8, 12.1 Hz, Ha-6"), 4.23 (1H, d, *J* = 2.0, 12.1 Hz, Hb-6"), malonyl: 3.09 (2H, s, H_2-2'")
panaxynol (**15**)	5.13 (1H, d-overlapped, *J* = 9.9 Hz, Ha-1), 5.30 (1H, t-like, *J* = 16.1 Hz, Hb-1), 5.83 (1H, ddd, *J* = 5.4, 11.5, 16.8 Hz, H-2), 4.83 (1H, d, *J* = 5.4 Hz, H-3), 3.09 (1H, d, *J* = 7.6 Hz, H-8), 5.33 (1H, d-overlapped, *J* = 9.9 Hz, H-9), 5.48 (1H, dt, *J* = 7.6, 9.9 Hz, H-10), 2.00 (1H, q, *J* = 6.9 Hz, H-11), 1.22-1.40 (10H, br s, H-12, 13, 14, 15, 16), 0.84 (3H, t, *J* = 7.6 Hz, H-17), 2.16 (1H, t, *J* = 7.6 Hz, 3-OH)
sucrose	5.17 (1H, d, *J* = 3.8 Hz, H-1), 3.20 (1H, dd, *J* = 9.2, 3.1 Hz, H-2), 3.49 (1H, t, *J* = 9.2 Hz, H-3), 3.15 (1H, t, *J* = 9.2 Hz, H-4), 3.67 (1H, m, H-5), 3.53 (2H, d, *J* = 4.6 Hz, H-6), 3.43 (2H, s, H-1′), 3.91 (2H, d, *J* = 7.6 Hz, H-3′), 3.80 (1H, t, *J* = 7.6 Hz, H-4′), 3.69 (1H, m, H-5′), 3.59 (2H, d, *J* = 3.8 Hz, H-6′)
glucose	4.89 (1H, d, *J* = 3.8 Hz, H-1), 3.40 (1H, t, *J* = 9.2 Hz, H-2), 3.09 (1H, dd, *J* = 9.2, 3.8 Hz, H-3), 3.52-3.55 (1H, m, H-4), 3.02 (1H, t, *J* = 9.2 Hz, H-5), 3.58 (1H, dd, *J* = 11.5, 2.3 Hz, H-6), 3.41-3.44 (1H, m, H-6'),

*: Underlined δ_H are assigned in Fig. 3-5.

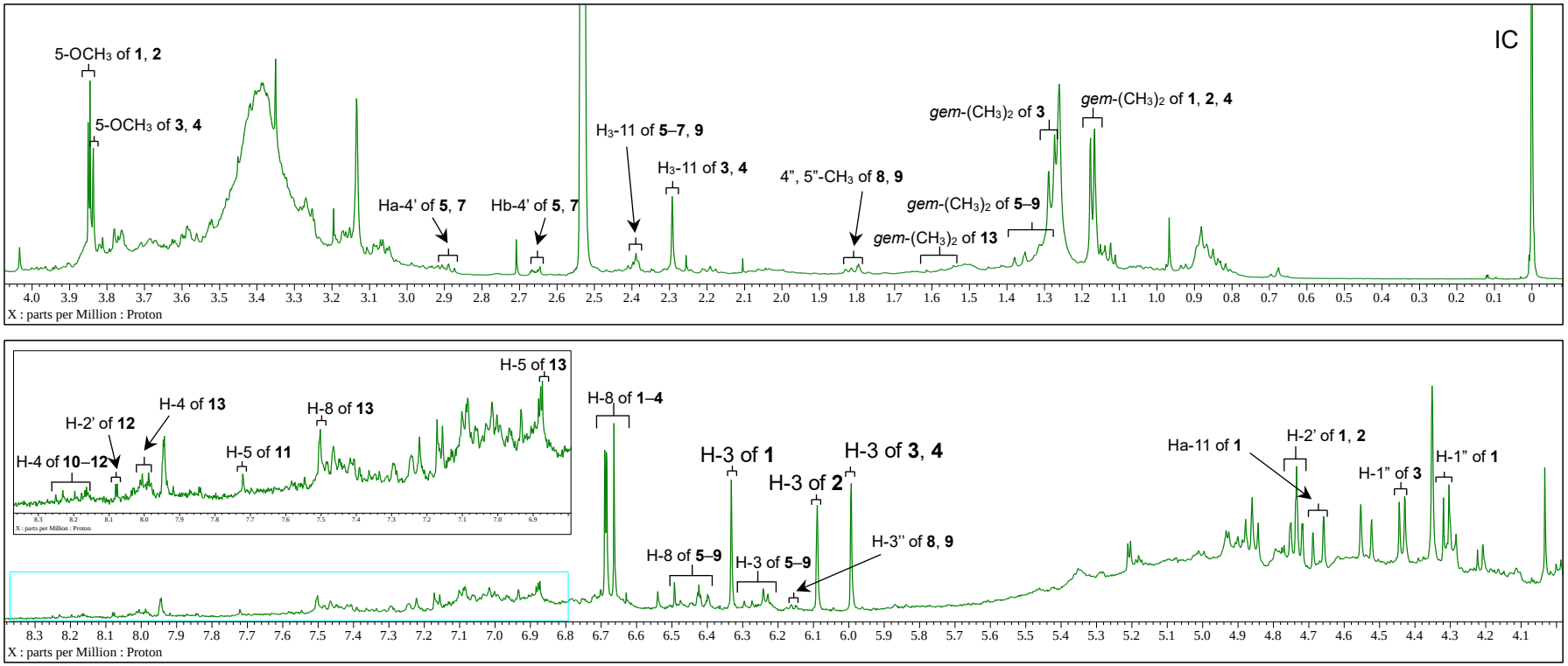

Fig. 3-5. ^{1}H NMR assignments of characteristic signals of compounds **1**–**13** in 70% MeOH extract of Mongolian *S. divaricata* roots (M64, lower part). Upper range, 0.0–4.0 ppm; Lower range, 4.0–8.3 ppm.

^{1}H NMR profiling of 24 specimens of Mongolian *S. divaricata* that were collected in 2015 and 2019 and two Chinese SR samples was conducted to characterize the metabolites, especially sugars and polyacetylenes as well as chromones and coumarins. All specimens and SR samples showed similar profiles regarding chromones and coumarins in the ^{1}H NMR spectrums (Fig. 3-6). Although coumarins were not detected in several specimens, chromones (δ_H 5.99-6.69 ppm) were detected in all specimens from Mongolia and SR samples (Table 3-8). Regarding sugars (δ_H 3.00-5.50 ppm), the intensity of sugar signals varied greater by growing conditions (wild or cultivated) than growing regions. For instance, the intensity of sugar signals in the cultivated type of SR sample C10 was substantially higher than in the wild type of SR sample C9 and Mongolian specimens. In contrast, several Mongolian specimens had characteristic signals to polyacetylenes (δ_H 5.86, 1.20-1.40 ppm).

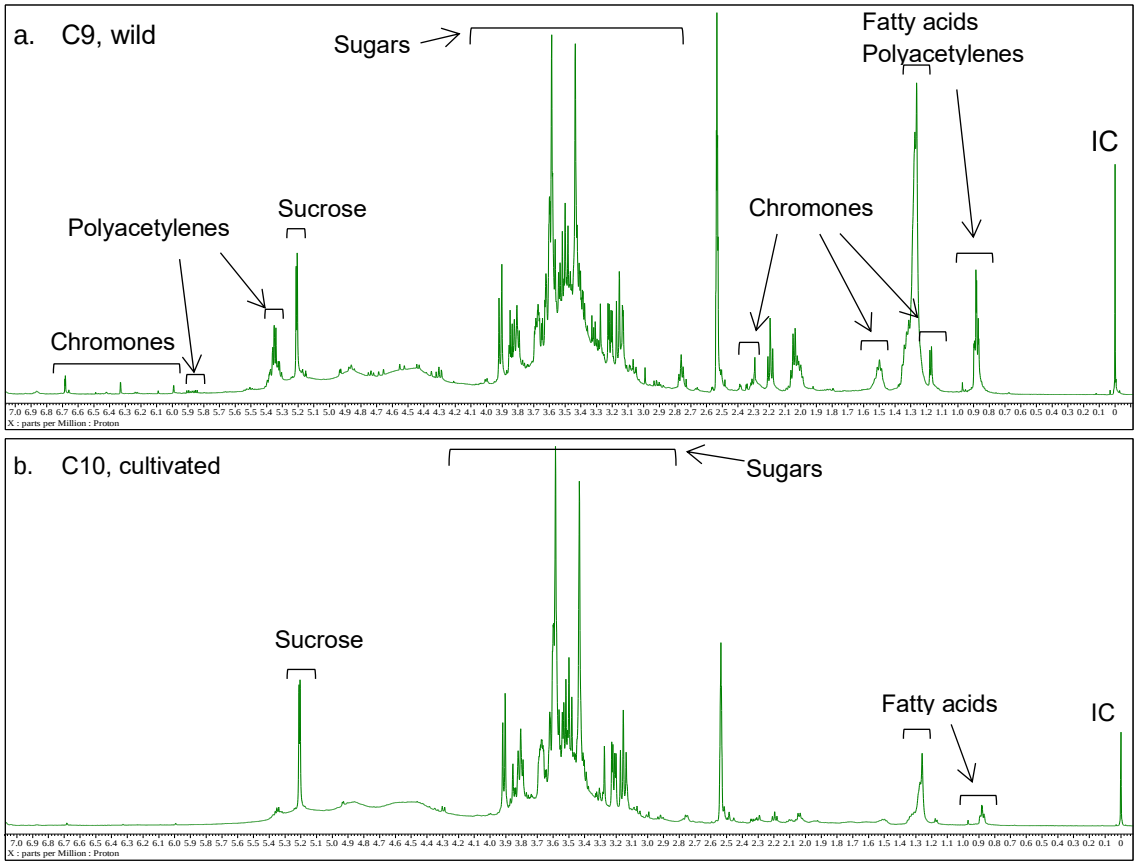

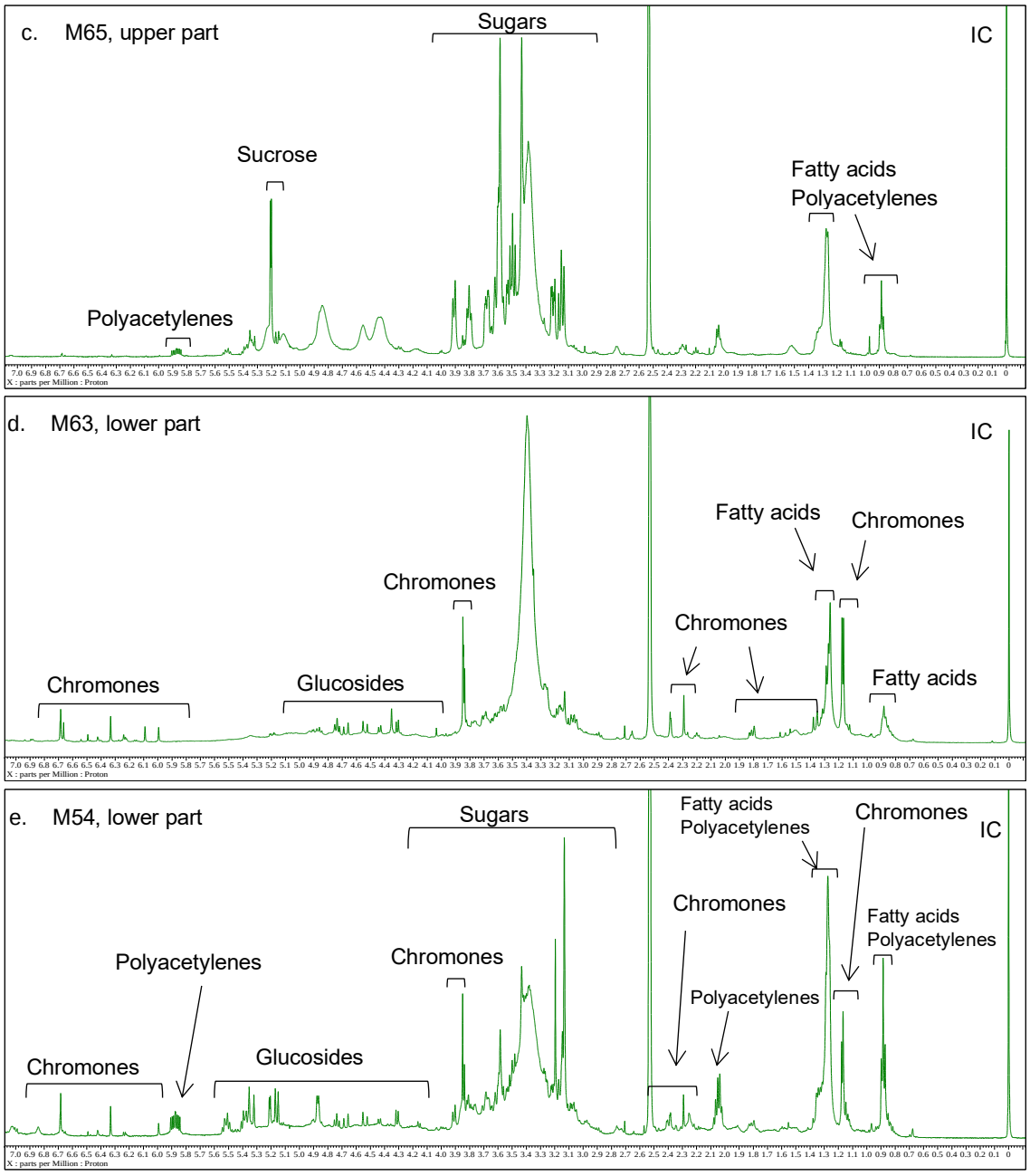

Fig. 3-6. ^{1}H NMR spectrums of Chinese SR samples C9 (a), C10 (b) and Mongolian plant specimens M65, upper part (c); M63, lower part (d); M54, lower part (e) of the root.

Table 3-8. ^{1}H NMR profiling of Mongolian *S. divaricata* specimens and Chinese SR samples.

Cmpd*	δ_H (ppm)	Pattern of signal	Bayan-Ovoo		Norovlin					Bayan-Uul					Holonbuir				Bulgan				Khalkhgol		Kherlem		China	
			M59	M60	M61	M63	M44	M45	M46	M47	M48	M49	M50	M51	M55	M56	M57	M58	M62	M52	M53	M54	M1	M64	M65	M66	C9	C10
poly., FA	0.87	t at H_3-17	+	+	+	+	+	+	+	+	+	+	+	+	+	+	+	+	+	+	+	+	+	+	+	+	+	+
1, **2**, **4**	1.17, 1.18	s, *gem*-$(CH_3)_2$	+	+	+	+	+	+	+	+	+	+	+	+	+	+	+	+	+	+	+	+	+	+	+	+	+	+
15, FA	1.22-1.40	s, *gem*-$(CH_3)_2$	+	+	+	+	+	+	+	+	+	+	+	+	+	+	+	+	+	+	+	+	+	+	+	+	+	+
3	1.27, 1.29	s, *gem*-$(CH_3)_2$	+	+	+	+	+	+	+	+	+	+	+	+	+	+	+	+	+	+	+	+	+	+	+	+	+	+
5, **6**	1.26-1.36	s, *gem*-$(CH_3)_2$	+	+	+	+	+	+	+	+	+	+	+	+	+	+	+	+	+	+	+	+	+	+	+	-	+	+
8, **9**	1.35, 1.38	s, *gem*-$(CH_3)_2$	+	+	+	+	+	+	+	+	+	+	+	+	+	+	+	+	+	+	+	+	+	+	+	-	+	+
13	1.57, 1.81	s, H_3-4", 5"	-	-	-	-	-	-	-	+	-	-	-	-	+	-	-	+	+	+	+	+	-	+	-	-	-	+
8, **9**	1.79, 1.83	s, H_3-4", 5"	+	+	+	+	+	+	+	+	+	+	+	+	+	+	+	+	+	+	+	+	+	+	+	+	+	+
15	2.19	t, 3-OH	+	-	+	+	-	-	-	-	-	+	+	+	+	+	+	+	+	+	-	-	+	+	+	+	+	+
3, **4**	2.29	s, H_3-11	+	+	+	+	+	+	+	+	+	+	+	+	+	+	+	+	+	+	+	+	+	+	+	+	+	+
5–**7**	2.38-2.39	s, H_3-11	+	+	+	+	+	+	+	+	+	+	+	+	+	+	+	+	+	+	+	+	+	+	+	+	+	+
1–**4**	3.84-3.85	s, 5-OCH_3	+	+	+	+	+	+	+	+	+	+	+	+	+	+	+	+	+	+	+	+	+	+	+	+	+	+
1	4.31	d, H-1"	+	+	+	+	+	+	+	+	+	+	+	+	+	+	+	+	+	+	+	+	+	+	-	+	+	-
5	4.35	d, H-1"	-	-	-	-	-	+	+	+	-	+	-	+	-	-	+	-	+	-	-	+	-	-	-	-	+	-
3	4.44	d, H-1"	+	+	+	+	+	+	+	+	+	+	+	+	+	+	+	+	+	+	+	+	+	+	-	+	+	-
sucrose	5.20	d, H-1	+	+	+	-	+	+	+	+	+	+	+	+	+	+	+	+	+	+	+	+	+	+	+	+	+	+
poly.	5.83	ddd, H-2	+	-	-	-	-	+	+	+	-	-	-	+	+	+	+	+	-	+	+	+	+	-	-	+	+	-
3, **4**	5.99	s, H-3	+	+	+	+	+	+	+	+	+	+	+	+	+	+	+	+	+	+	+	+	+	+	+	+	+	+
2	6.09	s, H-3	+	+	+	+	+	+	+	+	+	+	+	+	+	+	+	+	+	+	+	+	+	+	+	+	+	-
8, **9**	6.15	dq, H-3"	-	-	-	-	+	+	-	+	-	+	+	+	+	-	+	+	+	+	+	-	-	-	-	-	-	-
5–**9**	6.22-6.29	s, H-3	+	+	+	+	+	+	+	+	+	+	+	+	+	+	+	+	+	+	+	+	+	+	+	+	+	-
1	6.33	s, H-3	+	+	+	+	+	+	+	+	+	+	+	+	+	+	+	+	+	+	+	+	+	+	+	+	+	+
1–**4**	6.66-6.69	s, H-8	+	+	+	+	+	+	+	+	+	+	+	+	+	+	+	+	+	+	+	+	+	+	+	+	+	+
5–**9**	6.42-6.49	s, H-8	+	+	+	+	+	+	+	+	+	+	+	+	+	+	+	+	+	+	+	+	+	+	+	+	+	-
10–**13**	6.89-8.05	s, H-5	-	-	-	+	+	+	+	+	+	-	-	-	-	-	-	-	+	-	-	-	-	+	-	-	-	-
10, **13**	7.54, 7.78	s, H-8	-	-	-	+	-	-	-	-	-	-	-	-	-	-	-	-	+	-	-	-	-	+	-	-	-	-
10–**12**	8.07-8.16	d, H-2'	-	-	-	+	-	-	-	-	-	-	-	-	-	-	-	-	-	-	-	-	-	+	-	-	-	-
10–**13**	7.98-8.24	s, H-4	-	-	-	+	-	-	-	-	-	-	-	-	-	-	-	-	+	-	-	-	-	+	-	-	-	-
5–**9**	13.19-13.24	s, 5-OH	-	-	-	-	-	-	-	-	-	-	-	-	-	-	-	-	-	-	-	-	-	+	-	-	-	-

*: fatty acids (FA), polyacetylenes (poly.)

+: detected; -: not detected

3.2.7 Quantification of compounds by qHNMR analysis

Among the chromones signals assigned in ^{1}H NMR spectrum of the extract, the H-3 signals of **1** and **2** were clearly observed as singlets at δ_H 6.33 and δ_H 6.09, respectively, and those of **3** and **4** were observed redundantly at δ_H 5.99 due to their similar structure (Fig. 3-7). These 3 signals could be used for the rapid quantification of major chromones in the extracts by qHNMR analysis. Therefore, the qHNMR analysis for the quantification of dihydrofurochromones **1**–**3** was performed on 24 Mongolian specimens and two SR samples. The integral values of the H-3 signals of **1** (δ_H 6.33, s), **2** (δ_H 6.09, s), and **3** (including **4**) (δ_H 5.99, s) were referred to those of DSS-*d*$_6$ at δ_H 0.00 for determining their contents. Although the H-3 signal of **3** overlapped with that of **4**, the molecular weight of **3** was applied to calculate the content of **3**, as the content of **4** was less than 3.6% of **3** when determined in the HPLC. As a result, the content of **3** determined by qHNMR method was 0.10–0.97% and slightly higher than that by the HPLC method (0.10–0.99%) (Table 3-9). The content of **1** determined by the qHNMR method was 0.20–1.95% and slightly lower than that by the HPLC method (0.20–2.08%). The content of **2** was 0.01–0.35% in both methods.

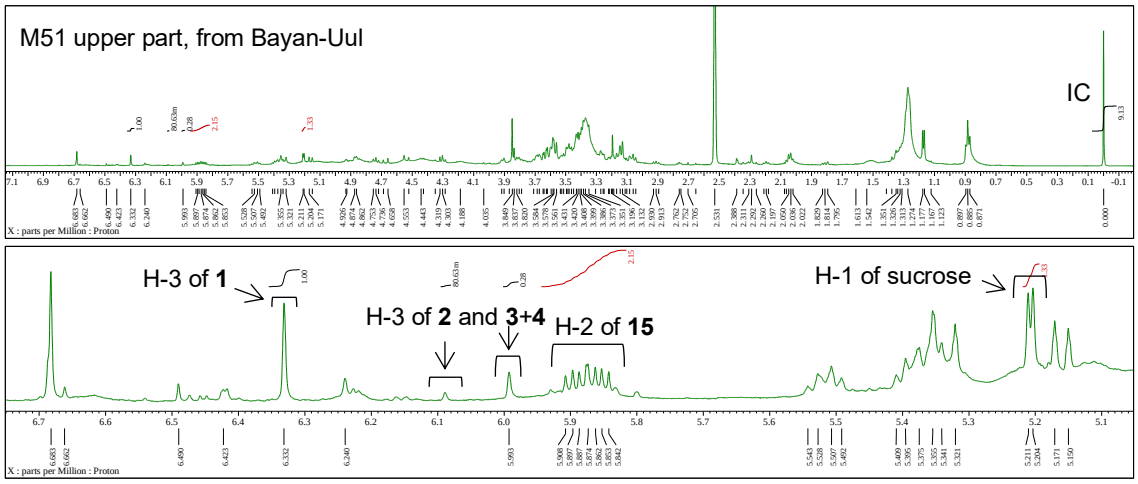

Fig. 3-7 qHNMR spectrum of 70% MeOH extract of M51 upper part from Bayan-Uul in DMSO-*d*$_6$. Upper: -0.1–7.1 ppm; Lower: 5.1–6.7 ppm.

For estimating sugar levels, carbohydrate signals (δ_H 3.00–5.50) in ^{1}H NMR spectra of the extracts were compared with signals of sucrose and glucose (Fig. 3-6, 3-8 a, b). As shown in Fig. 3-6, sucrose was the most abundant sugar in the extracts, with clear signals at δ_H 3.43 (2H, s, H-1′), 3.59 (2H, d, J = 3.8 Hz, H-6′), 5.17 (1H, d, J = 3.8 Hz, H-1) (Table 3-7). Although the anomeric proton signal of sucrose (δ_H 5.17) did not showed baseline separation, its integral value was used for estimating sucrose level by comparing it with the value of the signal of DSS-d_6 (IC) at 0.00 (Table 3-9). Nineteen specimens contained an extremely lower amount of sucrose (0.11–9.76%) than the 2 Chinese SR samples and the 2 Mongolian specimens (M65, M66). The level of sucrose was the highest in the cultivated SR sample C10 (25.91%) and was 13.06% in the wild SR sample C9. Two specimens (M65, M66) had a higher amount of sucrose (16.19 and 17.48%, respectively), while 2 specimens (M61, M64) had a trace amount of sucrose. The specimens and SR samples with higher sucrose levels exhibited a higher yield of extracts (Table 3-9). The yield of the extracts from the majority of Mongolian specimens was from 9.1 to 27.3%, while Chinese SR samples and 3 specimens (M65, M66, M1) exhibited 2–3 fold higher yield.

For investigating the level of polyacetylenes, the signals in the extracts were compared with the signals of panaxynol (**15**) since it is a major polyacetylene in SR (Figs 3-6, 3-7) [6,71,72]. In several specimens, a strong signal at δ_H 5.83 derived from H-2 signal of polyacetylenes including **15** was detected (Fig. 3-6, Table 3-9). The integral value of the signal at δ_H 5.83 was used for calculating polyacetylenes level by comparing with that of DSS-d_6 (IC). Seven Mongolian specimens contained a substantial amount of polyacetylenes (1.04–2.91%), while 8 Mongolian specimens and the wild type of SR sample C9 contained a lower amount of polyacetylenes (0.23–0.91%). The other 9

specimens and cultivated type of SR sample C10 had no polyacetylenes signal.

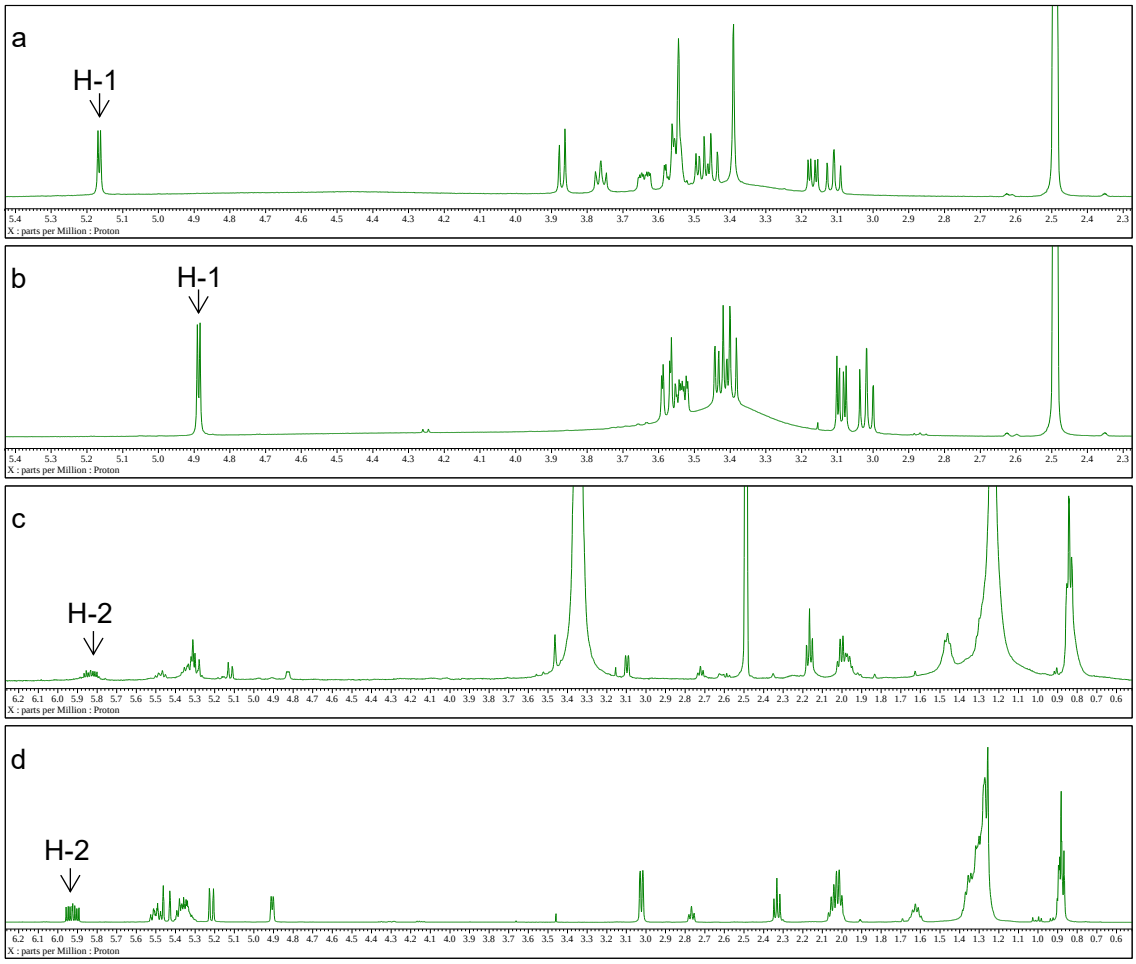

Fig. 3-8 ^{1}H NMR spectrums of sucrose (a), glucose (b), and panaxynol (c) in DMSO-*d*$_6$ and panaxynol (d) in $CDCl_3$.

Table 3-9. Content (%) of compounds in Mongolian specimens and Chinese SR samples by qHNMR analysis.

No.	Field No.	n[a]	Locality	Root parts	Yield[b] (%)		HPLC analysis			qHNMR analysis							
					Mean	SD	1	2	3	1	2	3	Total	Sucrose[c]	RSD	Polyacetylenes[c]	RSD
M59	MIV112	2	Bayan-Ovoo, Khentii prov.	low	15.33	0.12	0.75	0.04	0.39	0.47	0.04	0.37	0.88	1.16	1.09	1.04	0.67
M60	MIV114	3		mid	16.56	1.07	0.88	0.03	0.27	0.69	0.03	0.27	0.99	0.57	1.83	nd	nd
M61	MII060	1	Norovlin, Khentii prov.	low	17.30	0.00	0.92	0.10	0.42	0.71	0.10	0.43	1.24	nd	-	nd	-
M63	JB1501	3		low	12.13	0.32	1.16	0.35	0.45	0.85	0.35	0.48	1.68	0.11	0.91	nd	-
M44	MIV017	3		low	20.03	0.49	1.65	0.03	0.99	1.34	0.03	0.97	2.34	1.65	0.09	nd	-
M45	MIV019	3		low	22.40	0.17	1.62	0.05	0.31	1.37	0.06	0.32	1.75	2.25	0.73	1.81	2.44
M46	MIV025	2		low	17.82	0.20	0.73	0.06	0.42	0.64	0.05	0.42	1.11	2.43	0.62	0.35	0.52
M47	MIV030	3	Bayan-Uul, Dornod prov.	low	17.47	0.49	0.92	0.08	0.39	0.67	0.08	0.39	1.14	1.42	0.78	2.06	0.78
M48	MIV033	3		up	19.44	2.31	0.83	0.03	0.47	0.65	0.03	0.48	1.16	2.07	0.24	nd	-
M49	MIV039	3		up	16.43	0.92	1.10	0.09	0.23	0.85	0.09	0.23	1.17	1.24	1.48	nd	-
M50	MIV041	3		up	22.63	1.71	0.79	0.04	0.30	0.65	0.04	0.31	1.00	1.96	0.31	nd	-
M51	MIV049	3		up	26.00	0.58	2.08	0.11	0.43	1.95	0.12	0.46	2.53	1.76	0.43	2.04	0.74
M55	MIV105	3	Holonbuir, Dornod prov.	low	17.57	0.26	0.69	0.01	0.17	0.56	0.01	0.18	0.75	1.63	0.36	2.91	1.58
M56	MIV106	3		up	21.43	0.35	1.06	0.03	0.24	0.96	0.03	0.25	1.24	1.57	0.08	0.78	1.13
M57	MIV109	3		up	16.57	0.32	0.63	0.05	0.13	0.55	0.05	0.14	0.74	0.89	0.81	nd	-
M58	MIV110	3		mid	27.30	0.20	1.05	0.02	0.43	0.95	0.02	0.44	1.41	2.37	0.15	0.23	0.75
M62	MII100	2	Bulgan, Dornod prov.	low	12.39	1.35	0.62	0.03	0.23	0.49	0.03	0.23	0.75	1.17	1.73	0.91	-
M52	MIV098	2		low	16.30	0.46	0.91	0.03	0.20	0.76	0.02	0.20	0.98	0.90	0.60	1.11	0.59
M53	MIV099	3		up	21.77	0.38	0.67	0.04	0.11	0.55	0.03	0.12	0.7	1.89	0.81	0.18	4.60
M54	MIV102	3		low	15.90	0.26	1.04	0.03	0.30	1.01	0.02	0.30	1.33	0.93	0.59	1.57	0.34
M1	JB1502	3	Khalkhgol, Dornod prov.	low	39.44	1.13	0.45	0.03	0.10	0.44	0.03	0.10	0.57	9.76	1.55	0.36	1.15
M64	JB1506	2		low	9.10	0.14	0.49	0.24	0.35	0.44	0.24	0.32	1.00	nd	-	nd	-
M65	MIV136	3	Kherlem Bayan-Ulaan, Khentii prov.	up	46.63	0.15	0.24	0.06	0.12	0.24	0.06	0.12	0.42	16.19	0.87	0.47	0.82
M66	MIV137	3		up	39.99	0.20	0.50	0.03	0.37	0.49	0.03	0.37	0.89	17.48	1.41	0.27	3.45
C9	28814	3	Inner Mongolia	piece	42.60	1.65	1.02	0.13	0.56	1.03	0.13	0.64	1.80	13.06	1.52	0.68	1.52
C10	28813	3	Hebei prov.	piece	62.83	0.75	0.20	0.02	0.19	0.20	0.00	0.20	0.40	25.91	1.29	nd	-

[a]: The number of replicates.

[b]: The yield of extracts and contents are indicated as mean and standard deviation (SD).

[c]: Levels of sucrose and polyacetylenes are indicated as mean and relative standard deviation (RSD). not detected (nd); not available (-).

3.3 Discussion

The purities of 13 reference compounds used in HPLC quantification was 60.94–99.06% (Table 3-1). Reference standard compounds isolated from natural sources often contain impurities. Using the isolates as reference standards for targeted quantitative analysis might not be accurate. Therefore, reliable purity assessment by qHNMR analysis is preferred to determine the accurate purity. As recommended by the Committee of Japanese Pharmacopoeia, various applications of qHNMR analysis have been reported for the purity assessment of reference compounds in the quantification tests of crude drugs [44,73,74]. Therefore, purity assessment of 13 reference compounds by qHNMR analysis could afford reliable results despite some of them had lower purities than 90%.

In HPLC chromatograms of Mongolian specimens and Chinese SR samples, 13 compounds were observed, but the peaks of some compounds were different (Fig. 3-1). Coumarins (**10**–**13**) and 4 chromones (**4**, **6**, **7**, and **8**) were detected below the LOQ (not detected) or trace amount (tr) in some samples (Table S1). Chromones (**1**, **2**, **3**, and **9**) were detected in all specimens. The specimens collected in September (M1, M63) contained a remarkably higher amount of **2** compared with other specimens (Fig. 3-2b). Similar findings that the content of **2** increased markedly after September in cultivated *S. divaricata* roots have been reported [13]. Two specimens (M65, M66) from Kherlem Bayan-Ulaan field in the Khentii prov. (Table S1) showed chemical and morphological similarities to the cultivated type of SR samples such as the low amount of chromones as well as the yellow-colored root (without any cracks), which suggests that these specimens might be growing in the similar condition as the cultivated type of SR samples (Fig. 3-9). Therefore, these abnormal specimens (M1, M63–M66) were excluded from further multivariate analysis.

Fig. 3-9. Mongolian specimens M65, M66 from Kherlem Bayan-Ulaan field, Khentii prov. and cultivated type of SR sample C4 obtained from Hebei prov.

The OPLS-DA based on HPLC data revealed that **14** contributed to discriminate the specimens from Bayan-Uul, although in chapter 2, **14** was used to discriminate those from Ondorkhaan and Bayan-Ovoo. Moreover, major chromones **1**–**3** were discriminatory marker compounds for the specimens from the far eastern part of Mongolia, Khalkhgol and Tamsagbulag. After adding the specimens from the northeastern part, Bayan-Uul and Norovlin, **1**–**3** contributed most to discriminate the specimens from the northeastern part, as the variation of contents was extremely high in the specimens from Khalkhgol. Based on these results, the specimens from the northeastern part had superior property regarding the contents of major chromones.

A few approaches regarding ^{1}H NMR based fingerprinting and metabolomic analysis of SR extracts have been reported but used additional separation or fractionating for sample preparation [42,75]. This is the first time that is evaluating Mongolian *S. divaricata* roots by ^{1}H NMR analysis without additional separation. In principle, ^{1}H NMR spectroscopy, which can provide direct quantitative information because the intensity of the proton signal is proportional to the molar concentration of the analyte, does not need a chromatographic separation step and calibration curve preparation of

reference standards. Thereby, a quantitative ^{1}H NMR method was performed on Mongolian specimens to determine the content of major chromones. However, the qHNMR analysis has disadvantages as its low sensitivity and requiring that the target signal should be stable and should not overlap with any other peaks. In this chapter, the quantification of **1**–**3** by HPLC method and the qHNMR method were compared. The content of **1** in several specimens, as determined by the qHNMR method, was slightly lower than the content determined by the HPLC method (Table 3-9), because of loss or decomposition of the compound during the sample preparation. For polar compounds such as **1**, molecular interaction during the sample extraction can occur within each other or with other polar solvents [76] to result in decomposition of the compound. Although the H-3 signal of **3** overlapped with that of **4**, approximate content of **3** was obtained. Because, the content of **4** was less than 3.6% of **3** in the HPLC quantification. Therefore, qHNMR method can be used for determining the approximate contents of major chromones. A detailed study, including validation of the method and optimization of sample extraction, is necessary to improve its application.

Estimation of sucrose and polyacetylenes levels by qHNMR method in the extracts of 24 Mongolian specimens and Chinese 2 SR samples revealed that Mongolian specimens had less amount of sucrose than the Chinese SR samples, resulting in lower yield of extract (Table 3-9). This result supported the previous reports that the cultivated type of SR was characterized by sucrose [42] and had a higher yield of extract than the wild type [69]. During cultivation on cropland, sucrose will increase due to the nutrition of the soil environment. For this reason, Mongolian wild growing *S. divaricata* contained less amount of sucrose. Meanwhile, some of the Mongolian specimens contained a substantial amount of polyacetylenes including **15**. Severe drought stress during the

growth of the plant, *S. divaricata* has been reported to reduce the amount of **15** [77]. Accordingly, the difference in environmental and soil conditions could affect the amount of **15** and other polyacetylenes. In contrast, the contents of **1** and **3** in *S. divaricata* roots increased during drought stress by withholding water for 20 and 12 days, respectively, in the field [77]. When we compared the meteorological condition of each region such as mean temperature and mean precipitation (Table 3-10), the mean precipitations of Dashbalbar from the northeastern part and Khalkhgol from the far eastern part during plant growth season from April to September were situated midway among eastern Mongolian regions and the production areas of SR in China. Generally, high rainfall levels are preferred for plant growth. Therefore, balancing of drought stress and the suitable water content in soil is important for plant growth and contents of chromones. The regional differences in the chromone content described above will be useful for selecting prospective cultivation place.

Table 3-10. Monthly mean temperature and precipitation of eastern Mongolian regions and the production area of SR in China (1981-2010)

Month	Mean temperature* (°C)							Mean precipitation* (mm)						
	Khentii prov.		Dornod prov.			China		Khentii prov.		Dornod prov.			China	
	Ondorkhaan	Bayan-Ovoo	Choibalsan	Dashbalbar**	Khalkhgol	Inner Mongolia	Heilongjiang	Ondorkhaan	Bayan-Ovoo	Choibalsan	Dashbalbar	Khalkhgol	Inner Mongolia	Heilongjiang
	1035 m	926 m	747 m	706 m	689 m	1004 m	-	1035 m	926 m	747 m	706 m	689 m	1004 m	-
1	-23.7	-21.2	-20.4	-19.7	-24	-18.7	-18.2	2.2	2.2	2.4	2.5	3.5	2	2.2
2	-18.7	-16.7	-14.9	-15.4	-18.2	-14.2	-12.9	3.1	8.7	2.2	1.7	3.1	2	2.2
3	-7.4	-7.4	-6.8	-5.5	-9.1	-5.1	-3.6	4.3	4.4	3.2	2.4	5.1	5.2	6.9
4	3.4	3.9	3.8	3.9	3	5.7	7	5.6	8.6	5.6	5.7	13.2	7.7	22.3
5	11.5	11.6	12.4	11.2	11.5	13.6	15.1	15.6	16.7	15.2	15.3	17.5	24.3	31.8
6	17.8	18.1	18.6	18.1	18.6	19.2	21.2	39.6	40.3	35.5	39.4	42.7	44.8	73.1
7	20.4	20.3	20.9	21.1	20.9	21.6	23.4	54.6	65.4	74.3	103.7	98.3	74	141.6
8	17.9	18.1	18.8	18.0	18.9	19.8	21.6	54	73.6	56.4	60.3	66.5	60.6	99.7
9	11.1	11.6	11.8	11.3	12.1	13.3	14.9	20.8	20.9	28.4	26.3	22.7	24.9	40.6
10	0.9	1.1	2.1	0.6	2	4.1	5.7	6.8	12.9	10.7	9.2	7.6	13.1	19.7
11	-11.8	-10.5	-9.8	-11.8	-11	-6.8	-6.2	3.6	5.2	2.9	3.1	4.6	4.6	4.1
12	-20.9	-19	-17.2	-17.9	-20.4	-15.5	-15.5	2.3	3.9	3	4.1	6.3	3.1	5.1
Annual	0.0	0.8	1.6	1.2	0.4	3.1	4.4	212.5	262.8	239.8	273.7	291.1	266.3	449.3
Apr.-Sept.	13.7	13.9	14.4	13.9	14.2	15.5	17.2	190.2	225.5	215.4	250.7	260.9	236.3	409.1

*: Data is collected from Climat View data tool, Japan Meteorological Agency.
http://www.data.jma.go.jp/gmd/cpd/monitor/climatview/frame.php?s=7&r=1&d=0&y=2019&m=12&e=0&t=676.3789785714287&l=2278.1582666666672&k=0
**: Data is obtained from 2014 to 2019;
not avialable (-);

3.4 Summary of chapter 3

The simultaneous determination of 13 compounds in 44 Mongolian specimens as well as the Chinese SR samples was achieved using the HPLC-DAD method. All specimens from Mongolia contained dihydrofurochromones **1** and **3**, and their total amount exceeded the criterion assigned in the Chinese Pharmacopoeia. Moreover, the content of **1** was significantly higher in the Mongolian specimens than in Chinese SR samples. The specimens from Norovlin contained higher levels of total dihydrofurochromones (**1**–**4**). The levels of total dihydropyranochromones (**5**–**9**) were higher in the specimens from Bayan-Uul. The OPLS-DA based on HPLC data revealed that Mongolian specimens tended to be separated into three groups based on growing regions, in which 6 chromones (**1**, **2**, **3**, **5**, **7**, **14**) mostly contributed to each distribution. Meanwhile, the characterization and quantification of metabolites such as sugars and polyacetylenes by ^{1}H NMR and qHNMR analyses revealed that Mongolian specimens had a lower amount of sucrose than Chinese cultivated SR samples, and some of them contained a substantial amount of polyacetylenes including **15**. Furthermore, since the H-3 signals of **1**, **2**, and **3** (including **4**) were clearly observed in ^{1}H NMR spectra of the extracts, a quantitative determination of major chromones was performed to determine the approximate contents of **1**, **2**, and **3**. Therefore, qHNMR could be used for rapid quantification of major chromones, although further validation and optimization of the method are needed to improve its application.

Conclusion

Comprehensive research on quality evaluation of *S. divaricata* roots from Mongolia was conducted by various analytical methods such as LC-IT-TOF-MS, HPLC, and NMR. Each method has advantages and disadvantages for analyzing extracts of *S. divaricata* roots. In summary, the LC-IT-TOF-MS method was very useful for metabolomic profiling and metabolite identification together with multivariate statistical analysis to find metabolite markers on group separation (see the table below). In contrast, the HPLC method advantaged for the accurate quantification of metabolites but needs construction of calibration curves using reference standard compounds and development of chromatographic condition. Compared to the HPLC, the qHNMR method did not need calibration curve preparation of reference compounds and had simple procedures. In this study, LC-IT-TOF-MS combined with OPLS-DA achieved comprehensive metabolomic profiling of *S. divaricata* roots from Mongolia and finding characteristic compounds attributed to the geographical variation of Mongolian *S. divaricata* roots. HPLC-DAD analysis combined with OPLS-DA succeeded the simultaneous determination of characteristic compounds in Mongolian *S. divaricata* roots and supported regional differences of Mongolian *S. divaricata* roots. qHNMR analysis achieved the rapid quantification of major chromones, panaxynol, and sucrose in a single analysis. All these methods developed to evaluate *S. divaricata* roots, could be applied to estimate commercial SR samples.

Effort by analytical methods conducted on extracts of *S. divaricata* roots

Challenges	LC-IT-TOF-MS	HPLC-DAD	^{1}H NMR or qHNMR
Metabolomic profiling	◎	◎	◎
Identification of metabolites	◎	○	◎
Multivariate statistical analysis	◎	○	◎
Quantification of metabolites	○	◎	◎

The present study was concluded as follows:

S. divaricata roots from Mongolia could be natural sources of SR due to similar profiles with Chinese SR and higher levels of **1** and **3** which exceeded the value prescribed in Chinese Pharmacopoeia. Moreover, the geographical variation in contents of dihydrofurochromones as well as dihydropyranochromones was clarified by multivariate statistical analysis using LC-MS data and HPLC data. Among 8 regions of eastern Mongolia, Norovlin and Bayan-Uul in the northeastern part of Mongolia possessed a superior property such as higher contents of major chromones **1**–**3** and dihydropyranochromones **5**, **9**, and **14**, lower content of sucrose, and a substantial amount of polyacetylenes including **15**. Several pharmacological effects, including analgesic, anti-inflammatory, anti-allergic, anti-cancer, and anti-platelet aggregation activities, have been reported in **1**, **2**, **3**, **5**, **9**, and **15**. Therefore, the specimens from the north eastern part of Mongolia have the potential to be used as anti-inflammatory and analgesic drugs. Based on this study, the north eastern part was proposed as a prospective region for the cultivation of *S. divaricata* in Mongolia. These findings could contribute to the systematic collection and prospective cultivation of *S. divaricata* in Mongolia.

General experimental

1. Instrumentation and equipment

a. HPLC-DAD and ESI-IT-TOF-MS conditions

HPLC-DAD conditions: HPLC system (Shimadzu, Tokyo, Japan)

SCL-10AVP system controller, C-20AD binary pump,

DGU-20A degasser, IL-20AC auto-sampler,

CTO-20AC column oven, PD-M20A photo-diode-array (PDA) detector,

column: Atlantis T3 column (3 μm, 2.1 × 150 mm, Waters, MA, USA),

column temperature: 30°C, injection volume: 5 μL,

flow rate: 0.2 mL/min, detection wavelengths: 200–400 nm,

HR-ESI-MS conditions: Ion-trap time-of-flight mass spectrometer (IT-TOF-MS, (Shimadzu, Tokyo, Japan);

standard solution: trifluoroacetic acid sodium (TFA); dry gas pressure: 100 kPa;

nebulizer gas flow: 1.5 L/min; the ion accumulation time: 30 msec;

the ionization interface positive and negative;

source voltage: +4.5 kV (for positive) or –3.5 kV (for negative ionization modes);

curved desolvation line (CDL) and heat block temperature: 200°C;

molecular weight acquisition: *m/z* 100–2000 for MS and MS/MS;

the collision energy of collision-induced dissociation (CID): 50%;

data acquisition and processing software: the LCMS solution version 3.81.

b. ^{1}H NMR and qHNMR parameters

NMR spectrometer: JEOL JMN-ECA500 (500 MHz) and JEOL JMN-ECA800 (800 MHz) spectrometer (JEOL, Tokyo, Japan);

data acquisition and processing software: Delta 5.3.1 (JEOL, Tokyo, Japan);

chemical shifts of **1**–**13**: relative to DSS-d_6 at δ_H 0.00;

chemical shifts of **14**, **15**, sucrose, and glucose: relative to DMSO-d_6 at δ_H 2.49;

The parameters of ^{1}H NMR:	The parameters of qHNMR:
scans: 16	scans: 8
pulse angel: 45°	pulse angel: 90°
relaxation delay: 5 s	relaxation delay: 60 s
temperature: 295 K	temperature: 295 K

c. Other instruments

Column chromatography: DAION HP-21 (Fujifilm Wako Pure Chemical Corp.);

MPLC: Isolera One (Biotage Japan Ltd.); P–HPLC: DELTA 600 (Waters);

Evaporator: Multivapor (BUCHI); CEVI-SK-P5 (Bio Chromato);

Pulverizer: Wonder crusher (WC-3); Freeze-dryer: FDU-1110 (EYELA);

Multi-beads shocker: MB755U(S) (Yasui Kikai Corp.)

Centrifuger: KUBOTA 3740;

Ultramicro balance: Cubis MSA 2.7S-000-DM (Sartorius);

2. Chemicals and reagents

LC-MS grade reagents, including acetonitrile, methanol, and formic acid were purchased from Fujifilm Wako Pure Chemical (Osaka, Japan). Water was purified using a Milli-Q system (Millipore, MA, USA). Dimethyl sulfoxide-d_6 (DMSO-d_6), glucose, and sodium 3-(trimethylsilyl)-1-propane-1,1,2,2,3,3-d_6-sulfonate (DSS-d_6), which was used as certified reference materials for qHNMR analysis were purchased from Fujifilm Wako Pure Chemical. Sucrose was purchased from Nacalai Tesque (Kyoto, Japan). All other

chemicals were of analytical grade.

The following 21 reference compounds isolated and identified from the SR sample C9 were used as reference standards. (see chapter 1).

prim-*O*-glucosylcimifugin (**1**):
colorless amorphous solid
molecular formula $C_{22}H_{28}O_{11}$
HR-ESI-MS *m/z* 469.1689 $[M+H]^+$ (calcd. for $C_{22}H_{29}O_{11}$, 469.1704, Δ +0.3 mmu)
^{1}H NMR (Table 1-1)

cimifugin (**2**):
colorless needles
molecular formula $C_{16}H_{18}O_6$
HR-ESI-MS *m/z* 307.1185 $[M+H]^+$ (calcd. for $C_{16}H_{19}O_6$, 307.1176, Δ +0.7 mmu)
^{1}H NMR (Table 1-1)

4'-*O*-β-D-glucosyl-5-*O*-methylvisamminol (**3**):colorless needles
molecular formula $C_{22}H_{28}O_{10}$
HR-ESI-MS *m/z* 453.1762 $[M+H]^+$ (calcd. for $C_{22}H_{29}O_{10}$, 453.1755, Δ +0.9 mmu)
^{1}H NMR (Table 1-2)

5-*O*-methylvisamminol (**4**):
colorless needles
molecular formula of $C_{16}H_{18}O_5$
HR-ESI-MS *m/z* 291.1230 $[M+H]^+$ (calcd. for $C_{16}H_{19}O_5$, 291.1227, Δ +0.3 mmu)
^{1}H NMR (Table 1-2)

Sec-*O*-glucosylhamaudol (**5**):
colorless needles
molecular formula $C_{21}H_{26}O_{10}$
HR-ESI-MS *m/z* 439.1617 $[M+H]^+$ (calcd. for $C_{21}H_{27}O_{10}$, 439.1599, Δ +1.8 mmu)
^{1}H NMR (Table 1-3)

Hamaudol (**6**):
yellow needles
molecular formula $C_{15}H_{16}O_5$
HR-ESI-MS *m/z* 277.1077 $[M+H]^+$ (calcd. for $C_{15}H_{17}O_5$, 277.1077, Δ +0.6 mmu)
^{1}H NMR (Table 1-3)

3'-*O*-acetylhamaudol (**7**):
colorless needles
molecular formula $C_{17}H_{18}O_6$
HR-ESI-MS *m/z* 319.1190 $[M+H]^+$ (calcd. for $C_{17}H_{19}O_6$, 319.1176, Δ +1.4 mmu)
^{1}H NMR (Table 1-3)

Lebebouriellol (**8**):
colorless needles,
molecular formula of $C_{20}H_{22}O_7$
HR-ESI-MS *m/z* 375.1455 $[M+H]^+$ (calcd. for $C_{20}H_{23}O_7$, 375.1438, Δ +0.7 mmu)
^{1}H NMR (Table 1-3)

3'-*O*-angeloylhamaudol (**9**):
colorless needles
molecular formula $C_{20}H_{22}O_6$
HR-ESI-MS *m/z* 359.1487 $[M+H]^+$ (calcd. for $C_{20}H_{23}O_6$, 359.1489, Δ –0.2 mmu)
^{1}H NMR (Table 1-3)

Psoralen (**10**):
colorless needles
molecular formula $C_{11}H_6O_3$
HR-ESI-MS *m/z* 187.0394 $[M+H]^+$ (calcd. for $C_{11}H_7O_3$, 187.0390, Δ +0.4 mmu)
^{1}H NMR (Table 1-4)

Xanthatoxin (**11**):
colorless needles,
molecular formula $C_{12}H_8O_4$
HR-ESI-MS *m/z* 217.0525 $[M+H]^+$ (calcd. for $C_{12}H_9O_4$, 217.0495, Δ +3.0 mmu)
^{1}H NMR (Table 1-4)

Bergapten (**12**):
colorless needles,
molecular formula $C_{12}H_8O_4$
HR-ESI-MS *m/z* 217.0517 $[M+H]^+$ (calcd. for $C_{12}H_9O_4$, 217.0495, Δ +2.2 mmu)
^{1}H NMR (Table 1-4)

Deltoin (**13**): colorless prism
molecular formula $C_{19}H_{20}O_5$
HR-ESI-MS *m/z* 329.1400 $[M+H]^+$ (calcd. for $C_{19}H_{21}O_5$, 329.1384, Δ +1.8 mmu)
^{1}H NMR (Table 1-5)

3'-*O*-(6''-*O*-malonyl)-glucosylhamaudol (**14**): yellow amorphous powder
molecular formula $C_{24}H_{28}O_{13}$
HR-ESI-MS *m/z* 525.1616 $[M+H]^+$
^{1}H NMR and ^{13}C NMR (Table 1-7)

Panaxynol (**15**):
colorless oil
molecular formula $C_{17}H_{24}O$
HR-ESI-MS *m/z* 245.1927 $[M+H]^+$ (Calcd. for $C_{17}H_{25}O$, 245.1899, Δ +2.8 mmu)
UV λmax nm: 229, 241, 254, 269, and 285
^{1}H NMR (Table 1-6)

Praeruptorin B (**16**): colorless needles
molecular formula $C_{24}H_{26}O_7$
HR-ESI-MS *m/z* 449.1572 $[M+Na]^+$ (Calcd. for $C_{24}H_{27}O_7$, 449.1571, Δ +0.1 mmu)
UV λmax nm: 205 and 325
^{1}H NMR (Table 1-5)

Falcarindiol (**17**): colorless oil
molecular formula $C_{17}H_{24}O_2$
HR-ESI-MS *m/z* 261.2101 $[M+H]^+$ (Calcd. for $C_{17}H_{25}O_2$, 261.1849, Δ +25.2 mmu)
UV λmax nm: 220, 240, 255, 271, and 282
^{1}H NMR (Table 1-6)

Virol C (**18**): colorless oil
molecular formula $C_{17}H_{26}O_2$
HR-ESI-MS *m/z* 263.1996 $[M+H]^+$ (calcd. for $C_{17}H_{27}O_2$, 263.2006, Δ –1.0 mmu)
UV λmax nm: 214, 240, 253, 267, and 283
^{1}H NMR (Table 1-6)

Glycerol monolinoleate (**19**):
colorless oil
molecular formula $C_{21}H_{38}O_4$
HR-ESI-MS *m/z* 355 $[M+H]^+$ (Calcd. for $C_{22}H_{39}O_4$, 355.2843)
^{1}H NMR (Table 1-6)

Phellopterin (**20**): colorless needles
molecular formula $C_{17}H_{16}O_5$
HR-ESI-MS *m/z* 301.1079 $[M+H]^+$ (Calcd. for $C_{17}H_{17}O_5$, 301.1071, Δ +0.8 mmu)
UV λmax nm: 222, 268, and 313
^{1}H NMR (Table 1-5)

Isopimpinellin (**21**):
colorless needles
molecular formula $C_{13}H_{10}O_5$
HR-ESI-MS *m/z* 247.0652 $[M+H]^+$ (Calcd. for $C_{13}H_{11}O_5$, 247.0601, Δ +5.1 mmu)
^{1}H NMR (Table 1-5)

References

1. The Ministry of Health, Labour, and Welfare. The Japanese Pharmacopoeia. 17th edition (English version). The MHLW Ministerial Notification No. 64, Tokyo, Japan. (2016) 1971-1972
2. The State Pharmacopoeia Commision of China Pharmacopoeia of the People's Republic of China (English ed), China Medical Science Press, Beijing. (2015) 404-405
3. Kreiner J, Pang E, Lenon GB, Yang AWH. *Saposhnikoviae divaricata*: a phytochemical, pharmacological, and pharmacokinetic review. Chin J Nat Med (2017) 15: 255-264
4. Gao SL, Satsu H, Makino T. Inhibitory effect of bofutsushosan (fang feng tong sheng san) on glucose transporter 5 function *in vitro*. J Nat Med (2018) 72: 530-536
5. Baba K, Yoneda Y, Kozawa M, Fujita E, He WN, Qi YC. Studies on Chinese Traditional Medicine "Fang-Feng" (II) Comparison of several Fang-Feng by coumarins, chromones and polyacetylenes. Shoyakugaku Zasshi (1989) 216-221
6. Okuyama E, Hasegawa T, Matsushita T, Fujimoto H, Ishibashi M, Yamazaki M. Analgesic components of Saposhnikovia root (*Saposhnikovia divaricata*). Chem Pharm Bull (2001) 49: 154-160
7. Sasaki H, Taguchi H, Endo T, Yosioka I. The constituents of *Ledebouriella seseloides* Wolff. I. Structures of three new chromones. Chem Pharm Bull (1982) 30 (10):3555-3562
8. Yang JM, Jiang H, Dai HL, Wang ZW, Jia GZ, Meng XC. Polysaccharide enhances Radix Saposhnikoviae efficacy through inhibiting chromones decomposition in

intestinal tract. Sci Rep (2016) 6: 32698

9. Kang J, Sun JH, Zhou L, Ye M, Han J, Wang BR, Guo DA. Characterization of compounds from the roots of *Saposhnikovia divaricata* by high-performance liquid chromatography coupled with electrospray ionization tandem mass spectrometry. Rap Commun in Mass Spec (2008) 22: 1899-1911
10. Yokosuka A, Tatsuno S, Komine T, Mimaki Y. Chemical constituents of the roots and rhizomes of *Saposhnikovia divaricata* and their cytotoxic activity. Nat Prod Commun (2017) 12: 255-258
11. Yang JL, Dhodary B, Ha TKQ, Kim J, Kim E, Oh WK. Three new coumarins from *Saposhnikovia divaricata* and their porcine epidemic diarrhea virus (PEDV) inhibitory activity. Tetrahedron (2015) 71: 4651-4658
12. Ma SY, Shi LG, Gu ZB, Wu YL, Wei LB, Wei QQ, Gao XL, Liao N. Two new chromone glycosides from the roots of *Saposhnikovia divaricata*. Chem Biodiver (2018) 15: 6
13. Wang CC, Chen LG, Yang LL. Inducible nitric oxide synthase inhibitor of the Chinese herb - I. Saposhnikovia divaricata (Turcz.) Schischk. Cancer Lett (1999) 145: 151-157
14. Tai J, Cheung S. Anti-proliferative and antioxidant activities of *Saposhnikovia divaricata*. Oncol Rep (2007) 18: 227-234
15. Chun JM, Kim HS, Lee AY, Kim SH, Kim HK. Anti-inflammatory and antiosteoarthritis effects of *Saposhnikovia divaricata* ethanol extract: *In vitro* and *in vivo* studies. Evid-Based Compl Alt Med (2016) 1984238
16. Zhou J, Sun YY, Sun MY, Mao WA, Wang L, Zhang J, Zhang H. Prim-*O*-glucosylcimifugin attenuates lipopolysaccharide-induced inflammatory response in

RAW 264.7 macrophages. Pharmacog Mag (2017) 13: 378-384

17. Gao WF, Zhang XY, Yang WD, Dou DL, Zhang H, Tang YH, Zhong WL, Meng J, Bai Y, Liu YR, Yang L, Chen S, Liu HJ, Yang C, Sun T. Prim-*O*-glucosylcimifugin enhances the antitumour effect of PD-1 inhibition by targeting myeloid-derived suppressor cells. J Immunother Cancer (2019) 7:231
18. Jia QQ, Sun W, Zhang LY, Fu J, Lv YN, Lin YY, Han SL. Screening the anti-allergic components in Saposhnikoviae Radix using high-expression Mas-related G protein-coupled receptor X2 cell membrane chromatography online coupled with liquid chromatography and mass spectrometry. J Sep Sci (2019) 42: 2351-2359
19. Kang JS, Chin YW, Lee K, Kim YW, Choi BY, Keum YS. Identification of 4'-*O*-β-D-glucosyl-5-*O*-methylvisamminol as a novel epigenetic suppressor of histone H3 phosphorylation at Ser10 and its interaction with 14-3-3 ε. Bioorg Med Chem Lett (2014) 24: 4763-4767
20. Yang JM, Jiang H, Dai HL, Wang ZW, Jia GZ, Meng XC. Feeble Antipyretic, Analgesic, and Anti-inflammatory Activities were found with regular dose 4'-*O*-β-D-glucosyl-5-*O*-methylvisamminol, One of the conventional marker compounds for quality evaluation of Radix Saposhnikoviae. Pharmacog Mag (2017) 13: 168-174
21. Chang CZ, Wu SC, Kwan AL, Lin CL. 4'-*O*-β-D-glucosyl-5-*O*-methylvisamminol, an active ingredient of *Saposhnikovia divaricata*, attenuates high-mobility group box 1 and subarachnoid hemorrhage-induced vasospasm in a rat model. Behav Brain Func (2015) 11:28
22. Kamino T, Shimokura T, Morita Y, Tezuka Y, Nishizawa M, Tanaka K. Comparative analysis of the constituents in Saposhnikoviae Radix and Glehniae Radix cum Rhizoma by monitoring inhibitory activity of nitric oxide production. J Nat Med

(2016) 70: 253-259

23. Zhao B, Yang XB, Yang XW, Wu Q, Wang Y, Zhang LX, Xu W. Intestinal permeability of the constituents from the roots of *Saposhnikovia divaricata* in the human Caco-2 cell monolayer model. Planta Medica (2011) 77: 1531-1535
24. Han HS, Jeon H, Kang SC. Phellopterin isolated from *Angelica dahurica* reduces blood glucose level in diabetic mice. Heliyon (2018) 4: e00577
25. Khan S, Shin EM, Choi RJ, Jung YH, Kim J, Tosun A, Kim YS. Suppression of LPS-induced inflammatory and NF-kappa B responses by anomalin in RAW 264.7 macrophages. J Cell Biochem (2011) 112: 2179-2188
26. Kuo YC, Lin YL, Huang CP, Shu JW, Tsai WJ. A tumor cell growth inhibitor from *Saposhnikovae divaricata*. Cancer Invest (2002) 20: 955-964
27. Fujioka T, Furumi K, Fujii H, Okabe H, Mihashi K, Nakano Y, Mitsunaga H, Katano M, Mori M. Antiproliferative constituents from Umbelliferae plants. V. A new furanocoumarin and falcarindiol furanocoumarin ethers from the root of *Angelica japonica*. Chem Pharm Bull (1999) 47: 96-100
28. Meng Y, Yi L, Chen L, Hao J, Li DX, Xue J, Xu NY, Zhang ZQ. Purification, structure characterization and antioxidant activity of polysaccharides from Saposhnikovia divaricata. Chin J Nat Med (2019) 17: 792-800
29. Dong CX, Liu L, Wang CY, Fu Z, Zhang Y, Hou X, Peng C, Ran RX, Yao Z. Structural characterization of polysaccharides from *Saposhnikovia divaricata* and their antagonistic effects against the immunosuppression by the culture supernatants of melanoma cells on RAW264.7 macrophages. Int J Biol Macromol (2018) 113: 748-756
30. Chen LX, Chen XY, Su L, Jiang YY, Liu B. Rapid characterisation and identification

of compounds in Saposhnikoviae Radix by high-performance liquid chromatography coupled with electrospray ionisation quadrupole time-of-flight mass spectrometry. Nat Prod Res (2018) 32: 898-901

31. Kim MK, Yang DH, Jung M, Jung EH, Eom HY, Suh JH, Min JW, Kim U, Min H, Kim J, Han SB. Simultaneous determination of chromones and coumarins in Radix Saposhnikoviae by high performance liquid chromatography with diode array and tandem mass detectors. J Chromatogr A (2011) 1218: 6319-6330
32. Li W, Wang Z, Chen L, Zhang J, Han LK, Hou JA, Zheng YN. Pressurized liquid extraction followed by LC-ESI/MS for analysis of four chromones in Radix Saposhnikoviae. J Sep Sci (2010) 33: 2881-2887
33. Chen N, Wu Q, Chi G, Soromou LW, Hou J, Deng Y, Feng H. Prime-O-glucosylcimifugin attenuates lipopolysaccharide-induced acute lung injury in mice. Intern Immunopharmacology 2013; 16: 139-147
34. Steuer AE, Brockbals L, Kraemer T. Metabolomic Strategies in biomarker research-new approach for indirect identification of drug consumption and sample manipulation in clinical and forensic toxicology. Front in Chem (2019) 7:
35. Lu Y, Chen C. Metabolomics: Bridging chemistry and biology in drug discovery and development. Curr Pharmacol Rep (2017) 3: 16-25
36. Li DS, Wu YF, Wei PP, Gao X, Li M, Zhang CB, Zhou ZJ, Lu WY. Metabolic engineering of Yarrowia lipolytica for heterologous oleanolic acid production. Chem Engin Sci (2020) 218: 7
37. Tomita M, Nishioka T. Forefront of metabolome research. Japan. Springer-Verlag Tokyo (2003) 5-6
38. Shi YH, Zhu S, Ge YW, Toume K, Wang ZT, Batkhuu J, Komatsu K. Characterization

and quantification of monoterpenoids in different types of peony root and the related Paeonia species by liquid chromatography coupled with ion trap and time-of-flight mass spectrometry. J Pharm and Biomed Anal (2016) 129: 581-592

39. Ge YW, Zhu S, Yoshimatsu K, Komatsu K. MS/MS similarity networking accelerated target profiling of triterpene saponins in Eleutherococcus senticosus leaves. Food Chem (2017) 227: 444-452
40. Ghosson H, Schwarzenberg A, Jamois F, Yvin JC. Simultaneous untargeted and targeted metabolomics profiling of underivatized primary metabolites in sulfur-deficient barley by ultra-high performance liquid chromatography-quadrupole/time-of-flight mass spectrometry. Plant Meth (2018) 14: 62
41. Yoshitomi T, Wakana D, Uchiyama N, Tsujimoto T, Kawano N, Yokokura T, Yamamoto Y, Fuchino H, Hakamatsuka T, Komatsu K, Kawahara N, Maruyama T. Identifying the compounds that can distinguish between Saposhnikovia root and its substitute, Peucedanum ledebourielloides root, using LC-HR/MS metabolomics. J Nat Med (2020) 74(3):550-560
42. Yoshitomi T, Wakana D, Uchiyama N, Tsujimoto T, Kawano N, Yokokura T, Yamamoto Y, Fuchino H, Hakamatsuka T, Komatsu K, Kawahara N, Maruyama T. ^{1}H NMR-based metabolomic analysis coupled with reversed-phase solid-phase extraction for sample preparation of Saposhnikovia roots and related crude drugs. J Nat Med (2020) 74: 65-75
43. Song YL, Jing WH, Chen YG, Yuan YF, Yan R, Wang YT. ^{1}H nuclear magnetic resonance based-metabolomic characterization of Peucedani Radix and simultaneous determination of praeruptorin A and praeruptorin B. J Pharm Biomed Anal (2014) 93: 86-94

44. Tanaka R, Inagaki R, Sugimoto N, Akiyama H, Nagatsu A. Application of a quantitative ^{1}H-NMR (^{1}H-qNMR) method for the determination of geniposidic acid and acteoside in Plantaginis semen. J Nat Med (2017) 71: 315-320
45. Nguyen HT, Lee DK, Choi YG, Min JE, Yoon SJ, Yu YH, Lim J, Lee J, Kwon SW, Park JH. A H-1 NMR-based metabolomics approach to evaluate the geographical authenticity of herbal medicine and its application in building a model effectively assessing the mixing proportion of intentional admixtures: A case study of Panax ginseng Metabolomics for the authenticity of herbal medicine. J Pharm Biomed Anal (2016) 124: 120-128
46. Liu ZQ, Rochfort S. A fast liquid chromatography-mass spectrometry (LC-MS) method for quantification of major polar metabolites in plants. J Chromatogr B-Anal Tech Biomed Life Sci (2013) 912: 8-15
47. Xiu Y, Li X, Sun XL, Xiao D, Miao R, Zhao HX, Liu SY. Simultaneous determination and difference evaluation of 14 ginsenosides in Panax ginseng roots cultivated in different areas and ages by high-performance liquid chromatography coupled with triple quadrupole mass spectrometer in the multiple reaction-monitoring mode combined with multivariate statistical analysis. J Ginseng Res (2019) 43: 508-516
48. Li F, Gonzalez FJ, Ma XC. LC-MS-based metabolomics in profiling of drug metabolism and bioactivation. Acta Pharmaceutica Sinica B (2012) 2: 118-125
49. Magsar U, Baasansuren E, Tovuudorj M-E, Shijirbaatar O, Chinbaatar Z, Lkhagvadorj K, Kwon O. Medicinal plant diversity in the southern and eastern Gobi Desert region, Mongolia. J Ecol Env (2018) 42: 4
50. Jamyandorj J, Ligaa U, Otgonbileg K, Saaral N. Rare and useful plants cultivated in regions of countryside Kherlen. Mongolia. Ulaanbaatar Print (2011):242-243

51. Mongolia State Publishing. Overview of the Flora of Mongolia. (1989)
52. Zhu S, Sugiyama R, Batkhuu J, Sanchir C, Zou K, Komatsu K. Survey of Glycyrrhizae Radix resources in Mongolia: chemical assessment of the underground part of *Glycyrrhiza uralensis* and comparison with Chinese Glycyrrhizea Radix. J Nat Med (2009) 63: 137-146
53. Kitani Y, Zhu S, Omote T, Tanaka K, Batkhuu J, Sanchir C, Fushimi H, Mikage M, Komatsu K. Molecular analysis and chemical evaluation of *Ephedra* plants in Mongolia. Biol Pharm Bull (2009) 32: 1235-1243
54. Kitani Y, Zhu S, Batkhuu J, Sanchir C, Komatsu K. Genetic Diversity of *Ephedra* plants in Mongolia inferred from Internal Transcribed Spacer sequence of nuclear Ribosomal DNA. Biol Pharm Bull (2011) 34: 717-726
55. Tanaka K, Tamura T, Fukuda S, Batkhuu J, Sanchir C, Komatsu K. Quality evaluation of Astragali Radix using a multivariate statistical approach. Phytochem (2008) 69: 2081-2087
56. Magsar U. Description of S*aposhnikovia divaricata* Schischkin (Umbelliferae Juss.) in Mongolia. Ulaanbaatar, Mongolia. Proceedings of Institute of Botany, Mongolian Academy of Sciences. (2006): 51-55
57. Sanchir C, Batkhuu J, Boldsaikhan B, Komatsu K. Illustrated guide of Mongolian useful plants. (Ministry of Nature, Environment, and Tourism (MNET), Mongolia), Japan Cooperation Agency (JICA), Ulaanbaatar, Mongolia. (2003): 22
58. Ministry Notification No. A/43 of March 1, 2018. Ministry of Nature, Environment, and Tourism (MNET) Mongolia.
59. Yamamoto Y, Ko H, Sasaki H, Takeda O, Higuchi Y, Mukaido Y, Mori Y, Yamaguchi Y, Shiratori M. Survey on crude drug usage in Japan. Shoyakugaku Zasshi (2019) 73:

16-35

60. Ding L. The producing and selling analysis of *Saposhnikovia divaricata* (Turcz.) Schischk. Modern Chinese Medicine (2012) 14(3): 18-19
61. Kangmei Traditional Chinese Medicine Network. Insufficient supply of wild type of Saposhnikoviae Radix. 2020, 21th January http://www.kmzyw.com.cn/news/20200121/1579590488000.2246.html
62. Liu Y, Li L, Xiao YQ, Yao JQ, Li PY, Chen L, Yu DR, Ma YL. Rapid identification of the quality decoction pieces by partial least squares -based pattern recognition: grade classification of the decoction pieces of *Saposhnikovia divaricata*. Biomed Chromatogr (2016) 30: 1240-1247
63. Hiroshi S, Heihachiro T, Tohru E, Itiro Y. The Constituents of *Glehnia littoralis* Fr. Schmidt et Miq. Structure of a new coumarin glycoside, Ostenol-7-*O*-β-gentiobioside. Chem Pharm Bull (1980) 1847-1852
64. Lu M, Nicoletti M, Battinelli L, Mazzanti G. Isolation of praeruptorins A and B from Peucedanum praeruptorum Dunn. and their general pharmacological evaluation in comparison with extracts of the drug. Farmaco (2001) 56: 417-420
65. Baba K, Tabata Y, Kozawa M, Kimura Y, Arichi S. Studies on Chinese Traditional Medicine"Fang-Feng"-1-Structures and physiological activities of polyacetylene compounds from Saposhnikoviae Radix. Shoyakugaku Zasshi (1987) 41: 189-194
66. Fiandanese V, Bottalico D, Cardellicchio C, Marchese G, Punzi A. Stereoselective total synthesis of (*S*)-Virol C and (*S*)-1-dehydroxyvirol A. Tetrahedron (2005) 61: 4551-4556
67. Klimczak U, Wozniak M, Tomczyk M, Granica S. Chemical composition of edible aerial parts of meadow bistort (*Persicaria bistorta* (L.) Samp.). Food Chem (2017)

230: 281-290

68. Muller M, Byres M, Jaspars M, Kumarasamy Y, Middleton M, Nahar L, Shoeb M, Sarker S. 2D NMR spectroscopic analyses of archangelicin from the seeds of *Angelica archangelica*. Acta Pharmaceutica (2004) 277-285
69. Nishihara M, Nukui K, Osumi Y, Shiota H. Quality evaluation of Saposhnikoviae Radix (Differences between wild-type and cultivated products). Yakugaku Zasshi (2018) 138: 571-579
70. Li YY, Wang XX, Zhao L, Zhang H, Lv L, Zhou GC, Chai YF, Zhang GQ. High-performance liquid chromatography-electrospray ionization time-of-flight mass spectrometry analysis of Radix Saposhnikoviae for metabolomic research. J Chromatogr Sci (2013) 51: 99-106
71. Urbagarova BM, Taraskin VV, Shul'ts EE, Radnaeva LD, Anenkhonov OA, Ganbaatar Z, Boldanova NB. Biologically active compounds from the lipid fraction of *Saposhnikovia divaricata*. Chem Nat Comp (2017) 53: 138-140
72. Deng CH, Yang XH, Zhang XM. Rapid determination of panaxynol in a traditional Chinese medicine of *Saposhnikovia divaricata* by pressurized hot water extraction followed by liquid-phase microextraction and gas chromatography-mass spectrometry. Talanta (2005) 68: 6-11
73. Wu Y, He Y, He WY, Zhang YM, Lu J, Dai Z, Ma SC, Lin RC. Application of quantitative ^{1}H NMR for the calibration of protoberberine alkaloid reference standards. J Pharm Biomed Anal (2014) 90: 92-97
74. Pauli GF, Chen SN, Simmler C, Lankin DC, Godecke T, Jaki BU, Friesen JB, McAlpine JB, Napoitano JG. Importance of purity evaluation and the potential of quantitative ^{1}H NMR as a purity assay. J Med Chem (2014) 57: 9220-9231

75. Xin YY, Deng AJ, Du GH, Zhang JL, Qin HL. Fingerprinting analysis of *Saposhnikovia divaricata* using ^{1}H nuclear magnetic resonance spectroscopy and high performance liquid chromatography. J Integr Plant Biol (2010) 52: 782-792
76. Fukusaki E. Advanced technolgy of metabolomics and its practical application. Shiemushi Shuppan, Japan. (2008) 87-99
77. Men YQ, Wang DH, Li BZ, Su YL, Chen GL. Effects of drought stress on the antioxidant system, osmolytes and secondary metabolites of *Saposhnikovia divaricata* seedlings. Acta Physiol Plant (2018) 40: 191

Appendix

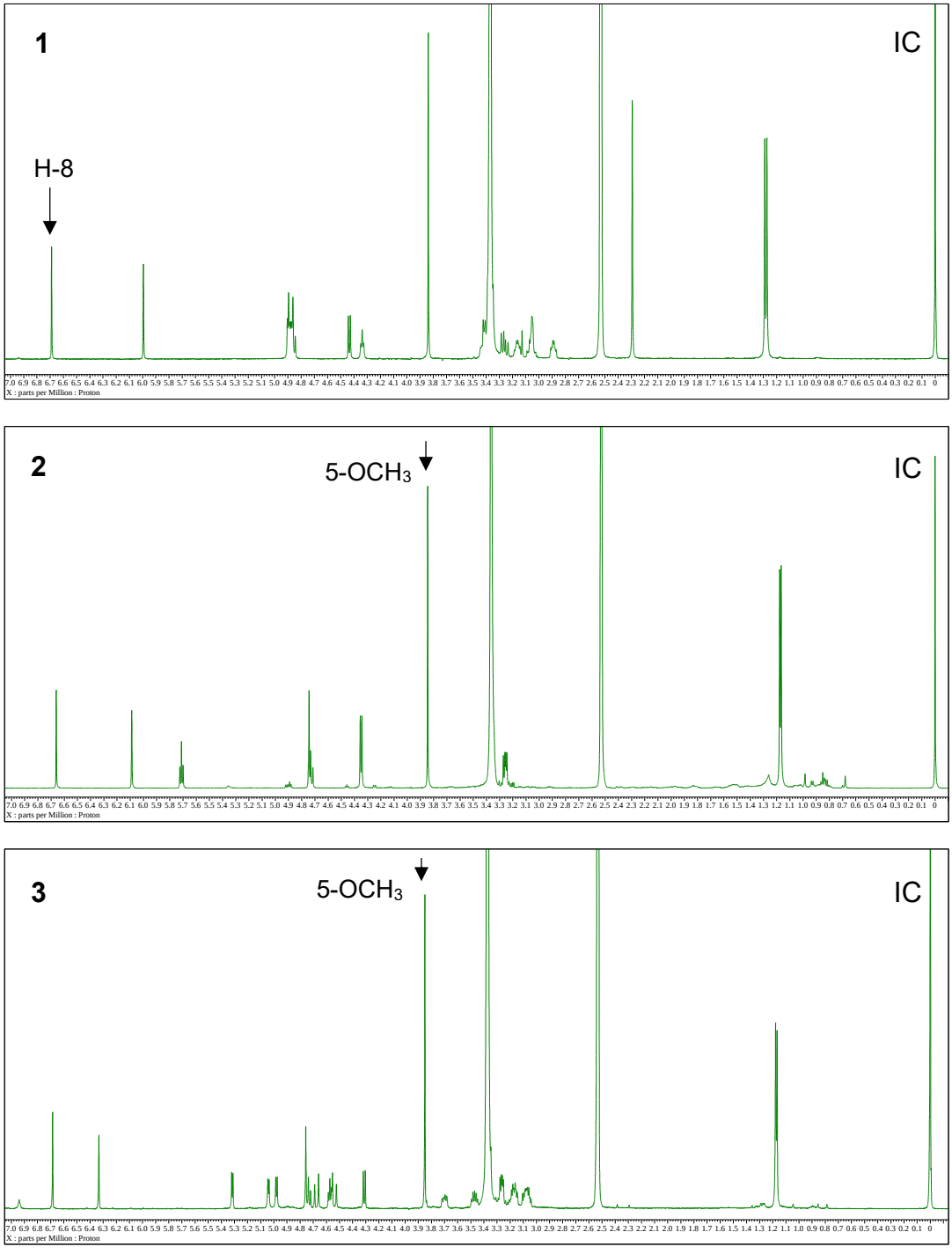

Fig. S1. The qHNMR spectra of compounds **1**–**13**. IC: the signal of internal calibrant DSS-d_6. Arrows: the selected signals of reference compounds for purity determination.

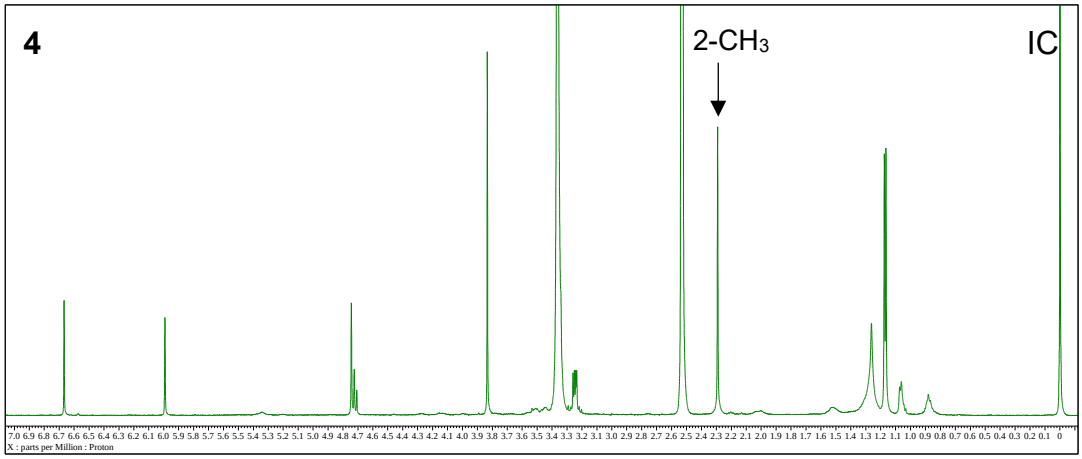
4
2-CH3
IC
X : parts per Million : Proton

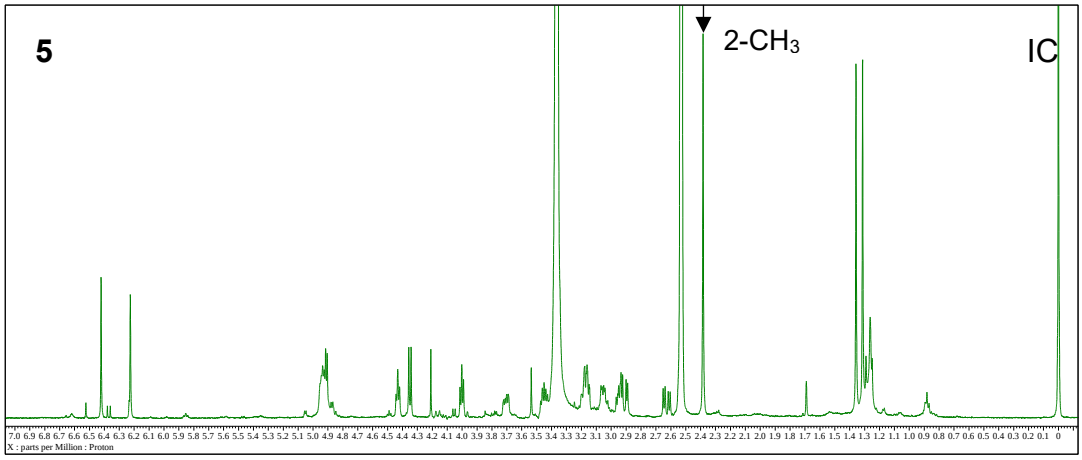
5
2-CH3
IC
X : parts per Million : Proton

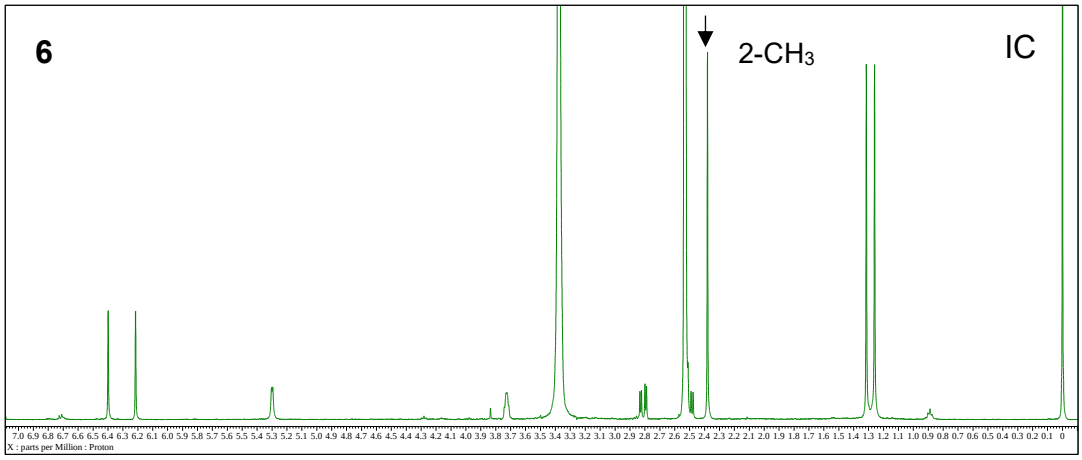
6
2-CH3
IC
X : parts per Million : Proton

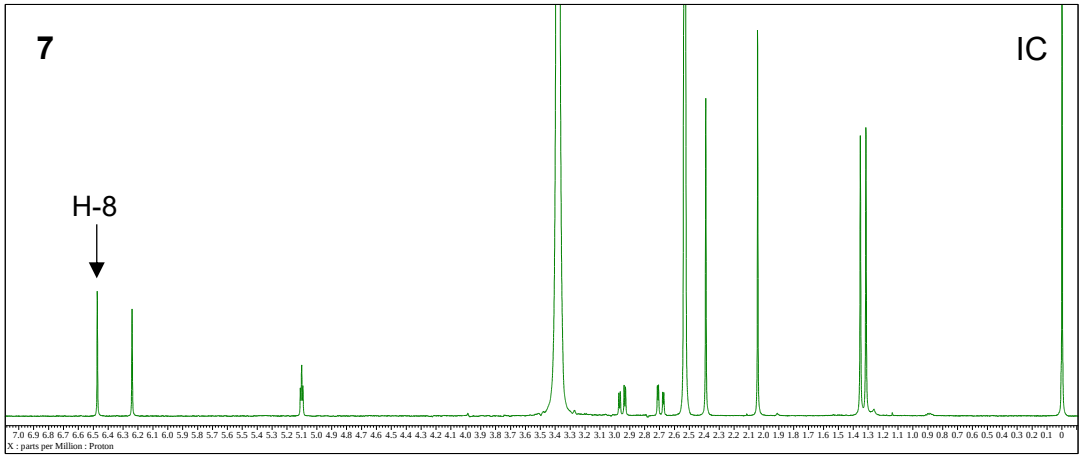
7
IC
H-8
X : parts per Million : Proton

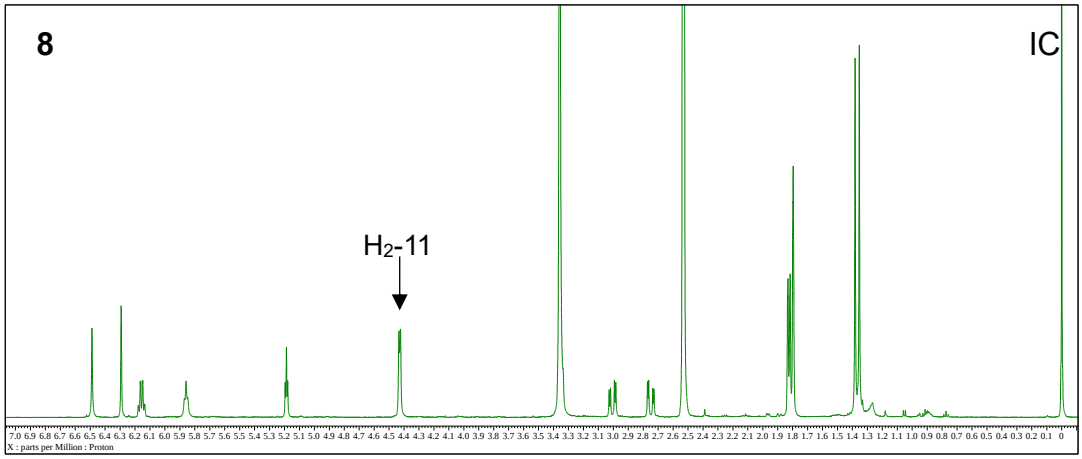
8
IC
H2-11
X : parts per Million : Proton

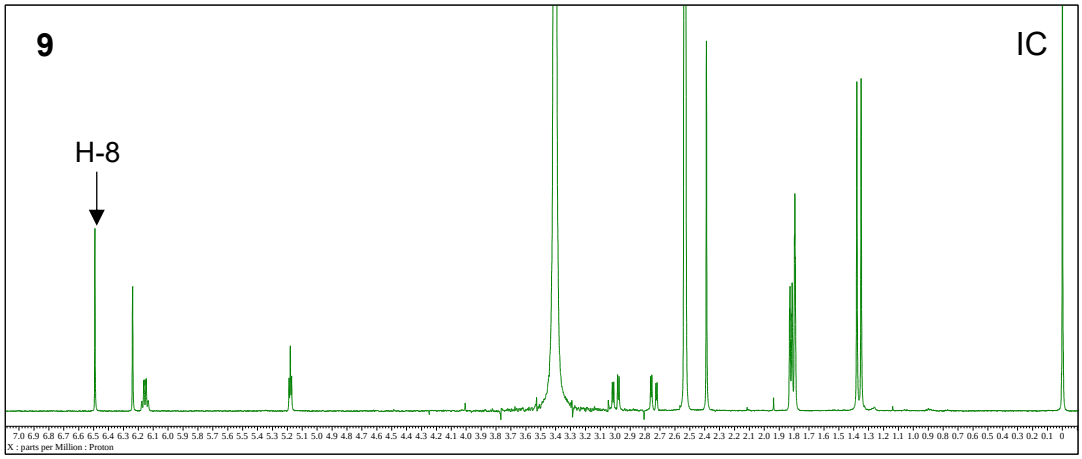
9
IC
H-8
X : parts per Million : Proton

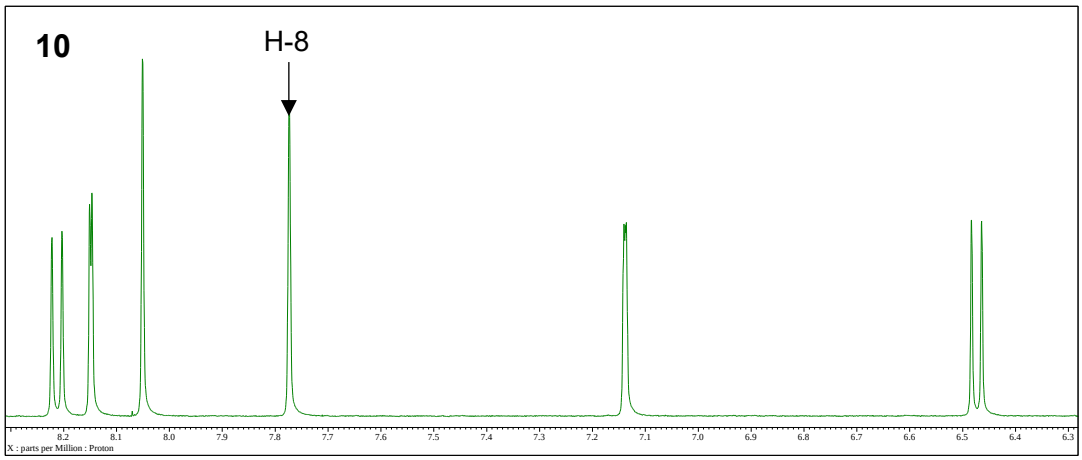
10
H-8
X : parts per Million : Proton

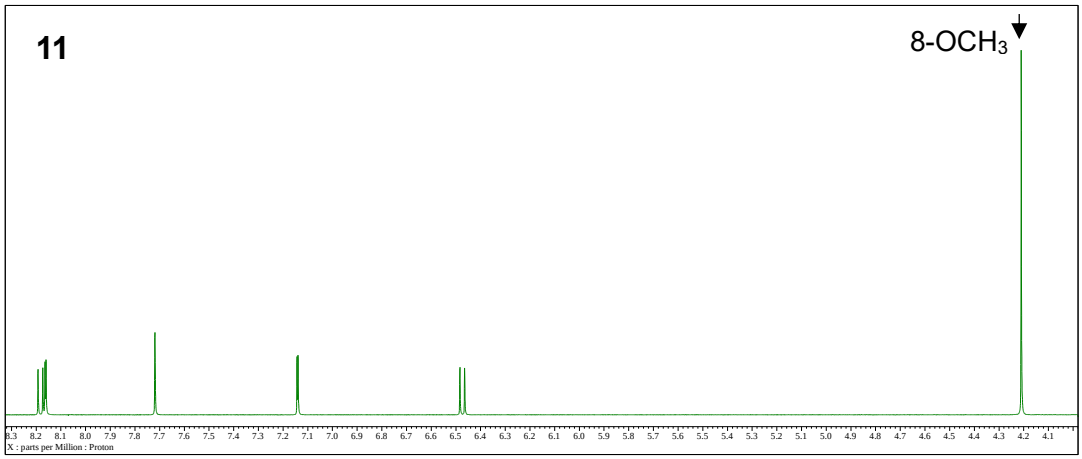
11
8-OCH3
X : parts per Million : Proton

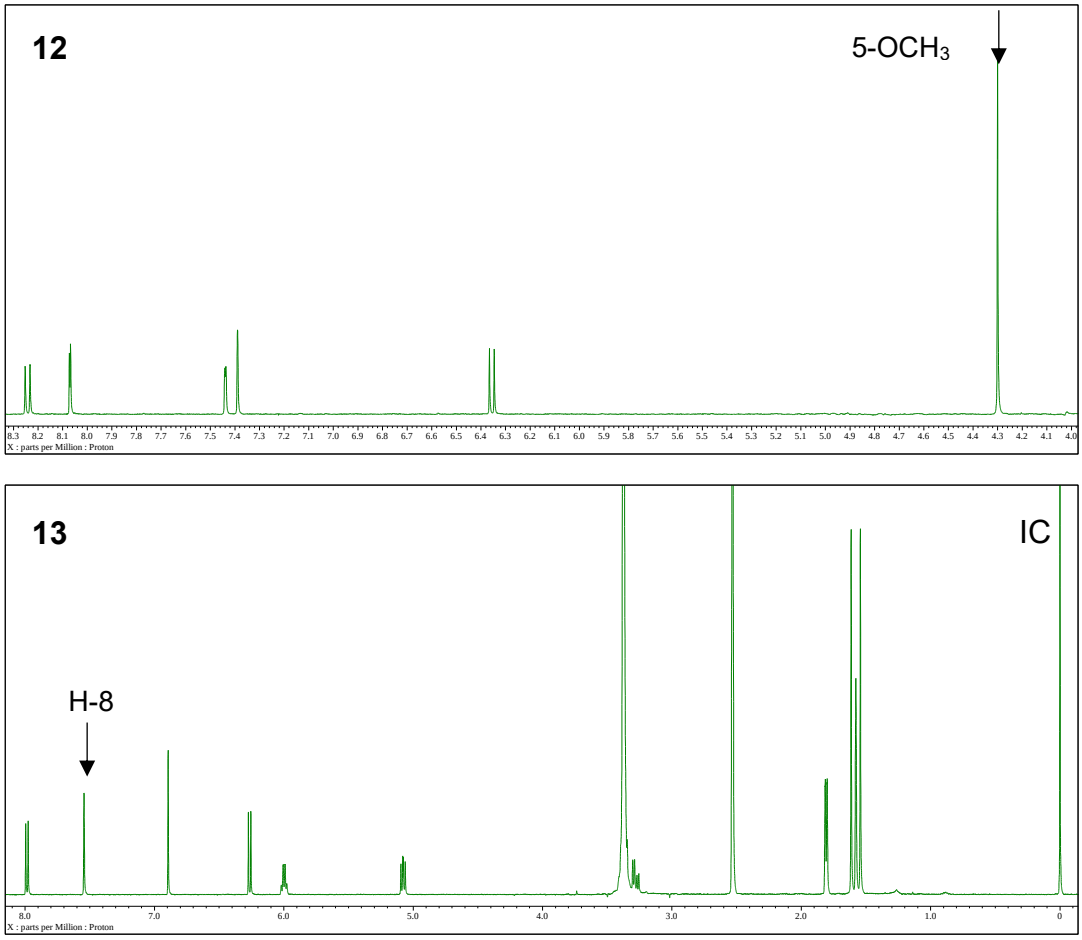

Fig. S1. continued.

Table S1. The contents (mg/g) of 13 compounds in plant specimens from Mongolia (A) and SR samples and specimens from China (B)

A

No.[a]	Field No.	Parts[b]	Type[c]	Locality		Dihydrofurochromones				Dihydropyranochromones					Coumarins			
						1	2	3	4	5	6	7	8	9	10	11	12	13
M2	MIII005	up	F	Ondorkhaan		3.9431	0.0748	1.1736	0.0275	0.6456	0.0352	0.0344	0.0294	0.8549	nd	nd	nd	0.0963
		B1				8.3110	0.2370	1.7429	0.0675	0.7929	0.0618	0.1323	0.1298	0.9574	nd	nd	nd	0.2698
		B2				9.1817	0.1911	2.4213	0.0705	1.0062	0.0700	0.1444	0.1408	1.1694	nd	nd	nd	0.3492
					Mean	7.1452	0.1676	1.7793	0.0552	0.8149	0.0557	0.1037	0.1000	0.9939	–	–	–	0.2384
					SD	2.8071	0.0836	0.6247	0.0240	0.1813	0.0182	0.0603	0.0614	0.1604	–	–	–	0.1293
M42	MIII071	A	F	〃		8.2999	0.6309	1.4214	0.1228	1.1971	0.6018	0.0374	0.1402	0.2979	nd	0.3265	0.0502	0.0061
		B				7.4124	0.4919	1.3713	0.0832	1.4011	0.3252	0.0632	0.0248	0.4914	nd	0.1091	nd	0.0061
		C				5.3148	0.5259	2.2785	0.0585	1.3775	0.0662	0.0680	0.0089	0.4389	nd	nd	nd	0.1197
		D				4.2696	0.4067	2.1629	0.0605	1.1477	0.0301	0.0464	0.0015	0.3592	nd	nd	nd	0.1155
					Mean	6.3242	0.5139	1.8085	0.0813	1.2808	0.2558	0.0537	0.0439	0.3968	–	0.1089	0.0126	0.0619
					SD	1.8554	0.0928	0.4787	0.0299	0.1272	0.2655	0.0143	0.0650	0.0855	–	0.1539	0.0251	0.0644
M43	MIII072	up	NF	〃		7.6556	0.3743	1.2605	0.1025	1.2252	0.0238	0.1182	0.0504	0.9133	nd	nd	nd	0.2312
		low				5.4208	0.2419	1.9688	0.0086	0.6268	0.0137	0.0595	0.0141	0.5180	nd	nd	nd	0.3064
					Mean	6.5382	0.3081	1.6147	0.0555	0.9260	0.0187	0.0889	0.0322	0.7156	–	–	–	0.2688
					SD	1.5802	0.0936	0.5008	0.0664	0.4231	0.0071	0.0415	0.0257	0.2795	–	–	–	0.0531
M3	MIII008	up	F	Bayan-Ovoo		13.8802	0.6182	2.0656	0.0711	0.6673	0.0558	0.0563	0.1350	1.2116	nd	0.0162	0.0284	0.1812
		mid				12.2723	0.4355	2.4587	0.0727	0.4300	0.0188	0.0340	0.0590	0.8814	nd	0.0140	nd	0.2217
		low				9.9893	0.4352	4.4944	0.0834	0.4897	0.0238	0.0185	0.0336	1.0822	nd	0.0149	nd	0.1363
					Mean	12.0473	0.4963	3.0062	0.0757	0.5290	0.0328	0.0363	0.0759	1.0584	–	0.0150	0.0095	0.1797
					SD	1.9552	0.1056	1.3037	0.0067	0.1234	0.0201	0.0190	0.0528	0.1663	–	0.0011	0.0164	0.0428
M4	MIII009	up	F	〃		10.0201	0.3322	1.0184	0.0739	0.9825	0.0430	0.0161	0.3880	1.2366	nd	nd	nd	0.0061
		mid				10.9155	0.3148	2.0611	0.0737	1.5997	0.0470	0.0204	0.2060	1.1115	nd	nd	tr	0.0980
					Mean	10.4678	0.3235	1.5398	0.0738	1.2911	0.0450	0.0182	0.2970	1.1741	–	–	–	0.0521
					SD	0.6332	0.0123	0.7373	0.0001	0.4364	0.0028	0.0031	0.1287	0.0884	–	–	–	0.0650
M5	MIII010	up	F	〃		4.0308	0.4450	0.8399	0.1362	0.8470	0.1091	0.1937	0.0683	0.4926	0.0201	nd	0.2666	0.0889
		low				3.9361	0.2218	1.2777	0.1102	0.4252	0.0226	0.0987	0.0299	0.3537	nd	nd	tr	0.0880
					Mean	3.9834	0.3334	1.0588	0.1232	0.6361	0.0659	0.1462	0.0491	0.4232	0.0201	–	0.2666	0.0885
					SD	0.0669	0.1579	0.3095	0.0183	0.2983	0.0612	0.0672	0.0272	0.0983	–	–	–	0.0007
M59*	MIV112	up	F	〃		9.6774	0.2876	2.4041	0.0662	1.2387	0.0477	0.0590	0.1491	0.7427	nd	0.0451	0.0031	0.1571
		low				7.5043	0.4415	3.9409	0.0651	0.9570	0.0280	0.0414	0.0332	0.5787	nd	nd	0.0038	0.1555
					Mean	8.5908	0.3646	3.1725	0.0657	1.0979	0.0379	0.0502	0.0912	0.6607	–	0.0451	0.0034	0.1563
					SD	1.5366	0.1088	1.0867	0.0008	0.1992	0.0140	0.0124	0.0820	0.1160	–	–	0.0005	0.0011
M60*	MIV114	up	F	〃		5.5077	0.1522	1.3771	0.0683	1.0173	0.0829	0.3772	0.2029	0.4694	nd	nd	nd	0.0061
		mid				8.8248	0.2591	2.6836	0.0890	1.2089	0.0826	0.2000	0.0799	0.6533	nd	0.0347	nd	0.1571
		low				6.8886	0.3753	2.9725	0.0876	0.8275	0.0128	0.0572	0.0161	0.3522	nd	nd	nd	0.0061
					Mean	7.0737	0.2622	2.3444	0.0816	1.0179	0.0594	0.2115	0.0996	0.4917	–	0.0347	–	0.0565
					SD	1.6663	0.1116	0.8501	0.0116	0.1907	0.0404	0.1603	0.0950	0.1518	–	–	–	0.0872

No.[a]	Field No.	Parts[b]	Type[c]	Locality		Dihydrofurochromones				Dihydropyranochromones					Coumarins			
						1	2	3	4	5	6	7	8	9	10	11	12	13
M61*	MII060	up	F	Norovlin		11.6117	0.4577	1.6647	0.0350	1.6483	0.0410	0.1963	0.1783	0.4370	0.0149	0.0102	0.0532	0.0061
		low				9.2019	0.9672	4.1788	0.1388	1.5539	0.0579	0.1634	0.0819	0.4552	nd	nd	nd	0.0061
					Mean	10.4068	0.7124	2.9217	0.0869	1.6011	0.0495	0.1799	0.1301	0.4461	0.0149	0.0102	0.0532	0.0061
					SD	1.7040	0.3602	1.7777	0.0734	0.0668	0.0120	0.0232	0.0682	0.0129	–	–	–	–
M63*	JB1501	up	F	,,		12.0915	1.6766	4.4348	0.0880	1.9650	0.0339	0.0453	0.0646	0.5621	nd	nd	nd	0.0061
		low				11.5689	3.5336	4.5323	0.2033	2.3752	0.1107	0.1188	0.2082	1.6708	nd	nd	nd	0.5699
					Mean	11.8302	2.6051	4.4835	0.1456	2.1701	0.0723	0.0820	0.1364	1.1164	–	–	–	0.2880
					SD	0.3696	1.3131	0.0689	0.0815	0.2901	0.0543	0.0520	0.1015	0.7840	–	–	–	0.3987
M44*	MIV017	up	F	,,		12.4730	0.2802	3.4695	0.0511	0.9091	0.0211	0.1226	0.4515	1.4543	nd	nd	nd	0.1250
		low				16.4821	0.3413	9.8912	0.0896	1.5077	0.0323	0.1918	0.2665	2.4585	nd	nd	nd	0.3821
					Mean	14.4776	0.3107	6.6803	0.0704	1.2084	0.0267	0.1572	0.3590	1.9564	–	–	–	0.2535
					SD	2.8349	0.0432	4.5409	0.0273	0.4232	0.0079	0.0490	0.1308	0.7101	–	–	–	0.1818
M45*	MIV019	up	F	,,		16.2180	0.3549	2.1331	0.0086	0.3653	0.0282	0.1490	0.3593	1.8494	nd	nd	nd	0.1705
		low				16.2160	0.5354	3.0653	0.0697	0.5294	0.0265	0.1727	0.1631	1.8883	nd	nd	nd	0.3275
					Mean	16.2170	0.4451	2.5992	0.0392	0.4473	0.0274	0.1609	0.2612	1.8689	–	–	–	0.2490
					SD	0.0014	0.1277	0.6592	0.0432	0.1160	0.0011	0.0168	0.1387	0.0275	–	–	–	0.1110
M46*	MIV025	up	F	,,		11.0206	0.2891	3.0078	0.0679	1.0168	0.0194	0.1883	0.1263	0.5685	nd	0.0445	nd	0.3262
		low				7.3399	0.5687	4.1659	0.1689	0.5929	0.0155	0.0515	0.0384	0.4793	nd	0.0214	nd	0.3262
					Mean	9.1802	0.4289	3.5868	0.1184	0.8049	0.0174	0.1199	0.0824	0.5239	–	0.0329	–	0.3262
					SD	2.6026	0.1976	0.8189	0.0714	0.2998	0.0027	0.0968	0.0621	0.0631	–	0.0163	–	–
M47*	MIV030	up	F	Bayan-Uul		7.2412	0.3133	1.8176	0.0673	0.5724	0.0392	0.1447	0.4286	0.8848	nd	0.0258	nd	0.0966
		low				9.1969	0.8481	3.8556	0.0830	0.7060	0.0127	0.0869	0.1813	0.8729	nd	nd	nd	0.3575
					Mean	8.2191	0.5807	2.8366	0.0751	0.6392	0.0260	0.1158	0.3050	0.8789	–	0.0129	–	0.2271
					SD	1.3829	0.3782	1.4411	0.0111	0.0944	0.0188	0.0408	0.1749	0.0084	–	0.0183	–	0.1845
M48*	MIV033	up	F	,,		8.2834	0.2863	4.7172	0.1613	2.0282	0.0628	0.5911	0.1281	1.0370	nd	nd	nd	0.1114
M49*	MIV039	up	F	,,		10.9580	0.8881	2.2675	0.0086	1.9578	0.0534	0.1869	0.2119	1.4596	nd	nd	nd	0.0915
M50*	MIV041	up	F	,,		7.9201	0.3650	3.0203	0.1154	2.4814	0.0606	0.2402	0.2280	2.0294	nd	nd	nd	0.1342
M51*	MIV049	up	F	,,		20.7937	1.1400	4.2660	0.0086	1.5638	0.0552	0.4979	0.1063	2.5173	nd	nd	nd	0.2772
M6	MIII011	up	F	Holonbuir		12.2137	0.7146	0.8545	0.1047	1.2623	0.4441	0.7322	0.3498	2.1873	nd	nd	0.0139	0.2844
		mid				12.5645	0.7734	1.6118	0.0606	1.8727	0.4813	1.0136	0.2009	2.0237	nd	nd	0.0010	0.5958
		low				9.2185	0.3298	4.4021	0.1003	1.2843	0.0247	0.1967	0.0937	1.4759	nd	nd	nd	0.4948
					Mean	11.3322	0.6060	2.2895	0.0885	1.4731	0.3167	0.6475	0.2148	1.8956	–	–	0.0074	0.4583
					SD	1.8389	0.2409	1.8684	0.0243	0.3462	0.2536	0.4150	0.1286	0.3726	–	–	0.0091	0.1589
M55*	MIV105	up	F	,,		2.6495	0.1786	0.4644	0.0757	0.4203	0.2362	0.1280	0.2985	0.9405	nd	nd	0.0266	0.0967
		low				6.8753	0.1341	1.7236	0.0710	0.8715	0.0213	0.0979	0.0936	1.5005	nd	nd	0.0019	0.2896
					Mean	4.7624	0.1563	1.0940	0.0734	0.6459	0.1287	0.1129	0.1961	1.2205	–	–	0.0143	0.1932
					SD	2.9881	0.0314	0.8904	0.0033	0.3190	0.1520	0.0213	0.1448	0.3960	–	–	0.0175	0.1364
M56*	MIV106	up	F	,,		10.5571	0.2887	2.4312	0.0086	1.1738	0.0264	0.1362	0.2197	0.6283	nd	0.0420	nd	0.4126
M57*	MIV109	up	F	,,		6.3106	0.5098	1.2758	0.3199	0.8607	0.1788	0.2677	0.2144	0.5038	nd	0.0535	0.2744	0.0061
M58*	MIV110	up	F	,,		5.3109	0.2975	1.1261	0.1014	1.2870	0.4680	0.2463	0.2063	0.5762	0.0425	0.0667	0.0780	0.3481
		mid				10.4850	0.2126	4.3221	0.0866	1.3514	0.0846	0.2208	0.1255	1.2688	nd	0.0663	0.0193	0.2876
		low				15.6178	0.3224	10.0211	0.1581	1.8513	0.0899	0.2749	0.1271	1.5711	nd	0.5233	nd	0.3567
					Mean	10.4712	0.2775	5.1564	0.1154	1.4966	0.2142	0.2473	0.1530	1.1387	0.0425	0.2188	0.0487	0.3308
					SD	5.1535	0.0576	4.5058	0.0377	0.3089	0.2198	0.0271	0.0462	0.5101	–	0.2638	0.0415	0.0377

No.[a]	Field No.	Parts[b]	Type[c]	Locality		Dihydrofurochromones				Dihydropyranochromones					Coumarins			
						1	2	3	4	5	6	7	8	9	10	11	12	13
M62*	MII100	up	F	Bulgan		9.0875	0.2371	1.9011	0.0530	1.3379	0.1825	0.1933	0.0686	1.7915	nd	0.0198	0.0034	0.0908
		mid				7.8219	0.2913	2.2400	0.0485	0.6323	0.0472	0.0455	0.0251	1.0252	nd	nd	nd	0.2046
		low				6.2365	0.3457	2.3179	0.0462	0.5551	0.0334	0.0348	0.0124	1.2292	nd	nd	nd	0.2149
					Mean	7.7153	0.2913	2.1530	0.0492	0.8418	0.0877	0.0912	0.0354	1.3487	–	0.0198	0.0034	0.1701
					SD	1.4285	0.0543	0.2216	0.0034	0.4314	0.0824	0.0886	0.0295	0.3969	–	–	–	0.0689
M9	MIII012	up	F	〃		9.6842	0.5600	0.8081	0.1695	1.1836	0.4456	0.1341	0.1675	0.9024	nd	nd	0.0150	0.1406
		mid				12.2024	0.8628	1.8849	0.3949	1.3729	0.5234	0.2300	0.0586	1.0977	nd	nd	0.0246	0.2008
					Mean	10.9433	0.7114	1.3465	0.2822	1.2783	0.4845	0.1821	0.1131	1.0000	–	–	0.0198	0.1707
					SD	1.7807	0.2141	0.7614	0.1594	0.1338	0.0550	0.0678	0.0770	0.1381	–	–	0.0068	0.0426
M52*	MIV098	up	F	〃		3.8872	0.2245	0.7802	0.0086	1.0702	0.0778	0.2182	0.3304	1.5306	nd	nd	0.0317	0.3578
		low				9.1435	0.2663	1.9594	0.0593	1.0501	0.0273	0.1286	0.1627	2.0195	nd	nd	nd	0.4405
					Mean	6.5153	0.2454	1.3698	0.0340	1.0602	0.0525	0.1734	0.2466	1.7751	–	–	0.0317	0.3991
					SD	3.7168	0.0296	0.8339	0.0358	0.0142	0.0357	0.0633	0.1186	0.3457	–	–	–	0.0585
M53*	MIV099	up	F	〃		6.7166	0.3599	1.1479	0.1929	0.9225	0.4029	0.2925	0.3385	1.6878	nd	0.0391	0.0285	0.3081
M54*	MIV102	up		〃		8.0121	0.2464	2.3736	0.0086	1.6299	0.0233	0.0343	0.0804	0.3841	nd	nd	nd	1.3820
		low				10.4435	0.2644	3.0375	0.0086	1.5061	0.0424	0.0984	0.0694	0.6865	nd	nd	nd	0.0061
					Mean	9.2278	0.2554	2.7055	0.0086	1.5680	0.0328	0.0664	0.0749	0.5353	–	–	–	0.6941
					SD	1.7193	0.0128	0.4695	0.0000	0.0875	0.0135	0.0453	0.0078	0.2138	–	–	–	0.9729
M1*	JB1502	up	F	Khalkhgol		9.2553	0.4721	1.5875	0.0734	0.9050	0.0932	0.0755	0.0847	0.3720	0.0842	0.1564	0.0711	0.0061
		low				4.4898	0.2960	0.9534	0.0521	0.6141	0.0878	0.2283	0.0360	0.4196	0.0192	0.0817	0.0118	0.0061
					Mean	6.8725	0.3840	1.2705	0.0627	0.7595	0.0905	0.1519	0.0603	0.3958	0.0517	0.1191	0.0415	0.0061
					SD	3.3697	0.1245	0.4484	0.0151	0.2056	0.0039	0.1080	0.0345	0.0337	0.0460	0.0529	0.0419	0.0000
M64*	JB1506	up	F	〃		5.4503	3.5790	3.0538	0.1279	0.6716	0.0596	0.0418	0.2757	0.6389	nd	0.0512	0.0688	0.1202
		low				4.9107	2.3599	3.4794	0.0949	0.5446	0.0441	0.0371	0.1617	0.4726	nd	0.0530	0.0510	0.1132
					Mean	5.1805	2.9694	3.2666	0.1114	0.6081	0.0519	0.0395	0.2187	0.5557	–	0.0521	0.0599	0.1167
					SD	0.3816	0.8620	0.3009	0.0233	0.0898	0.0110	0.0033	0.0806	0.1176	–	0.0013	0.0126	0.0049
M10	MIII019	up	NF	〃		3.7918	0.3574	1.4356	0.0086	0.7792	0.0226	0.1103	0.0530	0.8906	nd	nd	nd	0.0927
		mid				5.4947	0.4127	2.2748	0.0626	0.2544	0.0091	0.0352	0.0135	0.5106	nd	nd	nd	0.3419
		low				3.6424	0.2803	1.6675	0.0536	0.1707	0.0116	0.0193	0.0015	0.2439	nd	nd	nd	0.2283
					Mean	4.3097	0.3501	1.7926	0.0416	0.4014	0.0144	0.0549	0.0227	0.5483	–	–	–	0.2210
					SD	1.0290	0.0665	0.4334	0.0289	0.3298	0.0072	0.0486	0.0269	0.3250	–	–	–	0.1248
M21	MIII020	up	F	〃		8.6713	0.4961	2.1668	0.0838	0.5683	0.0242	0.0268	0.0817	0.2043	nd	nd	nd	0.1120
M29	MIII022	up	F	〃		8.0527	0.2903	4.5381	0.1394	2.5403	0.1162	0.6022	0.0799	1.5310	0.0080	0.0194	tr	0.0061
		low				7.7000	0.2577	6.6054	0.1568	1.2400	0.0678	0.3706	0.0453	1.0448	0.0072	0.0207	tr	0.0902
					Mean	7.8764	0.2740	5.5717	0.1481	1.8901	0.0920	0.4864	0.0626	1.2879	0.0076	0.0200	–	0.0482
					SD	0.2494	0.0231	1.4618	0.0123	0.9195	0.0342	0.1637	0.0245	0.3437	0.0005	0.0009	–	0.0594
M20	MIII023	up	F	〃		6.6194	0.3425	1.1878	0.0086	0.9106	0.0929	0.1578	0.1026	0.5320	nd	nd	nd	0.0061
		low				7.8512	0.4089	2.0246	0.0738	0.5825	0.0164	0.0295	0.0371	0.4327	nd	nd	nd	0.1232
					Mean	7.2353	0.3757	1.6062	0.0412	0.7465	0.0547	0.0936	0.0698	0.4823	–	–	–	0.0647
					SD	0.8710	0.0469	0.5917	0.0461	0.2320	0.0542	0.0907	0.0463	0.0702	–	–	–	0.0828

No.[a]	Field No.	Parts[b]	Type[c]	Locality		Dihydrofurochromones				Dihydropyranochromones					Coumarins			
						1	2	3	4	5	6	7	8	9	10	11	12	13
M21	MIII024	up	NF	Khalkhgol		8.0078	0.6814	2.9026	0.0780	0.5785	0.0590	0.1256	0.1314	0.8049	nd	nd	tr	0.1506
		low		(continued)		4.6593	0.4115	3.6520	0.1207	0.1865	0.0099	0.0227	0.0105	0.1692	nd	nd	nd	0.0920
					Mean	6.3336	0.5465	3.2773	0.0993	0.3825	0.0344	0.0741	0.0709	0.4871	–	–	–	0.1213
					SD	2.3677	0.1908	0.5299	0.0302	0.2771	0.0347	0.0728	0.0854	0.4495	–	–	–	0.0414
M22	MIII025	up	NF	″		5.6870	0.5348	1.0558	0.0756	1.9891	0.0533	0.2121	0.1516	0.4877	nd	nd	tr	0.1094
		low				10.4903	1.0154	3.0902	0.1452	1.9934	0.0500	0.0456	0.0150	0.0424	nd	nd	nd	0.1158
					Mean	8.0887	0.7751	2.0730	0.1104	1.9913	0.0516	0.1289	0.0833	0.2651	–	–	–	0.1126
					SD	3.3964	0.3398	1.4385	0.0492	0.0030	0.0024	0.1177	0.0966	0.3148	–	–	–	0.0045
M23	MIII027	up	NF	″		7.0509	0.6610	1.5032	0.0680	1.0833	0.0543	0.0825	0.2000	0.7337	nd	nd	0.0041	0.1721
		low				7.5074	0.5193	1.7964	0.0675	0.6711	0.0318	0.0358	0.0407	0.4096	nd	nd	nd	0.3460
					Mean	7.2791	0.5902	1.6498	0.0677	0.8772	0.0430	0.0591	0.1204	0.5716	–	–	0.0041	0.2590
					SD	0.3228	0.1002	0.2073	0.0004	0.2915	0.0159	0.0330	0.1127	0.2292	–	–	–	0.1230
M33	MIII028	B1	NF	″		5.2528	0.2952	3.7152	0.0552	2.1323	0.0339	0.0358	0.0407	0.4096	nd	nd	nd	0.3460
M34	MIII046	up	NF	″		4.7194	0.2667	2.0277	0.0964	1.8733	0.0751	0.0727	0.0863	1.2354	nd	nd	nd	0.0913
		low				13.6903	1.5872	1.7104	0.0996	1.2014	0.3734	0.1570	0.0606	0.8609	nd	0.0411	0.0288	0.6719
					Mean	9.2049	0.9269	1.8691	0.0980	1.5373	0.2242	0.1149	0.0734	1.0481	–	0.0411	0.0288	0.3816
					SD	6.3434	0.9337	0.2244	0.0022	0.4751	0.2109	0.0595	0.0181	0.2648	–	–	–	0.4106
M35	MIII049	A	F	″		18.5681	1.2425	1.0992	0.1444	0.9097	0.1440	0.0995	0.1990	0.3011	nd	nd	0.1229	0.0061
		E				10.3840	0.5817	1.9835	0.0724	0.9138	0.0512	0.0302	0.0144	0.3874	nd	nd	nd	0.0061
		H				6.4215	0.3690	1.6963	0.0521	0.5085	0.0189	0.0199	0.0130	0.3327	nd	nd	nd	0.0061
					Mean	11.7912	0.7311	1.5930	0.0896	0.7773	0.0714	0.0498	0.0754	0.3404	–	–	0.1229	0.0061
					SD	6.1943	0.4555	0.4511	0.0485	0.2328	0.0650	0.0433	0.1070	0.0437	–	–	–	0.0000
M36	MIII050	up	NF	″		10.3745	1.1111	1.7364	0.1022	1.2896	0.2091	0.1724	0.1106	1.1826	nd	0.0603	0.0681	0.1106
		low				8.9434	0.7834	3.2234	0.0980	1.1086	0.0397	0.1361	0.0412	1.0538	nd	nd	nd	0.0905
					Mean	9.6590	0.9472	2.4799	0.1001	1.1991	0.1244	0.1542	0.0759	1.1182	–	0.0603	0.0681	0.1006
					SD	1.0119	0.2317	1.0515	0.0030	0.1280	0.1198	0.0256	0.0491	0.0911	–	–	–	0.0143
M37	MIII051	B1	NF	″		18.2335	1.5426	3.4881	0.1468	1.8997	0.3994	0.2885	0.2009	0.7268	nd	nd	0.0399	0.5805
		B2				16.5238	1.4530	3.1589	0.1437	1.9391	0.3150	0.2630	0.1329	0.8171	nd	nd	nd	0.7053
					Mean	17.3786	1.4978	3.3235	0.1453	1.9194	0.3572	0.2757	0.1669	0.7720	–	–	0.0399	0.6429
					SD	1.2089	0.0633	0.2328	0.0022	0.0279	0.0597	0.0180	0.0480	0.0639	–	–	–	0.0883
M65*	MIV136	up	–	Kherlem Bayan-Ulaan		2.4113	0.5905	1.1968	nd	0.6689	0.0198	0.1032	0.1083	0.2687	nd	nd	nd	nd
M66*	MIV137	up	–	″		5.0109	0.2964	3.6755	0.0880	1.1410	0.0266	0.0817	0.1510	0.7287	nd	nd	nd	nd

B

No.[a]	TMPW No.	Parts[b]	Type[c]	Production area[d]		Dihydrofurochromones				Dihydropyranochromones					Coumarins			
						1	2	3	4	5	6	7	8	9	10	11	12	13
C1	Cn076	up	W	Inner Mongolia Autonomous Region		3.4757	0.3954	1.6149	nd	1.7875	0.0423	0.0852	0.0613	0.3509	nd	nd	nd	nd
C2	Cn262	up	W	,,		4.5342	0.3103	1.9618	0.0339	1.3996	0.0345	0.0619	0.0276	0.2953	nd	nd	nd	nd
		mid				4.7166	0.5105	2.9930	0.0735	1.7210	0.0474	0.0534	0.0126	0.2945	nd	nd	nd	nd
		low				2.7943	0.6234	2.0574	0.0734	1.2214	0.1585	nd	0.0163	0.1947	nd	nd	nd	nd
					Mean	4.0150	0.4814	2.3374	0.0603	1.4473	0.0802	0.0576	0.0188	0.2615	–	–	–	–
					SD	1.0611	0.1586	0.5698	0.0228	0.2532	0.0682	0.0060	0.0078	0.0578	–	–	–	–
C3	21596	up	–	–		3.0268	1.4139	3.1632	0.1771	2.8178	0.1560	0.0760	0.1069	0.8106	nd	nd	nd	0.2956
		low				1.9965	1.0354	4.2190	0.5053	0.7674	0.0481	0.0920	0.0517	0.3307	nd	nd	nd	0.1134
					Mean	2.5117	1.2247	3.6911	0.3412	1.7926	0.1021	0.0840	0.0793	0.5706	–	–	–	0.2045
					SD	0.7286	0.2677	0.7465	0.2321	1.4499	0.0763	0.0113	0.0390	0.3393	–	–	–	0.1288
C4	21601	up	C	–		3.6942	0.2948	2.7973	0.0985	0.5832	0.0255	0.0569	nd	0.0572	nd	nd	nd	nd
		mid				1.9774	0.2260	2.0251	0.0725	0.4012	0.0487	0.0561	nd	0.0412	nd	nd	tr	nd
		low				1.3244	0.3109	1.8189	0.0680	0.2991	0.0695	0.0874	nd	0.0375	0.0698	0.0435	0.0036	nd
					Mean	2.3320	0.2772	2.2138	0.0797	0.4278	0.0479	0.0668	–	0.0453	0.0698	0.0435	0.0036	–
					SD	1.2241	0.0451	0.5158	0.0165	0.1439	0.0220	0.0178	–	0.0105	–	–	–	–
C5	21602	up	W	–		4.2511	3.7700	3.6983	0.4815	2.8278	0.1925	0.0280	0.1373	0.3475	nd	0.0567	0.0045	nd
C6	24482	piece	–	–		2.5184	0.6310	2.4996	0.1579	0.6529	0.0649	0.0641	nd	0.0653	0.1237	0.0543	0.0324	nd
C7	27840	up	W	Dorbod Mongol Autonomous County, Heilongjiang prov.		3.4769	0.6203	10.5145	0.3535	2.5665	0.0848	0.0641	0.1178	0.3965	nd	nd	0.0001	0.1396
		mid				6.0867	1.5290	11.0892	0.3915	3.2565	0.1692	0.0799	0.0942	0.4608	nd	nd	0.0704	0.1357
		low				4.3052	1.2262	7.6323	0.2931	1.8003	0.0955	0.0579	0.0554	0.4364	nd	nd	0.0136	0.1764
					Mean	4.6229	1.1252	9.7453	0.3461	2.5411	0.1165	0.0673	0.0891	0.4312	–	–	0.0280	0.1505
					SD	1.3336	0.4627	1.8523	0.0496	0.7284	0.0459	0.0113	0.0315	0.0324	–	–	0.0373	0.0224
C8	27486	up	W	Inner Mongolia Autonomous Region		3.3622	0.6017	2.3569	0.0971	1.3319	0.0538	0.0833	0.0329	0.1387	nd	nd	nd	nd
		low				2.1460	0.3362	1.8806	0.0682	0.8644	0.0187	0.0581	0.0140	0.0962	nd	nd	nd	nd
					Mean	2.7541	0.4689	2.1187	0.0826	1.0982	0.0362	0.0707	0.0235	0.1175	–	–	–	–
					SD	0.8600	0.1878	0.3368	0.0204	0.3306	0.0248	0.0178	0.0133	0.0300	–	–	–	–
C9	28814	piece	W	,,		10.2557	1.2683	5.5588	0.2080	1.6426	0.1236	0.1448	0.0896	0.6216	0.1192	0.0806	0.0397	0.1522
C10	28813	piece	C	Hebei prov.		1.9995	0.2435	1.9032	0.0858	0.3723	0.0254	0.0449	nd	0.0719	0.0380	0.0370	0.0050	nd

[a]: the specimens used for qHNMR analysis;

[b]: the root of specimens was divided into upper (up), middle (mid), and lower (low) parts; the root of specimen was divided into 4 equal parts from the base and labeled with A, B, C, and D; newly occurred root on the old root (B1 or B2); SR samples composed of piece cut (piece);

[c]: plant specimens with flower (F), without flower (NF), other specimens had no aerial parts (–), SR sample derived from wild (W) or cultivated (C) plant; other samples had no onformation (–);

[d]: production area was not clear (–);

nd: not detected; tr: trace amount; mean and SD are not available (–);

List of Publications

[1] Batsukh Z, Toume K, Javzan B, Kazuma K, Cai SQ, Hayashi Sh, Kawahara N, Maruyama T, Komatsu K (2020) Metabolomic profiling of Saposhnikoviae Radix from Mongolia by LC-IT-TOF-MS/MS and multivariate statistical analysis J Nat Med 74:170–188.

[2] Batsukh Z, Toume K, Javzan B, Kazuma K, Cai SQ, Hayashi S, Atsumi T, Yoshitomi T, Uchiyama N, Maruyama T, Kawahara N, Komatsu K (2020) Characterization of metabolites in *Saposhnikovia divaricata* roots from Mongolia J Nat Med (in press).

Acknowledgements

I would like to express my deepest gratitude to my supervisor Prof. Katsuko Komatsu, Section of Pharmacognosy, Division of Medicinal Resources, Institute of Natural Medicine, University of Toyama, for her excellent guidance, advice, and support during my doctoral research. Her immense knowledge and enthusiastic encouragements have continuously inspired me in my study. I am also very grateful for giving me an opportunity to work in this laboratory.

I would like to offer my special thanks to Associate Prof. Kazufumi Toume, Section of Pharmacognosy, Division of Medicinal Resources, Institute of Natural Medicine, University of Toyama, for his patient guidance and constructive suggestions throughout this study. He continually discussed with me how to improve my research and motivated me to make an effort to complete this research work.

I also would like to express my sincere thanks to Assistant Prof. Shu Zhu, Section of Pharmacognosy, Division of Medicinal Resources, Institute of Natural Medicine, University of Toyama, for her valuable advice and thoughtful discussion on my research.

I am greatly indebted to Prof. Batkhuu Javzan, School of Engineering and Applied Sciences, National University of Mongolia, who recommended me to study at the University of Toyama and cooperated in collecting the plant specimens in Mongolia.

I would like to extend my sincere gratitude to all participants Dr. Kouhei Kazuma, Dr. Atsumi Toshiyuki, Dr. Shigeki Hayashi, and Dr. Nobuo Kawahara, for great cooperation to this study and sample collection.

My grateful thanks are extended to Dr. Takuro Maruyama, Dr. Taichi Yoshitomi, and Dr. Nahoko Uchiyama for their support in the NMR measurement.

I would like to express my gratitude to the members of Dissertation Committee Associate Prof. Taishi Taura and Prof. Hiroyuki Morita for their valuable comments and suggestions.

I am also thankful to the past and present members of Section of Pharmacognosy, Division of Medicinal Resources, Institute of Natural Medicine, University of Toyama, especially Ms. Masako Yuki, Dr. Yue-Wei Ge, Ms. Mai Asanuma, Ms. Zhi-Yan Hou, Ms. Han-Pei Zhang, Mr. Yasenjiang Aximu, Mr. Qundong Liu, Ms. Huanhuan Yu, Ms. Aimi Shirakawa, Ms. Yuki Tomita, Mr. Kenichiro Hotta, Mr. Shin Kimijima, Ms. Shiori Takao, Ms. Shiho Hanazawa, Mr. Yoshimasa Yamamoto, Ms. Yuzhuo Dong, Mr. Ryouhei Kawasaki, Mr. Shunsuke Kitami, Mr. Tomomasa Kosuge, for their kind help and friendship during the memorable time in Toyama.

I would also like to thank the staffs of the Graduate School of Pharmaceutical Sciences and International Student Division for their administrative help and support.

I would like to acknowledge the Japanese Government through the Ministry of Education, Culture, Sports, Science, and Technology for the Monbukagakusho Scholarship and financial support.

Finally, I would like to express my gratitude to my parents, husband, sons, parents-in-law, sisters, brothers, relatives, and friends for their endless love, support, and encouragement which enabled me to achieve my PhD degree.

Zolboo Batsukh

July 2020

Toyama, Japan